Stony Brook University

INDOOR LOCALIZATION AND TRACKING USING BINARY INFORMATION

A Dissertation Presented

by

Li Geng

to

The Graduate School

in Partial Fulfillment of the

Requirements

for the Degree of

Doctor of Philosophy

in

Electrical Engineering

Stony Brook University

August 2015

Stony Brook University

The Graduate School

Li Geng

We, the dissertation committe for the above candidate for the

Doctor of Philosophy degree, hereby recommend

acceptance of this dissertation

Mónica F. Bugallo - Dissertation Advisor
Associate Professor, Department of Electrical and Computer Engineering

Petar M. Djurić - Chairperson of Defense
Professor, Department of Electrical and Computer Engineering

Thomas Robertazzi
Professor, Department of Electrical and Computer Engineering

Samir R. Das
Professor, Department of Computer Science

This dissertation is accepted by the Graduate School

Charles Taber
Dean of the Graduate School

Abstract of the Dissertation

INDOOR LOCALIZATION AND TRACKING USING BINARY INFORMATION

by

Li Geng

Doctor of Philosophy

in

Electrical Engineering

Stony Brook University

2015

Real-time localization and tracking of people and assets within buildings is in high demand in many applications. These tasks are very challenging in indoor environments due to the physics of signal propagation and the multi-path interference. Satellite-based technologies such as the Global Positioning Systems (GPS) are notoriously unreliable in indoor environments. As a result, a variety of novel technologies have been developed to fill this gap. This dissertation focuses on the use of binary information for indoor localization and tracking, and in particular, on the use of the Ultra High Frequency (UHF) Radio Frequency Identification (RFID) technology. RFID is a rapidly growing technology that uses

electromagnetic fields in the radio frequency range to transfer data. It greatly motivates and drives the research in indoor localization and tracking.

The main contribution of this dissertation is a novel framework for indoor localization and tracking based on binary information. Binary information indicates whether a device is present or absent within a predefined area. New models and Bayesian-based methods are proposed and investigated, primarily in the context of RFID systems composed of readers and tags. One novelty represents models of probabilities of tag detection. It also includes variability of this probability. For tracking, we propose the use of a particle filtering algorithm that operates on asynchronous data. In order to improve the tracking performance, especially in areas with intersections and at portals, novel tags called sense-a-tags (STs) with ability to detect other tags are added to the standard RFID system. The STs can passively detect and decode backscatter signals from tags in their proximity. With the proximity information provided by the STs, the system can improve the localization accuracy and can unambiguously estimate the direction of movement of a tagged object.

Constrained by the cost and energy requirements, a novel system containing no RFID readers is proposed. This system is composed of tags with capability of tag-to-tag communication. The tags can broadcast information to neighboring tags by backscattering. A real-time self-locating problem is formulated in this reader-free system and algorithms using binary information with low computational complexity are investigated. These algorithms preserve high accuracy in their performance.

Stimulated by the requirements of low energy consumption, robustness against node failure, and scalability, non-centralized processing has gained a great interest in recent years. Simple low-cost devices with capability of communicating among themselves greatly promotes the development of non-centralized processing in wide applications. A non-centralized tracking problem with networks of binary

directional sensors is presented and its extension to the novel reader-free RFID system is discussed.

Contents

List of Tables

List of Figures

List of Abbreviations

ANM	All-node-method
APIT	Approximate point in triangulation
CDF	Cumulative density function
DOA	Direction-of-arrival
GPS	Global Positioning System
IoT	Internet of things
KF	Kalman filter
MAP	Maximum a posterior
MMSE	Minimum mean square error
ONM	One-node-method
PDR	Pedestrian dead reckoning
PF	Particle filter
RBPF	Rao-Blackwellised Particle filter
RFID	Radio frequency identification
RMSE	Root mean square error
RSS	Received signal strength
SMC	Sequential monte carlo
ST	Sense-a-tag
TDOA	Time-difference-of-arrival

TOA	Time-of-arrival
UHF	Ultra-high frequency
UWB	Ultra-wide bandwidth
WSN	Wireless sensor network

Acknowledgements

Over the past years, I have worked with a number of people who have made my time at Stony Brook University enjoyable and rewarding. I would like to thank all of them.

First of all, I am deeply grateful to my two excellent advisors, Professors Petar M. Djurić and Mónica F. Bugallo for providing guidance and many thoughtful suggestions regarding the content and direction of my research program. I would also like to thank Mónica for teaching me the art of effective writing and presentation.

I would like to thank all my colleagues at the COSINE lab, Bingxin Shen, Vibha Mane, Cagla Tasdemir, Shishir Dash, Inigo Urteaga, Yunlong Wang, Zhiyuan Weng, Zhe shen, Kezi Yu, Lingqin Gan, Hechuan Wang. I would also like to thank Dr. Akshay Athalye for his guidance and expert suggestions in the experiments.

I thank Prof. Thomas G. Robertazzi and Prof. Samir R. Das for serving as my committee members and providing important advice and suggestions on my research. I would also like to thank all the people from the department of Women In Science and Engineering (WISE) and Center for Science and Mathematics Education (CESAME). I have had a great time and learnt a lot in working with them to teach science and engineering for high school students.

Finally, I would like to offer my sincere thanks to my parents Xianzhou Geng,

Qingjiao Li and my husband Ke Zhang for their unconditional love, encouragement and support during these years.

1

Introduction

1.1 Motivation

In the past decades, an intense research work has been carried out on target localization and tracking technologies that can operate in indoor environments. These technologies complement the fully-developed outdoor positioning so that ubiquitous location awareness can be achieved for the construction of the Internet of Things (IoT). In IoT, every object is expected to interact with people and other objects. Real-time localization and tracking of people and objects within buildings is in high demand for many applications. These applications can be seen in various settings, e.g., in health care systems to improve patient monitoring and safety and to locate in-demand portable medical equipments; in mine safety to track underground miners' locations; in public safety and military applications to track and navigate fire fighters and soldiers inside buildings; in warehouses for inventory management; in shopping malls for targeted mobile advertising.

Satellite-based technologies such as the Global Positioning Systems (GPS) are

notoriously unreliable in indoor environments since the signals emitted by satellites are not designed to penetrate most construction materials such as roofs, walls and other objects, and generally require line-of-sight transmission between receivers and satellites. As a result, a variety of novel technologies have been developed to fill this gap in order to make positioning ubiquitous.

Of the many existing wireless facilities that have been considered for indoor positioning systems, radio frequency based systems predominate today due to their availability and low cost [1, 2]. Systems using WiFi, Radio-frequency identification (RFID), ZigBee, Bluetooth, Ultrawide-band (UWB) and inertial measurements units in smart phones have been investigated in recent years.

RFID is a rapidly growing technology that transfers data from a tag to a reader by backscattering electromagnetic fields in the radio frequency range [3]. It greatly motivates and drives the research in indoor localization and tracking. RFID technology is also one of the pivotal enablers of the IoT, where it is anticipated that trillions of things will be equipped with RFID tags with the goal that the things interact with people and other objects, ultimately improving daily life [4]. The localization and tracking of these trillions of devices will be of critical importance.

Indoor positioning problems have been studied extensively in the context of RFID systems, using measurements such as received signal strength (RSS), angle, time or phase of arrival to support location-based services. It is expected that an explosion of advances of indoor positioning using binary information will follow in the near future. One rationale for this is the requirements of simple, inexpensive individual devices with limited resources (processing capabilities, memory, and power) deployed in large numbers for the construction of IoT and the ubiquitous location awareness. These devices require minimal assumptions about sensing

capabilities. It alleviates the requirements of sophisticated observations models such as the modeling of RSS which is known to be a thorny problem in indoor scenarios due to the attenuation, reflection and refraction by the objects and the multi-path interference. On the other hand, many sophisticated sensors or devices can also act as binary-detection devices easily by outputing binary report with predefining a threshold for the measurements.

1.2 Problem formulation

To address the localization problem, we consider a stationary target in a field with N reference nodes collecting observations related to the target. There are two cases of binary detection as illustrated in the previous section. One is of sensors/devices that output a binary report depending on the strength of the observed signal. The observation is assumed to be

$$y_i \quad = \quad h(\boldsymbol{x}) + v_i \tag{1.1}$$

- $\boldsymbol{x}$: a tag state, which is the location of the target,
- y_i: an observation from the i-th reference node, where $i = 1, \cdots, N$,
- v_i: a measurement noise of the i-th reference node, and
- h: a function describing the observation model.

The measurement y_i depends on the type of sensors, e.g., with acoustic sensors, the sensed information is the strength intensity (signal power) of the transmitted signals by the source. The attenuation of the signal is a function of the distance

from the source. The output binary information is determined by

$$n_i = \begin{cases} 1, & y_i >= \gamma \\ 0, & \text{otherwise} \end{cases} \tag{1.2}$$

where γ is a predefined threshold; and n_i is the binary output with $n_i \in \{0, 1\}$.

The other case is to model the probability of detection directly and the output binary information is assumed to follow a Bernoulli distribution

$$f(n; p_i) = \begin{cases} p_i, & n_i = 1 \\ 1 - p_i, & n_i = 0 \end{cases} \tag{1.3}$$

where $p_i \in [0, 1]$ is the probability of detection by the i-th reference node and it requires modeling based on experimental data from the real world.

The key to successful target localization lies in the effective extraction of useful information about the target's state from observations based on the observation model. Without loss of generality, we assume the target to be a tag[1](usually attached to an object) and the reference nodes are the readers in a RFID system as shown in Fig. 1.1 (a).

The tracking problem is different from the localization problem in that the tag is moving with time as shown in Fig. 1.1 (b). The primary objective of target tracking is to estimate the state trajectories of a moving target. Almost all maneuvering target tracking methods are model-based because knowledge of target motion is available and a model-based tracking algorithm will greatly outperform any model-free tracking algorithm if the underlying model turns out to be a good one. Various

[1] Since each tag has its unique identification, there is no data association problem. The localization of different tags is statistically independent due to this nature of the RFID system. Thus, we address the localization of one particular tag.

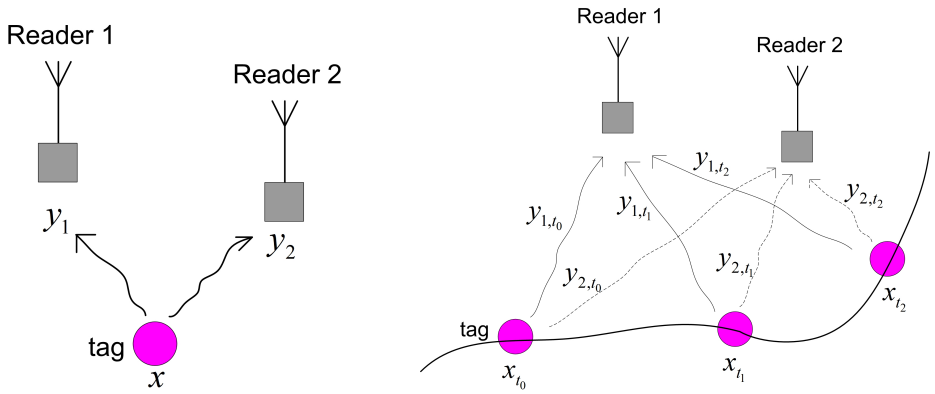

(a) A localization example (b) A tracking example

FIGURE 1.1: Examples for localization and tracking.

mathematical models of target motion have been developed over the past three decades [5]. Consider a tag moving in a field according to the state-space model given by

$$\boldsymbol{x}_{t_k} = f(\boldsymbol{x}_{t_{k-1}}) + \boldsymbol{u}_{t_k} \tag{1.4}$$

$$\boldsymbol{y}_{i,t_k} = h(\boldsymbol{x}_{t_k}) + \boldsymbol{v}_{i,t_k} \tag{1.5}$$

- $\boldsymbol{x}_{t_k}$: the tag state at t_k where $k = 1, 2, \cdots$. It can be the location of a tag, or the location and the velocity, or even the location, velocity, and acceleration depending on different application scenarios. The symbol t_k represents a time instant, where $t_{k-1} < t_k$. Furthermore,
- $\boldsymbol{y}_{i,t_k}$: an observation from the i-th reader at time t_k, where $i = 1, \cdots, N$,
- $\boldsymbol{u}_{t_k}$: a noise of the motion model at time t_k,
- $\boldsymbol{v}_{i,t_k}$: a measurement noise of the i-th reader,
- f and h: system functions (possibly non-linear).

The formulation of the tracking problem using binary information is a straightforward extension in the modeling of the binary observations as in equations (1.2) and (1.3).

1.3 Contributions

In this thesis, we formulate a novel framework for indoor localization and tracking based on binary information. New models and Bayesian-based methods are proposed and investigated. One novelty represents models of probabilities of tag detection. The use of a particle filtering algorithm is proposed that operates on asynchronous data for tracking.

In order to improve the tracking performance, especially in areas with intersections and at portals, the use of sense-a-tags (STs) with ability to detect other tags is introduced. The ST is a device that can not only communicate with the reader like standard passive tags but also can sense the communication between tags in its proximity and the reader. Improved accuracy is reported.

A novel system containing no RFID readers is proposed. This system is composed of tags with capability of tag-to-tag communication. The tags can broadcast information to neighboring tags by backscattering in presence of a continuous wave generated by an external excitor. The motivation of the new tag device stems from the cost and energy constraints as well as the vision of IoT, where it is anticipated that trillions of things will be equipped with simple tags and that these things can interact with each other. A real-time self-locating problem is formulated in this reader-free system and algorithms with low computational complexity are investigated.

Furthermore, a non-centralized method in a network of directional binary

sensors is investigated, where each node implements the algorithm based on its own measurement or measurements received from other nodes. The decentralized technique without a central unit use in-network processing and neighbor-to-neighbor communications. It can achieve lower energy consumption, higher robustness to node failure, and larger scalability comparing with the centralized methods.

1.4 Thesis organization

The remaining of this dissertation is organized as follows. In Chapter 2, we provide a brief overview of indoor positioning systems in the context of IoT, and in particular, the RFID systems. State-of-the-art localization and tracking methods using binary information are reviewed in Chapter 3. The particle filtering (PF)-based approach of real-time tracking of tagged objects in UHF RFID systems with asynchronous measurements are proposed in Chapter 4. In Chapter 5, the use of novel tags with ability to detect other tags is introduced in order to improve the tracking performance using only binary information, especially in areas with intersections and at portals. Furthermore, in Chapter 6, a novel reader-free system composed of tags with capability of tag-to-tag communication is proposed for the purpose of indoor positioning motivated by the cost and energy constraints. In Chapter 7, non-centralized tracking with networks of directional sensors are presented and its extension to the novel reader-free RFID system is discussed. Finally, the thesis concludes with some final remarks and future work in Chapter 8.

2

Indoor Positioning Systems in the Internet of Things

The Internet of Things (IoT) is a scenario in which uniquely identifiable physical objects or "things" observe their environment and transfer data they collect from each other, internet servers and people. The data is then analyzed and the results are used to make decisions and affect changes [6]. It was stated in the International Telecommunication Union report [7] that " A new dimension has been added to the world of information and communication technologies: from anytime, any place connectivity for anyone, we will have connectivity for anything". This vision requires ubiquitous location awareness of "anything" and hence a variety of indoor positioning systems have been proposed to complement the outdoor positioning technologies. This vision also requires tiny, simple and inexpensive individual devices with limited resources (processing capabilities, memory, and power) that are able to communicate with each other.

2.1 Indoor positioning techniques

As stated in Chapter 1, an intense research work has been carried out on wireless positioning technologies that can operate in indoor environments in recent years to achieve the indoor location awareness. In the market, companies providing outdoor map services like Google and Apple are also working on indoor positioning. Besides, many startups are also going after this market in exploring indoor positioning technologies, devices and systems [8]. These indoor positioning systems have been successfully applied in many applications such as asset tracking, inventory management and targeted mobile advertising. A variety of wireless facilities have been used for the construction of the systems such as WiFi, RFID, ZigBee, Bluetooth, UWB and Smartphones as shown in Figure 2.1 (see surveys on indoor localization systems in [1, 9] and a recent survey on indoor tracking problems in [10]).

FIGURE 2.1: The indoor positioning technologies.

Given that WiFi technology is widely deployed in many buildings, such as

museums, hospitals, airports and shopping malls, it requires no extra cost for the infrastructure of the indoor positioning system. Compared to other wireless technologies, WiFi has much higher throughput than ZigBee and each WiFi access point can cover a much wider area than Bluetooth. These advantages make WiFi a good candidate for indoor positioning. Existing work investigating the indoor positioning performance using WiFi signals can be found in [11, 12, 9]. Some of the well-known systems using WiFi are RADAR [13], Horus system [14], Herecast [15] and PlaceLab [16]. Just like other widely used wireless technologies, WiFi technology was not designed for localization and tracking purpose, and therefore the connectivity information, the RSS, or the phase measurements are exploited and the positioning accuracy could be very low. Furthermore, problems arise when the deployment of the access point is sparse and there are areas where the WiFi signals are not available. Researchers have proposed to integrate WiFi with various wireless devices such as laptops and mobile phones with embedded sensors in them such as the gyroscope and accelerometers [17, 18]. Pedestrian dead reckoning (PDR) technique [19] is applied, which determines the current position based on the previous position, step length and walking direction of the pedestrian, to assist the indoor positioning in the WiFi-blind area [20].

Unlike those built on top of existing infrastructure, RFID requires extensive deployment of infrastructure and customized tags attached to objects or people. However, with the requirements of the IoT construction and the continous development of RFID technology and smart tags, it is expected that every object will be equipped with these light and small RFID tags in the near future. Besides, the RFID technology can uniquely identify objects and persons tracked in the system, and hence provide many potential services for the demands of users.

These advantages make it superior to other wireless communication technologies for indoor positioning [21].

2.2 RFID system

RFID technology, which uses radio frequency electromagnetic fields to transfer data from a tag (usually attached to an object) with the purpose of automatic identification and tracking of the object, is seen as one of the pivotal enablers of the Internet of Things [4]. For more than a decade, the RFID technology has seen continuous technical advances combined with a decreased cost of the equipment, an increased reliability in performance, and a stable international standard, allowing us within the next years to equip virtually every object in an environment with small and cheap RFID tags [3]. Real-time identification and tracking of these tagged objects is in high demand and is important in the construction of IoT, providing the unique identity and location context to fulfill the various smart functions and the location-aware services and applications, e.g., in health care systems where RFID is applied to improve patient monitoring and safety, increase asset utilization with real-time tracking, reduce medical errors by tracking medical devices, and enhance supply-chain efficiencies [22]; in warehouses where inventory management, tracking and dispatching of goods is of paramount importance [23]; in library management where the location of books are readily obtained [24].

A RFID system usually consists of three main components: RFID tags, RFID readers, and a data processing subsystem [25].

- RFID tag: A RFID tag represents the actual data-carrying device of an RFID system, normally consists of coupling element and an electronic microchip [3]. Depending upon their operating principle, tags are classified into passive and

active patterns. An active tag has both internal power supply and an on-tag transmitter. It is able to actively send out messages (i.e., the ID of the tag) within a larger range at certain time intervals. A passive tag has no internal power source but backscatters to transmit its identification (ID) and harvests energy from the query signals from the reader. RFID systems with passive tags are more attractive due to the much lower cost.

- RFID reader: A RFID reader transmits a modulated RF signal through its antenna to the tags and receives data backscattered from the tags using a defined radio frequency and protocol. There are several different types of RFID antennas such as the dipole antenna and patch antenna. The antennas are important to the performance of a RFID system. Depending on the antenna design, the reading range can exceed 100 meters.

- Data processing subsystem: The data processing subsystem utilizes the data from the readers to execute localization and tracking algorithms and further to offer the location results to various applications.

RFID systems operate at widely different frequencies, ranging from 30 kHz to 5.8 GHz. The Ultra High Frequency (UHF) RFID systems operate in the 902–928 MHz band (North America) and they allow for detection ranges of several meters which makes them a good choice for localization and tracking [26].

2.3 Localization and tracking algorithms

There are many methods for localization and tracking. Examples include multilateration, proximity, fingerprint and Bayesian inference.

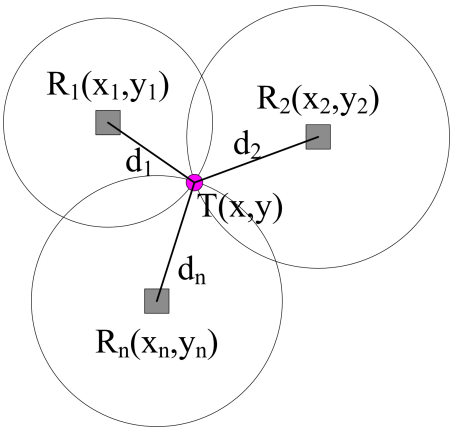

FIGURE 2.2: A multilateration positioning example.

- `Multilateration:` Multilateration estimates the coordinates of the target using the distances between the target node and at least three reference nodes with known coordinates as shown in Fig. 2.2. The location of the target is obtained by minimizing the differences between the measured distances and the estimated Euclidean distances. Assuming the estimated position of the target is $\hat{\boldsymbol{x}} = (\hat{x}, \hat{y})$, the error of the measured distance to the n-th reference node is $e_n = d_n - \sqrt{(\hat{x} - x_n)^2 + (\hat{y} - y_n)^2}$. The problem becomes an optimize problem

$$\hat{\boldsymbol{x}} = \arg\min_{\boldsymbol{x}} C(\boldsymbol{x}) \tag{2.1}$$

where $\boldsymbol{x} = [x, y]^T$ is the coordinates of the target and $C(\boldsymbol{x})$ is the cost function. Different criteria can be applied depending on the choice of $C(\boldsymbol{x})$, e.g., least squares estimation when $C(\boldsymbol{x}) = \sum_n ||e_n||^2$ and maximum likelihood estimation when $C(\boldsymbol{x}) = \sum_n \log p_E(e_n)$, where $p_E(e_n)$ is the distribution function of the measurement error. A Least Squares solution

to this problem can be found as

$$\hat{\boldsymbol{x}} = (X^T X)^{-1} X^T \boldsymbol{y}, \tag{2.2}$$

where

$$X = \begin{bmatrix} 2(x_1 - x_2) & 2(y_1 - y_2) \\ 2(x_1 - x_3) & 2(y_1 - y_3) \\ \vdots & \vdots \\ 2(x_1 - x_n) & 2(y_1 - y_n) \end{bmatrix} \quad \text{and} \quad \boldsymbol{y} = \begin{bmatrix} a - x_2^2 - y_2^2 + d_2^2 \\ a - x_3^2 - y_3^2 + d_3^2 \\ \vdots \\ a - x_n^2 - y_n^2 + d_n^2 \end{bmatrix}, \tag{2.3}$$

where $a = x_1^2 + y_1^2 - d_1^2$.

- `Proximity:` Proximity-based methods use binary information related to the presence or absence of the tag within the ranges of reader. These methods do not require any dedicated hardware or sophisticated measurement model, which makes it particularly suited for low-cost devices such as RFID tags [27]. The location of the target can be estimated by association method or the centroid method. With association method we simply estimate the target's location by equating it with that of the nearest reference node that detect the target. With centroid method, the estimated position of a tag is calculated as the central point of the positions of the reference nodes that detect the target. An extension to this method is the weighted centroid where the location is the weighted average of the candidates.

- `Fingerprint:` A fingerprint represents the characteristic or feature of signals at different positions, which is usually a RSS value in most literatures. The target location is estimated by matching the measurements with the stored fingerprints. Approaches from the theory of pattern recognition

[28] are commonly used in the fingerprint method. This method does not require a measurement model and hence they are very popular due to its simplicity. Nevertheless, it usually needs a great amount of off-line mapping information (fingerprints) and it is vulnerable to changes of the environment. Consequently, several map-free fingerprint positioning methods have been studied in recent years [9].

- `Bayesian inference:` Bayesian inference uses Bayes' rule to update the probability estimate for a hypothesis as additional evidence or observations is learned. Figure 2.3 (a) shows the principle for localizing a stationary tag by Bayesian inference, where $\boldsymbol{x} = [x_1, x_2]$ are the coordinates of the tag, and $y_i, i = 1, \cdots, N$ are a series of observations by N readers. We assume that given $\boldsymbol{x}$, the probabilities of y_i are independent of each other, and thus the system satisfies the Markovian condition. According to Bayes' rule, the position of the target can be obtained by the recursive equation

$$f(\boldsymbol{x}|y_1, y_2, \cdots, y_N) \quad \propto \quad f(y_N|\boldsymbol{x}) f(\boldsymbol{x}|y_1, y_2, \cdots, y_{N-1}) \tag{2.4}$$

The Bayesian network for tracking a moving tag is shown in Fig. 2.3 (b) and the Bayesian update in equation (2.4) can be computed as

$$\begin{aligned} f(\boldsymbol{x}_{t_k}|\boldsymbol{y}_{t_1}, \boldsymbol{y}_{t_2}, \cdots, \boldsymbol{y}_{t_k}) \quad \propto \quad & f(\boldsymbol{y}_{t_k}|\boldsymbol{x}_{t_k}) \\ & \times \int f(\boldsymbol{x}_{t_k}|\boldsymbol{x}_{t_{k-1}}) f(\boldsymbol{x}_{t_{k-1}}|\boldsymbol{y}_{t_1}, \boldsymbol{y}_{t_2}, \cdots, \boldsymbol{y}_{t_{k-1}}) d\boldsymbol{x}_{t_{k-1}}, \end{aligned} \tag{2.5}$$

where $\boldsymbol{y}_{t_k} = [y_{1,t_k}, y_{2,t_k}, \cdots, y_{N,t_k}]$, N is the number of reference nodes and t_k is the time instant. Depending on the application environment, Kalman Filters, Particle Filters and some other techniques can be used to represent

the density function and then to estimate the location by the Bayesian recursion [29].

Once the posterior distribution $f(\boldsymbol{x}_{t_k}|\boldsymbol{y}_{1:t_k})$ is obtained, the estimate of the state $\boldsymbol{x}_{t_k}$ can be computed using different criteria, i.e., the minumum mean-square error (MMSE) and the maximum a posteriori (MAP), in which the respective point estimates are given by

$$\hat{\boldsymbol{x}}_{t_k}^{MMSE} = \int \boldsymbol{x}_{t_k} f(\boldsymbol{x}_{t_k}|\boldsymbol{y}_{t_1:t_k}) d\boldsymbol{x}_{t_k} \tag{2.6}$$

$$\hat{\boldsymbol{x}}_{t_k}^{MAP} = \arg\max_{\boldsymbol{x}_{t_k}} f(\boldsymbol{x}_{t_k}|\boldsymbol{y}_{t_1:t_k}). \tag{2.7}$$

Among all the localization and tracking techniques, each approach has its own strengths and weaknesses. For instance, Bayesian inference can update the location dynamically and it usually requires less reference nodes, but it has a relatively high

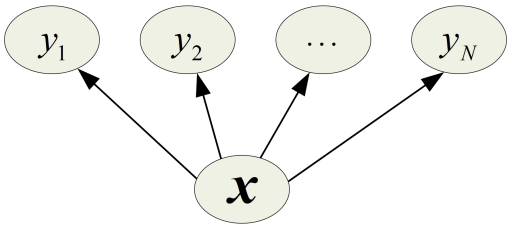

(a) For stationary localization

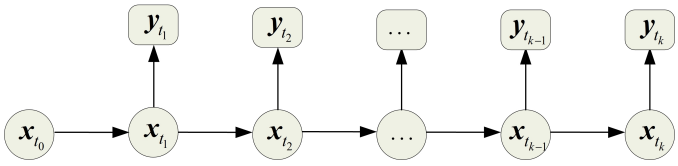

(b) For dynamic tracking

FIGURE 2.3: Bayesian network for localization and tracking problems.

computational complexity. The multilateration method requires less computation effort, but it is based on the signal propagation model, which is very vulnerable due to the indoor environment. The proximity method also requires less computation but it heavily relies on the placement and the density of the reference nodes. Integration of two or more algorithms may bring benefits such as improvement on accuracy and reduction of computation time.

2.4 State-of-art

Existing approaches to RFID localization and tracking vary and depend on the used of sensor information, the assumed models, and the implemented inference algorithms [30]. Regarding sensor information, research has been done on systems based on received signal strength (RSS) [31, 32, 33], tag detection events [34, 35, 36], direction-of-arrival (DOA) measurements [37] and measured phases of received signals from the tags [38, 39]. A model that merges RSS information with tag detection was proposed in [40]. With this model, a better accuracy was achieved in comparison to that of models that use either RSS or tag detection events. It was also reported that the RSS model alone was consistently less accurate than the tag detection model, which is primarily due to the difficulty in modeling superpositions of RF signals and as a result, the RSS in indoor environments.

The modeling problem of RFID signals has been addressed by various research groups. In [41], the model was learned by generating statistics related to the frequency of detection given different relative positions between the antenna and the tag. In [42], a probabilistic RFID model was obtained in a semi-autonomous fashion with a mobile robot. A method for bootstrapping the sensor model in a fully unsupervised manner was presented in [40]. In [43] for modeling the RFID

system, the authors used fuzzy set theory instead of probabilistic approaches.

The inference algorithms can be categorized into multilateration [33, 33], Bayesian inference [40, 38], k-nearest neighbor [31, 44], proximity [45, 46], and kernel-based learning methods [47]. For calculation of the location of an unknown tag, LANDMARC adopted the k-nearest neighbor algorithm, where distance was measured using the RSS received by the readers between the tag and a reference tag [31]. Instead of an offline RF fingerprint database search, [33] applied an adaptive Kalman filter and probabilistic map matching to minimize the effect of the measurement noises on distance estimation. The locations of the unknown tags were obtained using multilateration with respect to the RFID landmarks. A UHF RFID tracking system that exploits measured phases of the backscattered signals from RFID tags using multiple spatially distributed antennas and implements extended Kalman filtering was presented in [38].

2.5 Challenges

There are several practical issues when considering the localization and tracking problems in indoor environment [48]:

- `Multipath:` Multipath is the radio propagation phenomenon that results in radio signals reaching the receiving antenna by two or more paths. Severe multipath occurs indoors since the reflection, refraction, diffraction and absorption of radio signals are caused by the walls, furniture, objects and humans.

  In real environments, the RSS collected at node sites results from the signal summation of all the paths, and therefore easily varies. Hence, the

localization/tracking performance degrades for those approaches that are based on RSS. This issue affects not only RFID-based localization, but all RF-based localization in indoor scenarios.

- `Interference:` Interference occurs when unwanted signals alter, modify or disrupt the signal of interest and this phenomenon naturally presents a challenge to RFID localization/tracking. Again, for those positioning schemes based on RSS information, the deviation of RSS results in positioning errors.

- `Dense objects:` Localization of multiple objects constitutes a major challenge only for RFID systems, but also for many RF-based technologies. The RF signals are much more easily influenced when there are a large number of objects being tracked at the same time, and hence the localization/tracking accuracy abruptly suffers. One solution to this issue is to have the objects sparsely distributed, however, this is rather unpractical. A feasible solution with the assist of a novel tag device is investigated in this dissertation.

- `Cost and power constraints:` There is always a tradeoff between the positioning accuracy and the coverage (the number of reference nodes to be deployed) in any indoor positioning system due to the constraints of the infrastructure cost. Furthermore, the vision for ubiquitous location awareness requires positioning using tiny, simple and low-cost individual devices. These devices usually come with limited sources such as processing capabilities, memory, and power. No dedicated hardware and time synchronization is applicable for the device, which indicates that the

positioning algorithms must be able to deal with the asynchronous and unsophisticated measurements with low-computational complexity.

3

Overview of Positioning Using Binary Information

As stated along Chapter 2 of the challenges in indoor positioning systems, the severe multipath propagation and interference from unwanted signals render the inapplicability of the commonly-used RSS. Instead, we seek for solutions using binary information. Binary information indicates whether a device is present or absent within a predefined area. The methodology of positioning using binary information can be found in a wide literature and it can be categorized into proximity-based, connectivity-based and detection-event driven methods.

3.1 Proximity-based

Proximity-based method makes use of the binary information with respect to the nearby reference node with known positions. The location of the target can be estimated by the association method or the centroid method. With association method we simply estimate the target's location by equating it with that of the nearest reference node which detects the target. Figure 3.1 shows an example of

the proximity-based positioning method using association, where the location of the person is estimated using that of the central antenna which detects him. With centroid method, the estimated position of the target $\hat{\boldsymbol{x}} = [\hat{x}, \hat{y}]$, is calculated as the central point of the positions of N reference nodes with most reliable communication link quality which sensed the target.

$$\hat{\boldsymbol{x}} = \sum_{i=1}^{N} \boldsymbol{l}_i / N, \tag{3.1}$$

where $\boldsymbol{l}_i$ is the coordinates of the reference node i.

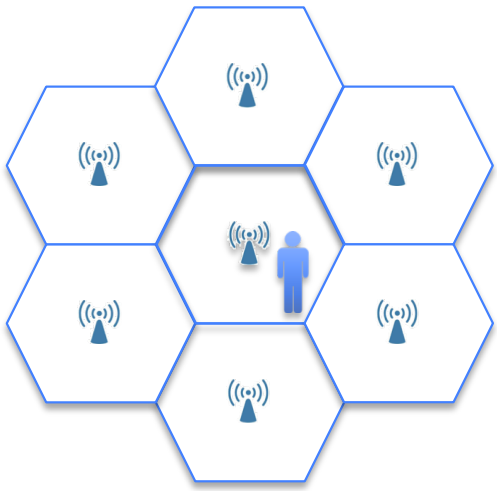

FIGURE 3.1: An example of proximity.

An extension to this method is the weighted centroid where the location is the weighted average of the candidates. The weights can be obtained using extra information such as RSS [31], hop count [49], or the number of detections [50].

APIT [51] (Approximate Point in Triangulation) algorithm is also a distance-free localization algorithm using binary information. The principle of APIT is to estimate the target location by segmenting the area into a large number of

triangular regions with different sets of three reference nodes. A test is performed to determine whether the target is in the triangle composed by every three reference nodes based on geometry. If there exists an adjacent point to the target which is further or closer to the three reference nodes simultaneously, the target is outside the triangle. Otherwise, the target is claimed to be inside the triangle and the count of this area (initialized by 0) is increased by 1. For example, the point A is closer than the target T to the points O, M, N respectively as shown in Figure 3.2. Then we know that T is outside $\triangle$OMN. The target location is estimated as the centroid of the area which has the maximum count, representing the overlapping area of all these non-zero triangles. For example, the overlap area is $\triangle$ABC in Figure 3.2 and the location of T is estimated as the centroid of $\triangle$ABC. It is shown that the scheme performs best when an irregular radio pattern and random node placement are considered. However, extra information such as RSS is needed for the test of the geometry.

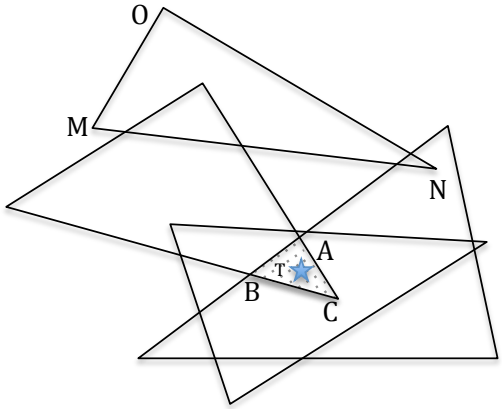

FIGURE 3.2: An illustration of the APIT algorithm.

Note that the accuracy of proximity-based method greatly relies on the deployment of the reference nodes (the density, the pattern, the sensing ranges,

etc.). The work in [52] provides the fundamental performance limits of localizing a target in a J-dimensional ($J \in \{1, 2, 3\}$) space using only binary proximity information. It was shown that the localization error at any point is of order $\frac{1}{\rho R^{J-1}}$, where ρ is the node density per unit area and R is the sensing range.

Besides, the scalability of the system using proximity is limited due to the requirement of a large deployment of the nodes. However, the key advantage of the proximity-based method is that it is suited for very low-cost devices such as RFID tags where the deployment of a large number of tags is not an issue [27]. It also has the advantages of low communication and computation overhead.

3.2 Connectivity-based

Connectivity-based method uses the sensed binary information from the local neighborhood to build hop-based virtual distances for localization [53] and it is also suited for low-cost devices. Figure 3.3 shows a graph of connectivity of a network. The red nodes represent the reference nodes with known positions and the yellow nodes represent the target nodes with unknown positions. The edge represents the radio link between two nodes indicating that these two nodes are within the communicating range of each other. The objective is to localize the yellow nodes with the location information of red nodes and the connectivity of the network.

In [54], a sensor network position estimation problem is formulated as a linear or semidefinite program, which is based on connectivity between nodes. Feasible solutions are described to the problem using convex optimization. Additionally, a method for placing rectangular bounds around the possible positions for the unknown nodes is given. However, this method requires centralized computation.

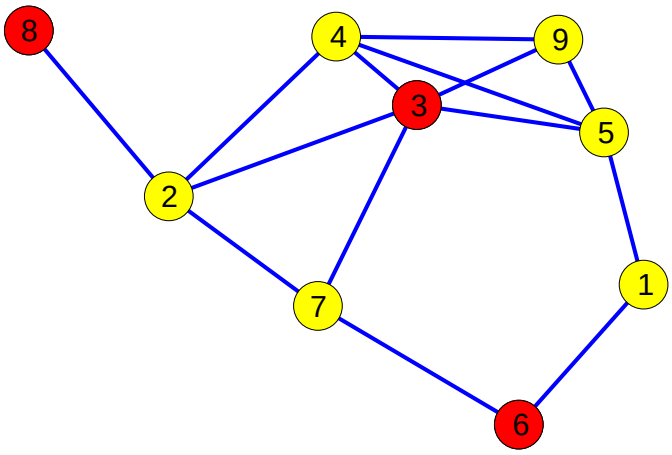

FIGURE 3.3: Graph of connectivity of a general network.

Similar work on localization from connectivity can be found in [53].

Compared to the proximity-based method, the connectivity-based method can provide better scalability at a cost of more communication and computation overhead and extra efforts for topology recognition.

3.3 Detection-event-driven

In detection-event-driven method, localization and tracking can be accomplished by analyzing simple event detections at low-cost devices. The detection model can be a simple disk model where the detection range is described by a circle with a fixed radius, a ring model where the uncertainty of detection occurs at a range larger than a certain threshold [52], or a probabilistic model where the probability of detection is modeled as a function of distance depending on the nature of the sensing devices/nodes [55, 56]. A detailed description of this method based on probabilistic model will be presented in Chapter 4.

3.4 Remarks

Note that the localization and tracking using binary information can be either centralized, where the information sensed by the nodes is transmitted to a fusion center, or non-centralized, where the information is processed locally by the nodes with some cooperative methods. The interest in distributed processing stems from the requirement of low energy consumption, high robust to node failure and scalability. Besides, the development of simple low-cost devices with device-to-device communication for the construction of IoT greatly promotes the implementation of distributed processing in wide applications.

A variety of analytical results are presented in [57] to aid in the design of localization and tracking systems based on not only the binary or the proximity measurements between sensors, but also the RSS or the quantized RSS received by the sensors. The Cramér-Rao bound is computed to compare the minimal attainable variances of unbiased location estimators for different cases. The results show that lower bounds for standard deviation in proximity-based systems are about 50% higher than the bounds for RSS-based systems. It is also shown that a system with just 3 bits of quantization can be enough in cases.

One final remark is that most of existing techniques are based on using location information provided by a set of reference nodes which are aware of their exact locations. The location uncertainty of the reference nodes is considered in the localization problem in [58].

4

Indoor Tracking Using Aggregated Binary Readings with RFID Systems

We address the problem of indoor tracking of tagged objects with Ultra High Frequency (UHF) Radio Frequency Identification (RFID) systems. A new and more realistic observation model of the system is proposed, where the probability of detecting a tag by a reader is described by a Beta distribution. We model the probability of detection as a function of both the distance and the angle between the tag and the reader. The considered model also accounts for the possibility of a tag being in a dead-zone, that is, in a space where the tag cannot be detected even if it is well within the range of a reader. For tracking, we propose the use of the particle filtering methodology that takes into account the asynchronous nature of the measurements. The needed parameters for modeling the system are obtained from laboratory experiments and the performance of the algorithm is shown by extensive computer simulations. The mathematical formulation of the problem is presented in Section 4.2. The new model is described in Section 4.3. The PF

method for tracking the targeted tags is introduced in Section 4.4. In Section 4.5, we provide simulation results that demonstrate the performance of the method. This chapter concludes with some final remarks in Section 4.6.

4.1 Introduction

RFID is a technology for transferring of data from a tag attached to an object with the purpose of its automatic identification and tracking. In this chapter the interest is in the use of UHF RFID systems for indoor tracking of objects with attached passive tags and based on aggregated binary measurements.

An important application of the RFID technology is accurate real time tracking of tagged objects in indoor environments. This remains a very challenging problem due to a number of reasons including missed detections in existing systems. An important class of approaches to localization and tracking of tagged objects is distance-based and relies on measurements that are either received signal strength (RSS), time-of-arrival (TOA), or time-difference-of-arrival (TDOA). The main difficulty of these approaches is the quality of the measurements, which are often distorted due to multipath and other interferences existing in indoor environments [48].

Some recent efforts on real time tracking in indoor environments include [59] and [38]. In [59], the authors use the RFID system to estimate the trajectory of a robot by using passive UHF RFID measurements. There, the tracking is "reader-based" meaning that the RFID tags are placed at fixed, known locations, and the mobile object has a portable reader [48]. In [38], the authors present a UHF RFID location tracking system that exploits the measured phases of the backscattered signals from RFID tags using multiple spatially distributed antennas, and they

implement the tracking by extended Kalman filtering.

In this chapter, the tracking of the tagged objects is performed by particle filtering [60]. This is a methodology that is applied to nonlinear problems with possibly non-Gaussian noises. The main objective of particle filtering is to track distributions of unknowns, which in our case are the posterior distributions of the locations and velocities of the tagged objects. This is achieved by propagating a set of particles of the possible values of the unknowns and associating with them weights, thereby obtaining random measures that approximate the desired distributions. There, the sensors transmit ID signals to a central unit only if the target is in their proximity. The nature of the problem of real time tracking of tagged objects in RFID systems allows for the use of as many particle filters as there are tags in the system. This is due to the fact that the source of the signal (backscattered by the tag) is clearly known to the readers. Thus, each tagged object is tracked by a dedicated particle filter, and all the particle filters used in the system operate independently.

We have studied the problem of indoor UHF RFID tag tracking based on aggregated binary measurements [61], [62], where we introduced a model for the probability of reading a tag that was a function of the distance from the tag to the reader [61]. The model was later extended to include variability of the probability of detecting a tag [62]. In this chapter, we expand this model and make it more realistic by (a) modeling the probability of detection also as a function of the angle between the tag and the reader's antenna and by (b) integrating into the model the probability of a tag being in a dead-zone. Dead zones are common in indoor tracking due to various factors including ground reflections or obstacles [63].

Tag responses are received by the readers following a standard protocol. A

reader makes a fixed number of queries whose overall duration can vary depending on the number of tags in its proximity, the forward link symbol timing parameters, the backscatter link frequency, and the backscatter encoding scheme [64]. This entails that the overall observation model has to capture this asynchronicity. We propose a tracking algorithm that accounts for it and we implement it by PF [65, 66]. Some work dealing with asynchronous measurements in traditional sensor networks can be found in [67, 68].

4.2 Problem formulation

Consider the problem of tracking objects with attached RFID tags that move in an area covered by a mesh grid of L RFID readers whose antennas have known locations. The RFID antennas are deployed as shown in Fig. 4.1 so that they provide full coverage. The nodes in the corners of the grid have only one antenna, the ones on the edges that are not corners have two, and all other nodes have three antennas. The RFID readers are located in the middle of each cell of the grid and are connected to three or four antennas depending on the deployment of the antennas. We note that each antenna is controlled by one reader. For example, reader R_6 has three antennas located at nodes 7, 8, and 12, while reader R_{14} is connected to four antennas located at nodes 17, 18, 22, and 23. The antennas at each node are connected to the nearby readers, e.g., node 8 has three antennas denoted by the right (red), the upper left (green), and the lower left (blue) sectors, where the red one is connected to reader R_7, the green one to R_3, and the blue one to R_6. The arrows indicate the orientation of the antennas.

The state of the system consists of a vector containing information about a

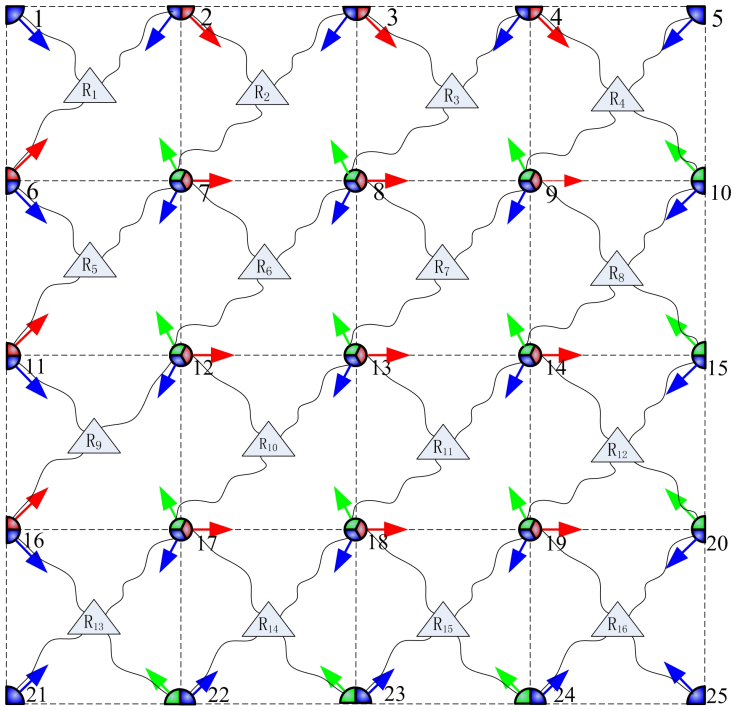

FIGURE 4.1: Deployment of the RFID readers (denoted by triangles) in the middle of the cells and antennas (denoted by sectors) in the nodes of the mesh grid. The curved lines represent the cables connecting the antennas and readers, and the arrows indicate the directionalities of the antennas.

particular tag[1] in the area of coverage at time instant t, and it is denoted by $x_t \in \mathbb{R}^{4\times 1}$, where $x_t = [x_{1,t}\ x_{2,t}\ \dot{x}_{1,t}\ \dot{x}_{2,t}]^\top$ and $t \in \mathbb{R}^+$. The first two elements of the vector denote the location of the tag in the two-dimensional Cartesian coordinate system at time instant t, and the other two elements are the components of the velocity. The tagged object moves according to the model [69]

$$\boldsymbol{x}_{t_2} \quad = \quad \boldsymbol{A}(t_1, t_2)\boldsymbol{x}_{t_1} + \boldsymbol{B}(t_1, t_2)\boldsymbol{v}_{t_2}, \tag{4.1}$$

where $\boldsymbol{x}_{t_2}$ is the state of the system at time instant t_2, and $\boldsymbol{v}_{t_2} \in \mathbb{R}^{2\times 1}$ is a noise

[1] We note that in RFID systems the tasks of tracking different tags are statistically independent, and therefore we only address the tracking of one tag.

vector with known distribution. Let $\Delta\tau \triangleq (t_2 - t_1)$ be the time period from t_1 to t_2, and $\boldsymbol{A}(t_1, t_2) \in \mathbb{R}^{4\times4}$ and $\boldsymbol{B}(t_1, t_2) \in \mathbb{R}^{4\times2}$ be the known transition and covariance matrices, respectively, given by

$$\boldsymbol{A} = \begin{pmatrix} 1 & 0 & \Delta\tau & 0 \\ 0 & 1 & 0 & \Delta\tau \\ 0 & 0 & 1 & 0 \\ 0 & 0 & 0 & 1 \end{pmatrix} \quad \text{and} \quad \boldsymbol{B} = \begin{pmatrix} \frac{\Delta\tau^2}{2} & 0 \\ 0 & \frac{\Delta\tau^2}{2} \\ \Delta\tau & 0 \\ 0 & \Delta\tau \end{pmatrix}.$$

Next we describe the system of readers that we use in the simulations and explain the difference between synchronous and asynchronous measurements. All the readers start their rounds of queries and complete them at different time instants due to various factors such as the number of tags in their proximity, the frequency of the backscatter link and the scheme of backscatter encoding. The readers repeat the rounds periodically. Note that the readers may start their rounds of queries at different time instants, however, for ease of explanation and for comparison purposes, we assume that all the readers start their rounds at the same time instant $(k-1)T_s$, where T_s is the intended sampling interval and $k = 1, 2, \cdots, T$. It is also assumed that the durations of the rounds are always shorter than T_s. More specifically, during the time interval between two time instants, $(k-1)T_s$ and kT_s, each RFID reader sends N queries with the purpose of detecting the tags in its area of coverage. Each observation represents the number of responses out of N trials that each reader gets. In a fictitious (ideal) synchronous system, all the observations are obtained by the readers at the sampling instants as shown in Fig. 6.2 (a). However, in real systems, the responses are obtained asynchronously. In the wide literature, the asynchronism of the readers is ignored and the general assumption is that all the observations are obtained by the readers

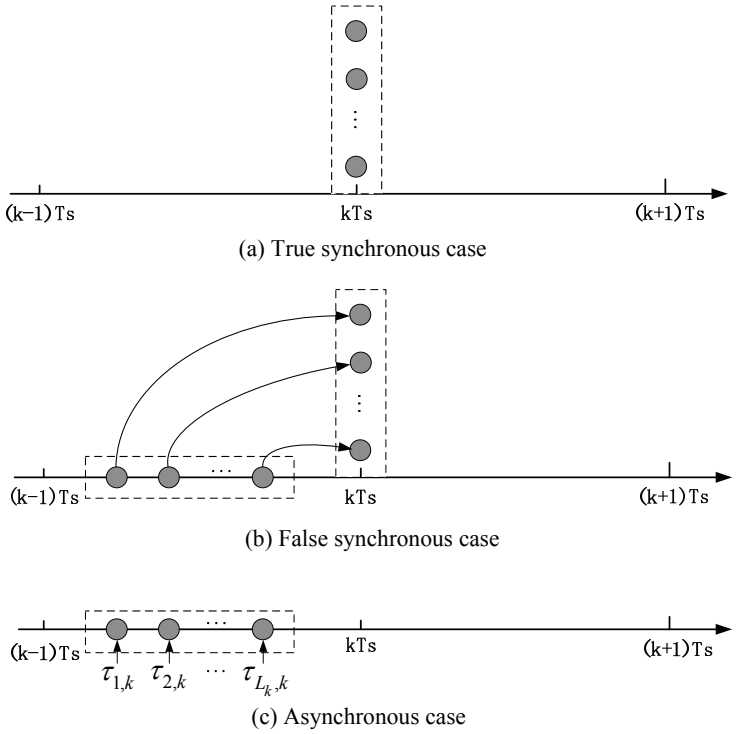

FIGURE 4.2: Synchronous vs. asynchronous measurements.

synchronously at the sampling instants as shown in Fig. 6.2 (b).

We denote the lth measurement in the kth round by $\boldsymbol{y}_{l,k} = \{\tau_{l,k}, i_{l,k}, n_{l,j,k} : j \in \{1,2,3,4\}, l \in \{1,2,\cdots,L_k\}, k \in \mathbb{N}^+\}$ where $\tau_{l,k}$ is the time instant of the lth measurements in the kth round, $i_{l,k} \in \{1,2,\cdots,L\}$ is the index of the reader that detected the tag, and $n_{l,j,k} \leqslant N$ is the number of received responses by reader $i_{l,k}$ with its jth antenna. We note that $\tau_{1,k} \leqslant \tau_{2,k} \leqslant \cdots \leqslant \tau_{L_k,k}$ with $L_k \leqslant L$ being the total number of readers that detected the tag. Our approach accounts for asynchronous measurements where the instants $\tau_{l,k}$ are assumed known (Fig. 6.2 (c)).

The readings collected for a particular tag until time instant kT_s are gathered in the observation set $\mathcal{Y}_{kT_s} = \{\boldsymbol{y}_{T_s}, \boldsymbol{y}_{2T_s}, \cdots, \boldsymbol{y}_{kT_s}\}$, where $\boldsymbol{y}_{kT_s} =$

$\{\boldsymbol{y}_{1,k}, \boldsymbol{y}_{2,k}, \cdots, \boldsymbol{y}_{L_k,k}\}$. The observations from each antenna in the system are assumed independent of each other. The objective is to track $\boldsymbol{x}_t$ in time given the observations and the assumed state-space model. A key component of the tracking is the model of the observations $\boldsymbol{y}_{kT_s}$. It is discussed in the next section.

4.3 The observation model and its evaluation

The observation model constitutes one of the major challenges when tracking with RFID systems, especially in indoor environments, since the number of detections of a reader in a set of queries depends on numerous factors including the distance from the antenna, the orientation of the antenna, and the multipath created by the indoor environment [48].

4.3.1 The observation model

In this section, a more realistic observation model is proposed. First, the probability of detection is modeled as a function of both the distance and angle from the tag to the reader. Then, we add to this model a mathematical representation that accounts for a tag being in a dead-zone. We refer to the proposed model that uses distance and angle as to DA-based model and the one considering distance only as D-based model, which is from previous work [62].

Figure 4.3 shows the distance, d, and the angle, θ, between a tag and an antenna located at points G and H in the global reference coordinate system u_1Ou_2, respectively. The angle, θ, represents the relative orientation between the antenna and the tag within a range of $(-\pi/2, \pi/2]$ rads, whereas d is the distance between G and H. Note that the location of the antenna is known, and it is denoted by $(l_{H,1}, l_{H,2})$.

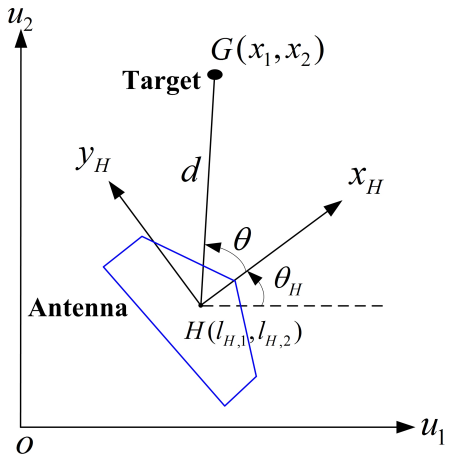

FIGURE 4.3: Representation of the distance and the angle between an antenna and a tag.

In order to simplify the expression of the observation function, we convert the Cartesian coordinates of the states $x_{1,t}$ and $x_{2,t}$ into polar coordinates d_t and θ_t, where d_t and θ_t are the distance and angle from the tag to the antenna at time instant t, respectively. The relationship between the Cartesian coordinates and the polar coordinates is given by

$$\begin{aligned} d_t &= \sqrt{(x_{1,t} - l_{H,1})^2 + (x_{2,t} - l_{H,2})^2}, \\ \theta_t &= \arctan((x_{2,t} - l_{H,1})/(x_{1,t} - l_{H,2})), \end{aligned} \tag{4.2}$$

where $l_{H,1}$ and $l_{H,2}$ are the Cartesian coordinates of the location of the antenna H.

For a given distance d and angle θ between the tag and the antenna (here we omit the subscript t for simplicity), the probability of the tag being detected by the associated reader is modeled as a random variable, $p(d, \theta)$, with a Beta distribution whose parameters are $\alpha(d, \theta) > 0$ and $\beta(d, \theta) > 0$, i.e., $Beta(\alpha(d, \theta), \beta(d, \theta))$, or

$$\pi(p(d, \theta)) \propto p(d, \theta)^{\alpha(d,\theta)-1}(1 - p(d, \theta))^{\beta(d,\theta)-1}. \tag{4.3}$$

We note that the choice of modeling probabilities with Beta distributions is common due to their flexibility in approximating posteriors on the interval [0,1] [70]. Furthermore, the Beta distribution is the conjugate prior of the binomial distribution, which allows for mathematical tractability [71].

The mean of the probability of detection of a tag at a distance d from the reader is assumed to have the form of a logistic regression given by

$$\mathbb{E}(p(d,\theta)) \quad = \quad \frac{1}{1+e^{(a_1+a_2d+a_3|\theta|)}}, \tag{4.4}$$

where a_1, a_2, and a_3 are the parameters of the model. The logistic regression and the polynomial in the exponent can capture the change in decay of probability as a function of both distance and angle and the logistic regression has a range $[0,1]$. This model reflects the nature of measurements from real-world experiments. Since the mean of a Beta random variable is given by $\alpha(d,\theta)/(\alpha(d,\theta)+\beta(d,\theta))$, one can write

$$\frac{\alpha(d,\theta)}{\alpha(d,\theta)+\beta(d,\theta)} \quad = \quad \frac{1}{1+e^{(a_1+a_2d+a_3|\theta|)}}. \tag{4.5}$$

In addition, the variance of the probability of detection of a tag at a distance d from the reader is assumed to have the form

$$\sigma^2(d,\theta) \quad = \quad c_1+c_2d+c_3d^2+c_4|\theta|+c_5\theta^2, \tag{4.6}$$

where $c_i, i = 1,\cdots,5$ is another set of parameters of the model. Modeling the variance with a polynomial comes as a result of a Taylor expansion of the variance as a function of distance and magnitude of the angle. The variance of a Beta random variable is given by $\alpha(d,\theta)\beta(d,\theta)/((\alpha(d,\theta)+\beta(d,\theta))^2(\alpha(d,\theta)+\beta(d,\theta)+1))$

[70], and therefore we write

$$\frac{\alpha(d,\theta)\beta(d,\theta)}{(\alpha(d,\theta)+\beta(d,\theta))^2(\alpha(d,\theta)+\beta(d,\theta)+1)} = c_1 + c_2 d + c_3 d^2 + c_4|\theta| + c_5\theta^2 \quad (4.7)$$

The parameters $\alpha(d,\theta)$ and $\beta(d,\theta)$ of the Beta distribution can be uniquely obtained by solving (4.5) and (4.7) for each pair of d and θ.

The previous model can be further extended and made more realistic by introducing the event that a tag can be in a dead-zone in the proximity of a reader. The probability of this event is defined as the probability that a tag is not detectable by an antenna given that the tag is in the field of view of the antenna.[2] Therefore, tags which are in a dead-zone will not be detected even though based on their proximity to the antenna one expects they should be detected. We denote this probability with λ, where $\lambda \sim Beta(\alpha_\lambda, \beta_\lambda)$. Then, the overall probability of detection becomes $(1-\lambda)p(d,\theta)$.

When the object is at a distance d and an angle θ from the reader as well as outside a dead-zone, the number of times that it is read by the reader in a set of N queries is modeled by a binomial distribution, that is, the probability that the number of reads is n is given by

$$P(n|p) = \binom{N}{n} p(d,\theta)^n (1-p(d,\theta))^{N-n}. \quad (4.8)$$

Here we note that we use the approximation that during the execution of a set of N queries the tag has not moved. Since $p(d,\theta)$ is random, the probability of the number of reads n should be obtained by averaging over all random $p(d,\theta)$ values

[2] Collision of tags is another event that prevents the reading of tags when they are in the field of view. For simplicity, in this chapter, we assume that the event of a collision is an event of a tag being in a dead-zone.

using the Beta distribution in (4.3). The number of reads n in a dead-zone is 0. Then for $P(n|d,\theta)$ we can write

$$P(n|d,\theta,\lambda) = \int_0^1 P(n|p)(1-\lambda)\pi(p)dp + \lambda\delta(n)$$

$$= (1-\lambda)\binom{N}{n}\frac{B(n+\alpha(d,\theta), N-n+\beta(d,\theta))}{B(\alpha(d,\theta),\beta(d,\theta))} + \lambda\delta(n), \tag{4.9}$$

where p represents $p(d,\theta)$ for simplicity, $\delta(n)$ is the Dirac impulse function, and $B(\cdot,\cdot)$ is the Beta function, that is,

$$B(a,b) = \int_0^1 u^{a-1}(1-u)^{b-1}du = \frac{(a-1)!(b-1)!}{(a+b-1)!}, \tag{4.10}$$

with a and b being integers. We then average over all λ as follows:

$$P(n|d,\theta) = \int_0^1 (1-\lambda)\binom{N}{n}\frac{B(n+\alpha(d,\theta), N-n+\beta(d,\theta))}{B(\alpha(d,\theta),\beta(d,\theta))}$$

$$\times\frac{\lambda^{(\alpha_\lambda-1)}(1-\lambda)^{(\beta_\lambda-1)}}{B(\alpha_\lambda,\beta_\lambda)}d\lambda + \int_0^1 \lambda\delta(n)\frac{\lambda^{(\alpha_\lambda-1)}(1-\lambda)^{(\beta_\lambda-1)}}{B(\alpha_\lambda,\beta_\lambda)}d\lambda$$

$$= \frac{\beta_\lambda}{\alpha_\lambda+\beta_\lambda}\binom{N}{n}\frac{B(n+\alpha(d,\theta), N-n+\beta(d,\theta))}{B(\alpha(d,\theta),\beta(d,\theta))} + \frac{\alpha_\lambda}{\alpha_\lambda+\beta_\lambda}\delta(n). \tag{4.11}$$

This is the key function of the tracking algorithm. It is defined by the parameters α_λ, β_λ, $\alpha(d,\theta)$, and $\beta(d,\theta)$. These parameters can be obtained from experiments where we vary the distance of a tag from an antenna and its angle with respect to it. As already pointed out in the previous section, to that end we use (5.3) – (4.7).

4.3.2 Evaluation of the observation model

In this section we justify the observation model by presenting data from real-world experiments. In the experiments, we used Smartrac UHF Spine RFID tags and an Impinj Speedway revolution Reader, which was connected to a single 6 dBIC gain patch antenna. Both the reader and the tags were compliant with the ISO 18000-6C (EPC Gen 2) protocol [64]. The tags were placed in an orientation facing the reader at various distances from the reader's antenna whose power level was set to 27 dBm. The reader was programmed to send out 50 queries. We measured the probability of detection as a ratio of the number of times a tag was read over the total number of queries. We also changed the orientation of the antenna so that we could obtain the probability of detection for different sets of (d, θ). For each d and θ we repeated the experiment 10 times. For each distance, we had 13 different angles, and there were 18 distances. We conducted the experiment twice in two different locations.

We modeled the mean of probability of detection according to (5.3) and applied least squares fitting to estimate the unknown parameters. The estimated values were $\widehat{a}_1 = -3.2699$, $\widehat{a}_2 = 0.4931$ and $\widehat{a}_3 = 0.0438$. The mean of the probability of detection as a function of distance and angle with the estimated parameters is shown in Fig. 4.4 (a). Similarly, we fitted the variance of the probability of detection using the function in (4.6). The obtained parameters of the model were $\widehat{c}_1 = 0.0448$, $\widehat{c}_2 = 0.0057$, $\widehat{c}_3 = -0.0011$, $\widehat{c}_4 = 0.0004$, and $\widehat{c}_5 = 0$. The plot of the resulting variance is shown in Fig. 4.4 (b). Note that the variance is clipped to zero when the distance is greater than 10 m.

We compared the proposed model in (5.3) with the model from our previous

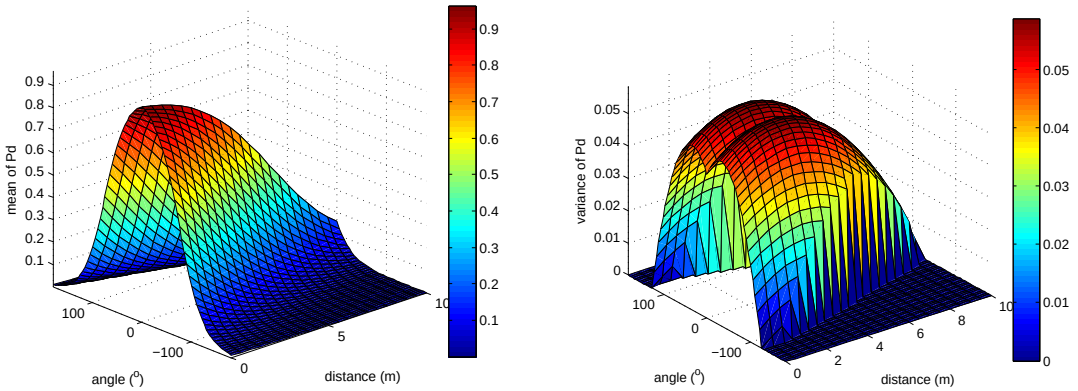

(a) (b)

FIGURE 4.4: Fitting of the mean and the variance of the probability of detection $p(d, \theta)$ of the proposed model (also referred to as the DA-based model).

work [62], where the probability of detection is a function of distance only in a specified field and is defined by

$$\mathbb{E}(\tilde{p}(d)) = \frac{I_{ij}(d)}{1 + e^{(\tilde{a}_1 + \tilde{a}_2 d)}}, \tag{4.12}$$

where $\tilde{a}_1$ and $\tilde{a}_2$ are the parameters of the model and $I_{ij}(d)$ is an indicator function defined by

$$I_{ij}(d) = \begin{cases} 1, & d \in \mathcal{R}_{ij} \\ 0, & \text{otherwise}, \end{cases} \tag{4.13}$$

with $\mathcal{R}_{ij}$ being the field of view of the jth antenna of the ith reader.

The variances of the data for this model were fitted with a quadratic function. The fitting results of the mean and the variance are displayed in Fig. 4.5. It appears that the mean of the D-based model fits the means obtained from raw data at given distances relatively well. However, the figure of the variance is much less convincing and it shows that the variability of the probability is high, which has

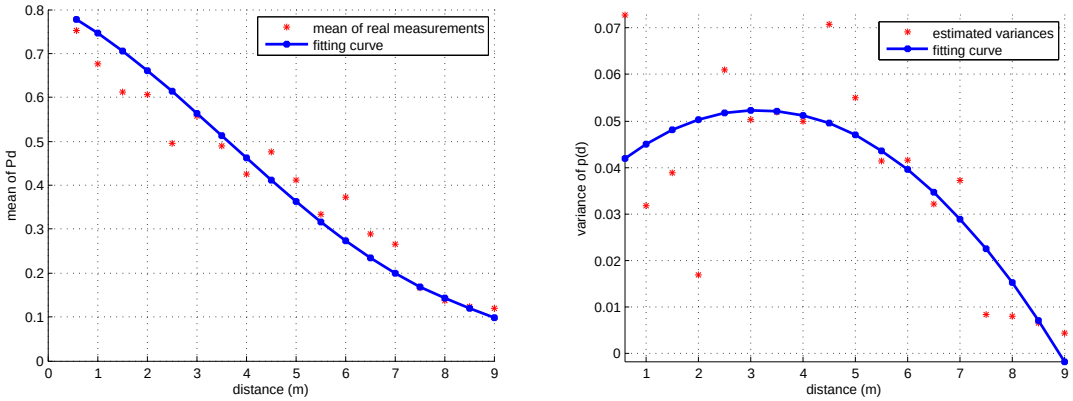

(a) (b)

FIGURE 4.5: Fitting of the mean and the variance of the probability of detection $p(d)$ as a function of distance for the distance-only model (also referred to as the D-based model).

been the motivation to include the angle as an additional parameter for modeling the probability of detection.

It was shown in our previous work that the probability of number of reads n for the D-based model is given by

$$\tilde{P}(n|d) = \binom{N}{n} \frac{B(n + \tilde{\alpha}(d), N - n + \tilde{\beta}(d))}{B(\tilde{\alpha}(d), \tilde{\beta}(d))}, \tag{4.14}$$

whereas the analogous expression for the DA-based model is (5.4). Figure 4.6 shows the probability of detection computed by these two models at different fixed distances and the obtained mean from real measurements at $d = 3$ m (represented by the red asterisks). Since the D-based model does not consider the angle as a parameter, we get a constant for the probability of detection over the range of angles, whereas the DA-based model shows how this probability decreases with the increase of angle as it should. We can see from Fig. 6 that the DA-based model with an angular component fits the real measurements well at a fixed distance

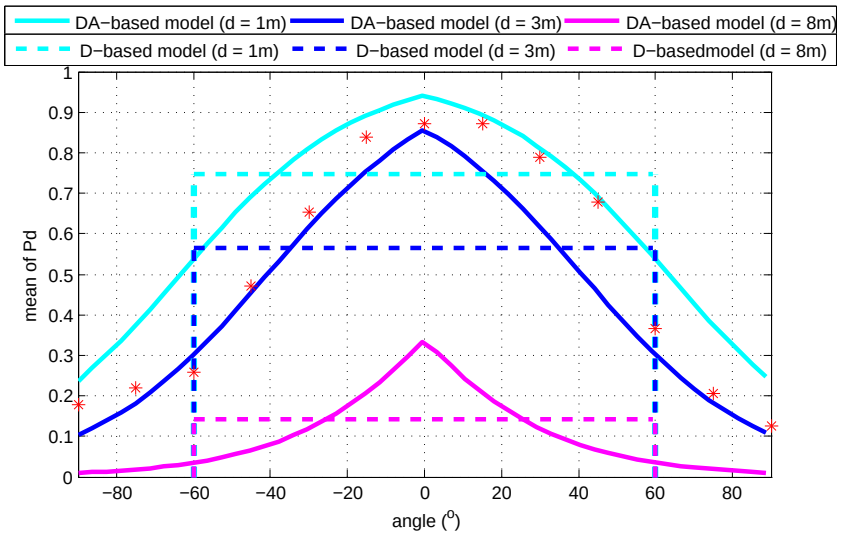

FIGURE 4.6: Probability of detection with different fixed distances. The DA-based model is given by (5.3) and the D-based model by (4.12). The red asterisks represent the mean of the real measurements of probability of detection at $d = 3$ m.

$d = 3$ m. Figure 4.7 shows the probability mass functions and the corresponding cumulative distribution functions of the number of readings for the two models at different fixed distances and angles. Each RFID reader is assumed to send $N = 50$ queries.

We can see that the probability mass functions and the cumulative distribution functions of n at different angles are almost the same for the D-based model, whereas for the DA-based model, the functions vary with the angle. For instance, in the DA-based model the probability of missed detections $P(n = 0|d = 4, \theta)$ is higher at $\theta = 60^\circ$ than at $\theta = 0^\circ$, which agrees with reality, whereas for the D-based model, it is the same.

We compared the performance of the two models by computing the mean of the probability of detection at certain distances and angles and validating the results

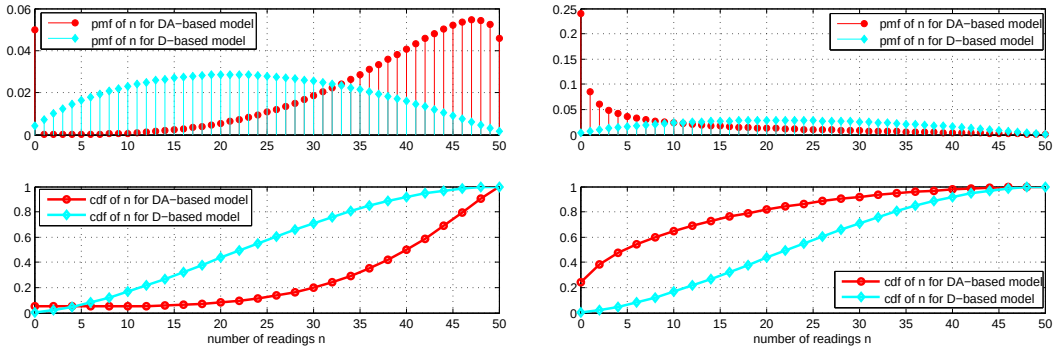

(a) $d = 4$ m and $\theta = 0^\circ$ (b) $d = 4$ m and $\theta = 60^\circ$

FIGURE 4.7: The probability mass functions and the cumulative distribution functions of the number of readings for the two models for different sets of (d, θ).

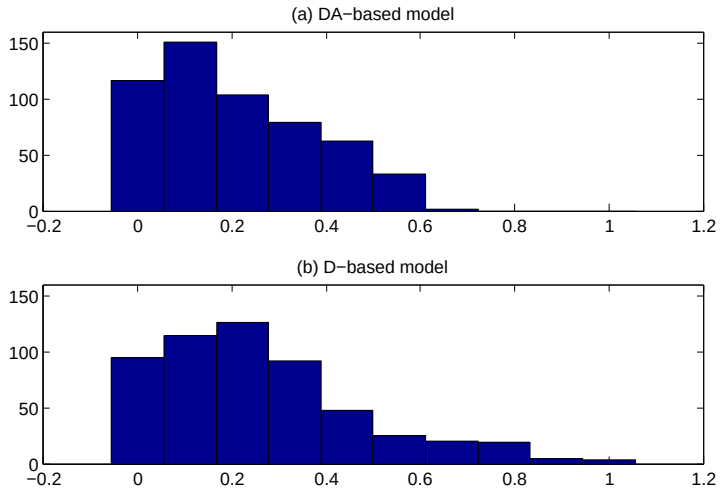

FIGURE 4.8: The histograms of prediction errors of the two models.

with real measurements. The mean square error (MSE) between the predicted results by the DA-based model and the real measurements is 0.071, while the MSE between the results by the D-based model and the real measurements is 0.113. The histograms of the prediction errors with the two models are displayed in Fig. 4.8. Thus, the proposed model achieves higher modeling accuracy than the D-based

model.

4.4 Proposed method

The highly nonlinear nature of the proposed observation model introduced in the previous section motivates the use of the PF methodology for tracking of the posterior distribution of the system state given the observations [65], [66], [29]. PF belongs to the family of Monte Carlo estimation methods and approximates the posterior density of the unknown state of the system by using a random measure χ_t composed of particles of the states, $\boldsymbol{x}_t^{(m)}$, and associated weights to the particles, $w_t^{(m)}$, i.e., $\chi_t = \{\boldsymbol{x}_t^{(m)}, w_t^{(m)}\}_{m=1}^{M}$. As new observations become available, the set of particles representing the possible values of the unknowns is propagated and the weights are updated accordingly following the Bayes' rule [29].

Suppose that at time instant t_1, a random measure of size M, $\chi_{t_1} = \{\boldsymbol{x}_{t_1}^{(m)},\ w_{t_1}^{(m)}\}_{m=1}^{M}$, is available, where $\boldsymbol{x}_{t_1}^{(m)}$ are the particles of the measure, and $w_{t_1}^{(m)}$ denotes the corresponding weights indicating the goodness of the particles. Upon reception of the next observation at t_2, the particles are propagated according to

$$\boldsymbol{x}_{t_2}^{(m)} \sim \pi(\boldsymbol{x}_{t_2}|\boldsymbol{x}_{t_1}^{(m)},\ \mathcal{Y}_{t_2}), \tag{4.15}$$

where $\pi(\boldsymbol{x}_{t_2}|\boldsymbol{x}_{t_1}^{(m)},\ \mathcal{Y}_{t_2})$ is the proposal distribution used for generation of new particles, $\boldsymbol{x}_{t_2}^{(m)}$, $t_2 > t_1$, and $\mathcal{Y}_{t_2}$ is the set of all measurements up to t_2. The general expression for computing the weights of the particles is given by

$$w_{t_2}^{(m)} \quad \propto \quad w_{t_1}^{(m)} \frac{p(\boldsymbol{y}_{t_2}|\boldsymbol{x}_{t_2}^{(m)}) p(\boldsymbol{x}_{t_2}^{(m)}|\boldsymbol{x}_{t_1}^{(m)})}{\pi(\boldsymbol{x}_{t_2}^{(m)}|\boldsymbol{x}_{t_1}^{(m)},\ \mathcal{Y}_{t_2})}, \tag{4.16}$$

where $p(\boldsymbol{y}_{t_2}|\boldsymbol{x}_{t_2}^{(m)})$ is the likelihood of the particle $\boldsymbol{x}_{t_2}^{(m)}$, and $p(\boldsymbol{x}_{t_2}^{(m)}|\boldsymbol{x}_{t_1}^{(m)})$ and $\pi(\boldsymbol{x}_{t_2}^{(m)}|\boldsymbol{x}_{t_1}^{(m)},\ \mathcal{Y}_{t_2})$ are the transition and the proposal distributions of the state computed at $\boldsymbol{x}_{t_2}^{(m)}$, respectively. We recall that the transition distribution of the state is readily obtained from (6.1) and the assumptions that we know the distribution of the noise vector $\boldsymbol{v}_t$, and that $\boldsymbol{v}_{t_1}$ and $\boldsymbol{v}_{t_2}$ are independent for $t_1 \neq t_2$. In the sequel, for $\pi(\boldsymbol{x}_{t_2}^{(m)}|\boldsymbol{x}_{t_1}^{(m)},\ \mathcal{Y}_{t_2})$ we use $p(\boldsymbol{x}_{t_2}^{(m)}|\boldsymbol{x}_{t_1}^{(m)})$, and (4.16) simplifies to

$$w_{t_2}^{(m)} \quad \propto \quad w_{t_1}^{(m)}\, p(\boldsymbol{y}_{t_2}|\boldsymbol{x}_{t_2}^{(m)}). \tag{4.17}$$

In a standard PF algorithm, once the weights of the particles are computed according to (5.7), they are normalized and a new random measure is formed, $\chi_{t_2} = \{\boldsymbol{x}_{t_2}^{(m)}, w_{t_2}^{(m)}\}_{m=1}^{M}$. This random measure is then used to obtain the estimate of $\boldsymbol{x}_{t_2}$, for example, by using the minimum mean square estimate

$$\widehat{\boldsymbol{x}}_{t_2} = \sum_{m=1}^{M} w_{t_2}^{(m)} \boldsymbol{x}_{t_2}^{(m)}. \tag{4.18}$$

An additional step of the algorithm, is to execute resampling so that we avoid a degeneration of the random measure. We implement resampling by drawing M particles from the current particle set $\boldsymbol{x}_{t_2}^{(m)}$ with probabilities proportional to their weights $w_{t_2}^{(m)}$. The current particle set is thereby replaced with the new one denoted by $\tilde{\boldsymbol{x}}_{t_2}^{(m)}$ and the weights $w_{t_2}^{(m)}$ are set to $1/M$, $\forall m$.

4.4.1 False synchronous case

In this subsection, we assume synchronicity, i.e., that all the measurements are considered to arrive at kT_s (see Fig. 6.2). Let the random measure at time instant $t = (k-1)T_s$ be $\chi_{(k-1)T_s} = \{\boldsymbol{x}_{(k-1)T_s}^{(m)}, w_{(k-1)T_s}^{(m)}\}_{m=1}^{M}$. First, we propagate the particles

to time instant kT_s by using

$$\boldsymbol{x}_{kT_s}^{(m)} \quad \sim \quad p(\boldsymbol{x}_{kT_s}|\boldsymbol{x}_{(k-1)T_s}^{(m)}). \tag{4.19}$$

Next, we compute the weights of these particles, and to that end we use

$$w_{kT_s}^{(m)} \quad \propto \quad w_{(k-1)T_s}^{(m)} \prod_{l=1}^{L_k} \prod_{j=1}^{J} \mathcal{L}\left(n_{l,j,k}, \boldsymbol{x}_{kT_s}^{(m)}\right), \tag{4.20}$$

where

$$\mathcal{L}\left(n_{l,j,k}, \boldsymbol{x}_{kT_s}^{(m)}\right) \quad = \quad \left\{ \frac{\beta_\lambda}{\alpha_\lambda + \beta_\lambda} \binom{N}{n_{l,j,k}} f\big(\boldsymbol{x}_{kT_s}^{(m)}, n_{l,j,k}\big) + \frac{\alpha_\lambda}{\alpha_\lambda + \beta_\lambda} \delta(n_{l,j,k}) \right\} \tag{4.21}$$

with $J \in \{3, 4\}$ represents the number of antennas a reader is associated to, and

$$f(\boldsymbol{x}_{kT_s}^{(m)}, n_{l,j,k}) = \frac{B\left(n_{l,j,k} + \alpha(\boldsymbol{x}_{kT_s}^{(m)}), N - n_{l,j,k} + \beta(\boldsymbol{x}_{kT_s}^{(m)})\right)}{B(\alpha(\boldsymbol{x}_{kT_s}^{(m)}), \beta(\boldsymbol{x}_{kT_s}^{(m)}))}, \tag{4.22}$$

where the $\boldsymbol{x}_{kT_s}^{(m)}$s in the argument of $\alpha(\cdot)$ and $\beta(\cdot)$ can readily be converted into polar forms, $d_{kT_s}^{(m)}$ and $\theta_{kT_s}^{(m)}$.

The above computation is an approximation and introduces several sources of errors. First, we recall that the particles $\boldsymbol{x}_{kT_s}^{(m)}$ are drawn from $p(\boldsymbol{x}_{kT_s}|\boldsymbol{x}_{(k-1)T_s}^{(m)})$, $m = 1, 2, \cdots, M$. Provided that the tag was indeed at the location given by the state $\boldsymbol{x}_{(k-1)T_s}^{(m)}$ at $(k-1)T_s$, and the validity of the transition model, the particles $\boldsymbol{x}_{kT_s}^{(m)}$ are, in principle good particles. The problem, however, is that the measurements are inaccurate for the following reasons: (a) the tag was moving during the interval of data acquisition, and therefore the distances of the tags and their angles with respect to the readers' antennas were changing all the time, (b), even though the rounds of queries started at the same time instant $(k-1)T_s$, they were completed

earlier than kT_s and at different time instants, and (c) for all the readers we have a common set of particles. With the synchronous approach, we simply ignore these errors and proceed as if the probabilities of detection of a tag did not change with the movement of the tag and if the querying occurred exactly from $(k-1)T_s$ to T_s.

4.4.2 The asynchronous case

Now we address the asynchronous case. Here our main strategy is to propagate and update the particles each time we receive a measurement. Let the last measurement in the $(k-1)$th rounds be from reader $i_{L_{k-1},k-1}$ and that after its processing, we obtained the random measure $\chi_{\tau_{L_{k-1},k-1}} = \{\boldsymbol{x}^{(m)}_{\tau_{L_{k-1},k-1}}, w^{(m)}_{\tau_{L_{k-1},k-1}}\}_{m=1}^{M}$. Now, we propagate the particles $\boldsymbol{x}^{(m)}_{\tau_{L_{k-1},k-1}}$ to time instant $(k-1)T_s$ according to

$$\boldsymbol{x}^{(m)}_{(k-1)T_s} \sim p(\boldsymbol{x}_{(k-1)T_s}|\boldsymbol{x}^{(m)}_{\tau_{L_{k-1},k-1}}). \tag{4.23}$$

The weights of these particles are not changed and therefore we have

$$w^{(m)}_{(k-1)T_s} = w^{(m)}_{\tau_{L_{k-1},k-1}}. \tag{4.24}$$

Suppose now that the first reading in the kth round came from the reader $i_{1,k}$ at $\tau_{1,k}$ and that the measurement was $\boldsymbol{y}_{1,k}$. First we propagate the particles according to

$$\boldsymbol{x}^{(m)}_{\tau_{1,k}} \sim p(\boldsymbol{x}_{\tau_{1,k}}|\boldsymbol{x}^{(m)}_{(k-1)T_s}). \tag{4.25}$$

Next we update the weights of the particles given the measurements $\boldsymbol{y}_{1,k}$. We use

$$w^{(m)}_{\tau_{1,k}} \propto \tfrac{1}{2} w^{(m)}_{(k-1)T_s} \prod_{j=1}^{J} \left(\mathcal{L}\left(n_{1,j,k}, \boldsymbol{x}^{(m)}_{(k-1)T_s}\right) + \mathcal{L}\left(n_{1,j,k}, \boldsymbol{x}^{(m)}_{\tau_{1,k}}\right)\right), \tag{4.26}$$

where $\mathcal{L}(\cdot,\cdot)$ is defined in (4.21). The computation of the weights according to (4.26) is an approximation to capture the phenomenon that the round of querying

took place from $(k-1)T_s$ to $\tau_{1,k}$. More specifically, an observation in our case represents aggregated binary measurements from one round of N queries. The location of the tag changes during these N queries and consequently the probability of detection changes. All the location points along this trajectory contribute equally to one acquired measurement. Therefore, ideally, we should average over the whole trajectory during this round. However, in our setup, for simplicity, we only draw particles for the ending time instant of a round. Thus, for the duration of the round we only have the locations of the particles at the beginning (from the previous round) and at the end of it. We make use of these two time instants to compute the approximate values of the weights. Obviously, we could modify this approximation by generating particles at time instants in between $(k-1)T_s$ and $\tau_{1,k}$ and computing the likelihood for these particles too.

Let now the next measurement be at $\tau_{2,k}$. Again, we first propagate the particles, and we use

$$\boldsymbol{x}_{\tau_{2,k}}^{(m)} \sim p(\boldsymbol{x}_{\tau_{2,k}}|\boldsymbol{x}_{\tau_{1,k}}^{(m)}). \tag{4.27}$$

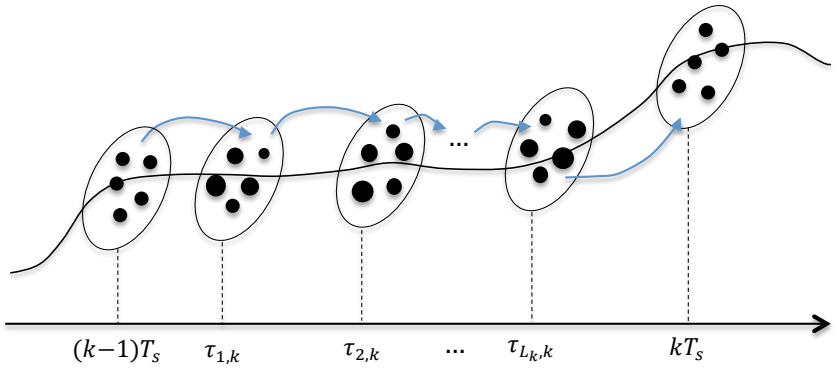

FIGURE 4.9: Particle propagations during each time interval.

We proceed with computation of the weights by

$$w_{\tau_{2,k}}^{(m)} \propto \frac{1}{2} w_{\tau_{1,k}}^{(m)} \prod_{j=1}^{J} \left(\mathcal{L}\left(n_{2,j,k}, \boldsymbol{x}_{(k-1)T_s}^{(m)} \right) + \mathcal{L}\left(n_{2,j,k}, \boldsymbol{x}_{\tau_{2,k}}^{(m)} \right) \right). \tag{4.28}$$

Now we have the random measure $\chi_{\tau_{2,k}} = \{\boldsymbol{x}_{\tau_{2,k}}^{(m)}, w_{\tau_{2,k}}^{(m)}\}_{m=1}^{M}$ and are ready for processing the readings of the next reader, $i_{3,k}$, which finishes its round at $\tau_{3,k}$. The steps are the same as for reader $i_{2,k}$. We repeat this procedure until the last reader completes its round of queries. With the processing of $\boldsymbol{y}_{L_k,k}$, we are ready to move on to time $(k+1)$th round of queries. Figure 4.9 shows the scenario of particle propagations during each time interval. A summary of the proposed PF algorithm is given in Table 4.1.

4.4.3 Extension to a more general setting

Here we extend the proposed method so that it can process data from readers that do not have to be synchronized at all. Thus we do not use the time instants kT_s. We denote the lth measurements at time instant τ_l by $\boldsymbol{y}_l = \{k_l, i_l, \tau_l, n_{j,l} : j \in \{1,2,3,4\}, l \in \mathbb{N}^+, k_l \in \mathbb{N}^+\}$, where τ_l is also the time instant of the completion of the k_lth round of reader i_l, as well as the starting time instant of the (k_l+1)th round of this reader. We note that $\tau_1 \leqslant \tau_2 \leqslant \tau_3 \leqslant \cdots$. Now suppose that the last available reading is at τ_{l-1} by reader i_{l-1} and that for this time instant we have the random measure $\chi_{\tau_{l-1}} = \{\boldsymbol{x}_{\tau_{l-1}}^{(m)}, w_{\tau_{l-1}}^{(m)}\}_{m=1}^{M}$. Let the next reading be at τ_l, $\boldsymbol{y}_l$. Once the reading is obtained, we propagate the particles by

$$\boldsymbol{x}_{\tau_l}^{(m)} \sim p(\boldsymbol{x}_{\tau_l} | \boldsymbol{x}_{\tau_{l-1}}^{(m)}). \tag{4.29}$$

We note that the tag moves during the time interval of the querying of the i_lth reader. Therefore, in computing the updated weights, we use an analogous

Table 4.1: PF algorithm for tracking in a UHF RFID system.

INITIALIZATION:
$\boldsymbol{x}_0^{(m)} \sim N(\boldsymbol{x}_0, \Xi)$ and $w^{(m)} = 1/M, \forall m$ where $\boldsymbol{x}_0$ is the prior knowledge of the states of the tag and Ξ is a predefined covariance matrix.
TRACKING:
for $k = 1, 2, \cdots$ perform the following: Generate the new particles according to $\boldsymbol{x}_{\tau_{1,k}}^{(m)} \sim p(\boldsymbol{x}_{\tau_{1,k}} \vert \boldsymbol{x}_{(k-1)T_s}^{(m)})$. Update the weights according to (5.6) and estimate $\widehat{\boldsymbol{x}}_{\tau_{1,k}}$. **for** $l = 2, 3, \cdots, L_k$ 1. `PROPAGATION` Generate the new particles according to $\boldsymbol{x}_{\tau_{l,k}}^{(m)} \sim p(\boldsymbol{x}_{\tau_{l,k}} \vert \boldsymbol{x}_{\tau_{l-1,k}}^{(m)})$, 2. `WEIGHT UPDATE` Update $w_{\tau_{l,k}}^{(m)}$ according to (4.28) and normalize. 3. `ESTIMATION` $\widehat{\boldsymbol{x}}_{\tau_{l,k}} = \sum_{m=1}^{M} w_{\tau_{l,k}}^{(m)} \boldsymbol{x}_{\tau_{l,k}}^{(m)}$. `RESAMPLING`: a) Draw M particles from the current particle set with probabilities proportional to their weights $w_{\tau_{l,k}}^{(m)}$. b) Replace the current particle set with the new one and set $w_{\tau_{l,k}}^{(m)} = 1/M, \forall m$. Propagate the particles $\boldsymbol{x}_{\tau_{L_k,k}}^{(m)}$ to time instant kT_s according to (4.23).

expression to (4.26), i.e., we have

$$w_l^{(m)} \quad \propto \quad \frac{1}{2} w_{l-1}^{(m)} \prod_{j=1}^{J} \left(\mathcal{L}\left(n_{j,l}, \boldsymbol{x}_{\tau_l *}^{(m)}\right) + \mathcal{L}\left(n_{j,l}, \boldsymbol{x}_{\tau_l}^{(m)}\right) \right), \tag{4.30}$$

where we need to know the particles $\boldsymbol{x}_{\tau_l *}^{(m)}$, that is, the particles of the states when they were updated at the previous reading of reader i_l, and l^* is the index of the $(k_l - 1)$th round of reader i_l. In principle, it is not difficult to maintain information about these particles, and they can readily be retrieved.

The next step is to compute the estimate of $\boldsymbol{x}_l$. As before, we use

$$\widehat{\boldsymbol{x}}_{\tau_l} = \sum_{m=1}^{M} w_{\tau_l}^{(m)} \boldsymbol{x}_{\tau_l}^{(m)}. \tag{4.31}$$

Finally, we may resample and thereby get ready for the reading of the next reader. Clearly, with this algorithm, there is no need to maintain any form of synchronism.

An important study of the methodology is its feasibility for real-time tracking. The actual implementation would very much depend on how many readers are in the system, how many tags need to be tracked, and what computational resources are used. Based on this information, one can design customized PF schemes for the problem. On the other hand, we would like to point out the following. The advantage of the false synchronous approach is that PF is applied periodically with one particle filter operating on all the measurements of a tag acquired within a period. Thereby one gains in computational efficiency and loses in estimation accuracy. By contrast, with the asynchronous approach, we have the opposite effect. If the average arrival rate of measurements per tag is κ, the number of tags to be tracked is K, and the rate of completion of PF recursions is ν, then, for successful real-time implementation, the number of processing units that perform PF needs to be greater than $\kappa K/\nu$.

4.5 Simulation results

In the simulations, our objective was to evaluate the performance of the proposed PF that uses the proposed model and asynchronous measurements and to compare it with other models and methods. To that end, we deployed 4×4 readers with

a separation distance of $D = 10$ m between them in a warehouse of size 40 m $\times$ 40 m as shown in Fig. 4.1. The objective was to detect and track the objects with tags (targets) during a period of 20 s with a sampling time $T_s = 1$ s. The process covariance matrix was given by $Q = diag(0.01, 0.01)$ and the initial speed was 1 m/s for both velocity components. The parameters of the observation model were the ones introduced in Section III. Note that there are no false alarms when tracking in RFID systems but missed detections are common.

The readers sent out queries every $T_s = 1$ s and the query period for each reader was generated using a $\mathcal{U}(0.2, 0.8)$, with the values being obtained from evaluation of the ISO 180006-C protocol and the experimental setup. In all the experiments, the PF algorithm used $M = 200$ particles. The tracking performance was evaluated using the average root mean square error (RMSE) of the position of the target as a function of time over 50 independent realizations. The RMSE for one realization was calculated as $\sqrt{(\hat{x}_{1,t} - x_{1,t})^2 + (\hat{x}_{2,t} - x_{2,t})^2}$ and the RMSE of a missed detection was set to 6 m. For the probability of being in a dead-zone, we had $\lambda \sim Beta(\alpha_\lambda, \beta_\lambda)$ with $\alpha_\lambda = 0.1875$ and $\beta_\lambda = 3.5625$, which corresponded to a mean of dead-zone probability of 0.05 and a variance of 0.01.

In the first experiment, we compared the tracking performance of the two models discussed in the previous subsection with the proposed asynchronous approach. The observations were generated according to the DA-based model due to its higher accuracy in describing real scenarios. We can see from Fig. 4.10 that the performance with the tracking algorithm using the DA-based model is much better than that using the D-based model.

In the second experiment, we compared the tracking performance of the DA-based model with asynchronous measurements for different grid resolutions. The

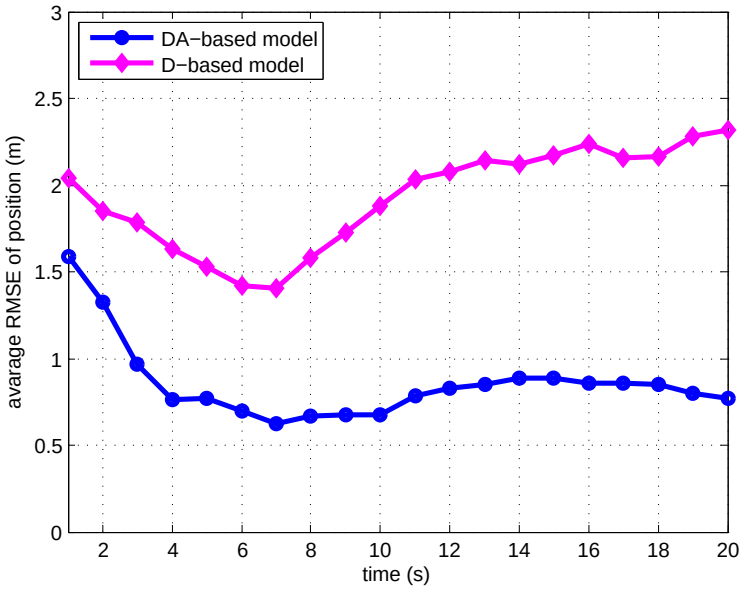

FIGURE 4.10: Tracking performances with the two models.

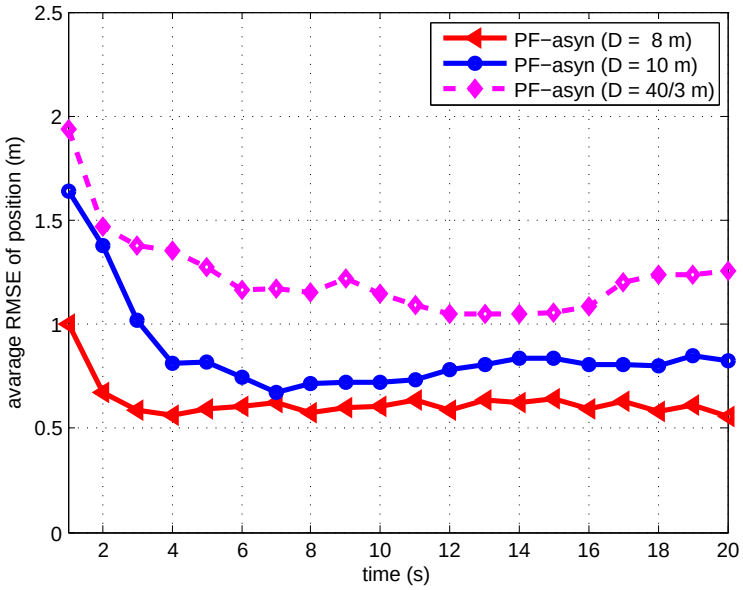

FIGURE 4.11: Tracking performance with different separation distances.

deployment of the antennas followed Fig. 4.1 and the results are shown in Fig. 4.11. We can see that the performance with smaller separation distance among readers,

D, achieved more accurate tracking results. However, smaller separation distance requires more readers and antennas, and thus the system is more expensive.

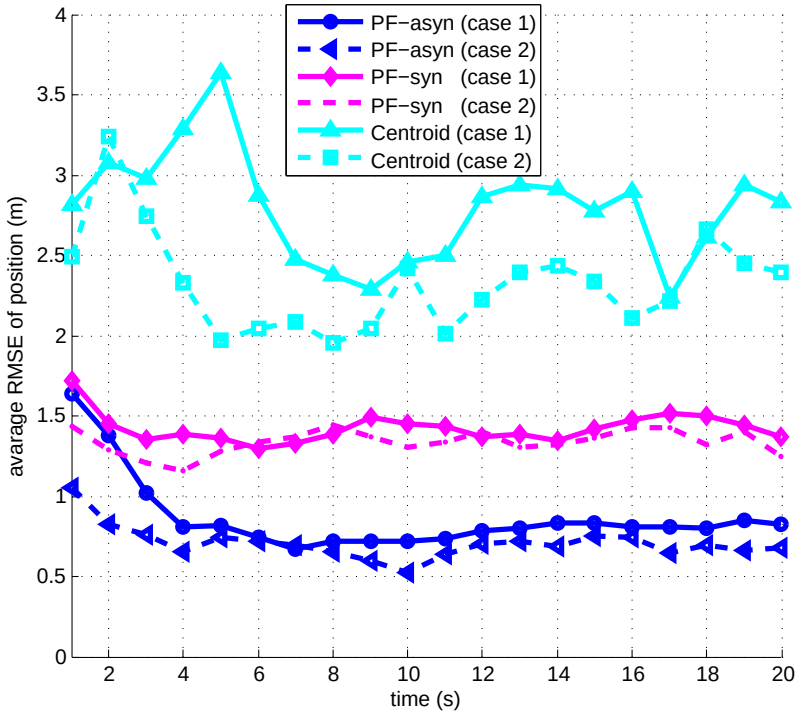

FIGURE 4.12: Tracking performances with different algorithms and with different number of antennas. In case 1, the deployment of the antennas follows Fig. 4.1 and in case 2, there are four antennas connected to each reader.

In the third experiment, we compared the performance of different tracking methods for two different cases of antenna deployment: (a) following Fig. 4.1; and (b) with four antennas connected to each reader. For the latter case, we needed more antennas. The separation distance was set to 10 m for both cases. We compared three methods: `PF-asyn` is the proposed PF method accounting for the asynchronous measurements, `PF-syn` is the PF method with wrongly assumed synchronism, and `CE-asyn` is a "centroid" method where the estimated position of the target is calculated as the central point of the positions of the detecting

antennas [72]. The results are shown in Fig. 4.12. We can see that the new proposed algorithm outperforms the other two methods. To be specific, for instance, the accuracy of `PF-asyn` is improved by half a meter on average in comparison to the `PF-syn` method. It is a reasonable improvement with respect to the simulation setup where the tags move at an initial velocity of 1 m/s and where the sampling interval was 1 s. As expected, the error with more antennas was reduced. In practical implementations, one could use as many antennas as a reader can support to achieve a better tracking performance but it will come with higher cost of the system.

In the fourth experiment, we evaluated the performance with different coefficients of variation, where the coefficient of variation is defined as the ratio of the standard deviation to the mean of the process signal. We compared the performance of our proposed PF method accounting for the asynchronous measurements (`PF-asyn`) and the PF method with wrongly assumed synchronism (`PF-syn`) with different separation distances D. We can see from the results in Fig. 4.13 that the performance of `PF-asyn` is consistently better than that of `PF-syn`. Note that the RMSE in the figure was obtained by averaging the RMSEs over time.

Finally, we simulated a scenario with different dead-zone probabilities and applied the proposed method. We set the variance of the dead-zone probability to be 0.01 and changed the value of the mean. As seen in Fig. 4.14, and as expected, the performance worsened as the probability of dead-zone increased. Also, more antennas in the system allow for improved tracking.

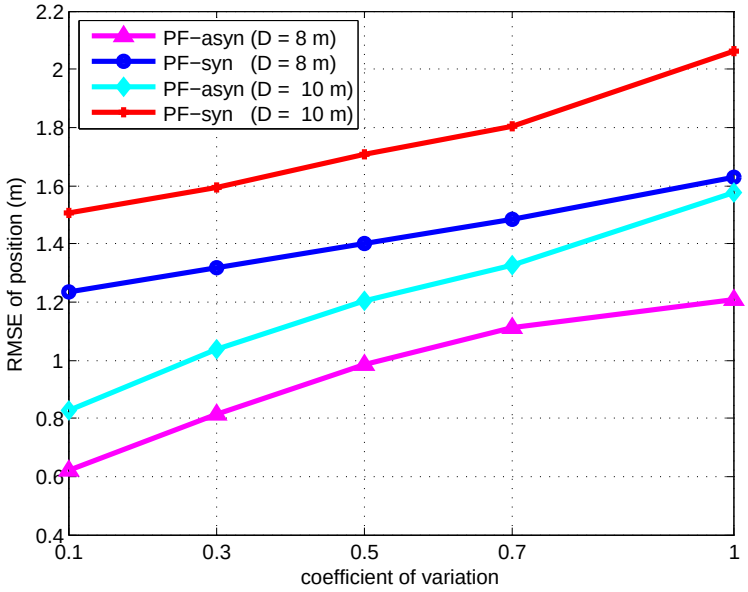

FIGURE 4.13: Tracking performances with different coefficients of variation.

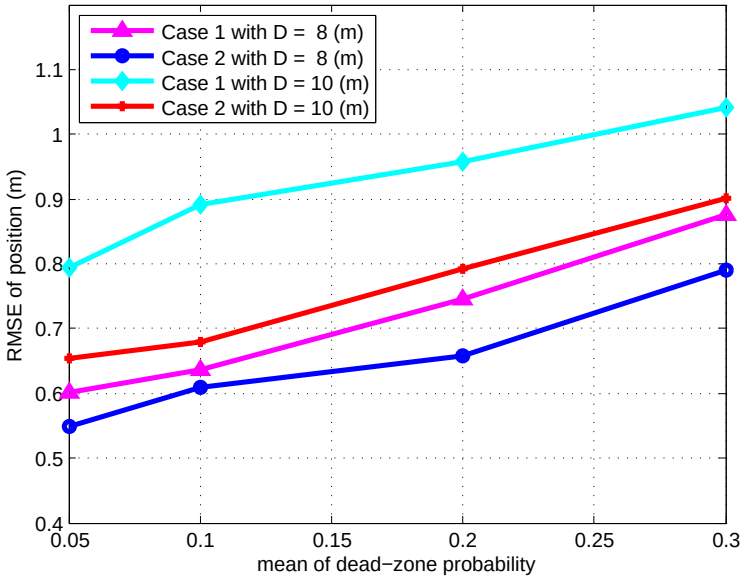

FIGURE 4.14: Tracking performances with different mean of probability of dead-zone.

4.6 Summary

In this chapter the problem of tracking tagged objects using asynchronous measurements in a Ultra High Frequency Radio Frequency Identification system was addressed. A more realistic parametric model for the probability of detection was proposed, which is a function of both the distance and the angle of the tag with respect to an antenna of the reader. This model also includes the variability of the probability of detection of a tag and the probability of a tag being in a dead-zone. Furthermore, we proposed a general method for processing asynchronous measurements using particle filtering. The parameters needed for the implementation of the method were obtained from real-world experiments and its performance was analyzed by extensive simulations.

5

Indoor Tracking with Asynchronous Binary Readings with Sense-a-tags

This chapter addresses the problem of real-time indoor tracking of tagged objects in UHF RFID systems with layout information and asynchronous readings. The method is based on binary detections and the model for the probability of detection is a function of both distance and angle between a tag and a reader and accounts for the possibility of a tag being in a dead-zone. A newly developed RFID component, called sense-a-tag (ST), is used to improve the tracking performance, especially in areas with intersections and at portals, where the estimation of the direction of movement is important. The ST is a semi-passive device that can not only communicate with the reader like standard passive tags but also can sense the communication between tags in its proximity and the reader. A multi-hypothesis particle filtering method is applied for the tracking and its performance is demonstrated by computer simulations. The formulation of the indoor tracking problem including the motion model and the asynchronous

observations is presented in Section 5.2. The PF method for tracking the targeted tags in constrained layout setups with multiple choices of movement direction and the novel ST devices is introduced in Section 5.3. In Section 5.4, we provide simulation results that demonstrate the performance of the method. The chapter concludes with some final remarks in Section 5.5.

5.1 Introduction

UHF RFID is a rapidly growing technology for real-time identification and tracking that can be applied in many settings including inventory management, health care systems and the Internet of Things [3]. In this chapter, we investigate the problem of real-time tracking of tagged objects in warehouse-like environments with layout information (intersections, shelves and walls). The objective is to track tagged objects moving between shelves and to estimate the direction of movement, which is especially important at intersections and portals for improved accuracy in inventory.

We have studied the problem of indoor UHF RFID tag tracking based on aggregated binary readings in Chapter 4 [62, 73]. The reader reports binary information indicating the detection of a tag and uses aggregated number of detections over a fixed number of queries. In this chapter, binary detections are used for real-time tracking, where tracking is updated as soon as a detection occurs and the model is from [73]. According to that model, the probability of detection is a function of both the distance and angle from the tag to the reader, and accounts for the possibility of a tag being in a dead-zone.

Tag responses are received by the readers asynchronously. We propose the use of the particle filtering (PF) methodology [66] that takes into account the

asynchronous nature of the readings. A study dealing with asynchronous readings in traditional sensor networks can be found in [67]. In the proposed approach, we also integrate available layout information, which improves the performance of the PF.

In this chapter we study the use of a newly developed low-cost device called sense-a-tag (ST) [74, 50]. An ST has the same functionality as a regular tag but can also detect communication between the reader and tags in its proximity. The ST can communicate this information to the reader by backscattering. With the information received from the STs, the system can improve the accuracy of localization and can unambiguously estimate the direction of movement of a tagged object [75]. The tracking of the direction of movement of a person or object close to some monitoring area is important in a number of applications. For example, it is critical to determine if tagged goods are moving into or out of a warehouse. Methods for estimation of the direction of movement in RFID systems can be found in [76], where two antennas are used and the direction of movement is estimated by measuring the times of detection of a tagged object from the signals of the antennas. An RFID system with STs and using PF for tracking purposes was introduced in [61]. The tracking problem was investigated in a very small area with one single reader. In this chapter, we extend the work from [61]. The main contribution is in a novel algorithm that operates with asynchronous readings and exploits the presence of STs in the RFID system.

5.2 Problem formulation

Consider the problem of tracking tagged objects (e.g., a warehouse worker or a forklift) that move in a warehouse. A possible deployment of a traditional reader-

only system is shown in Fig. 5.1. Each reader R_i is connected with three antennas denoted by the right (red), the upper left (green), and the lower left (blue) sectors. The arrows indicate the orientation of the antennas. We assume that the layout information is known and includes intersections V_i, invalid regions, shelves and walls.

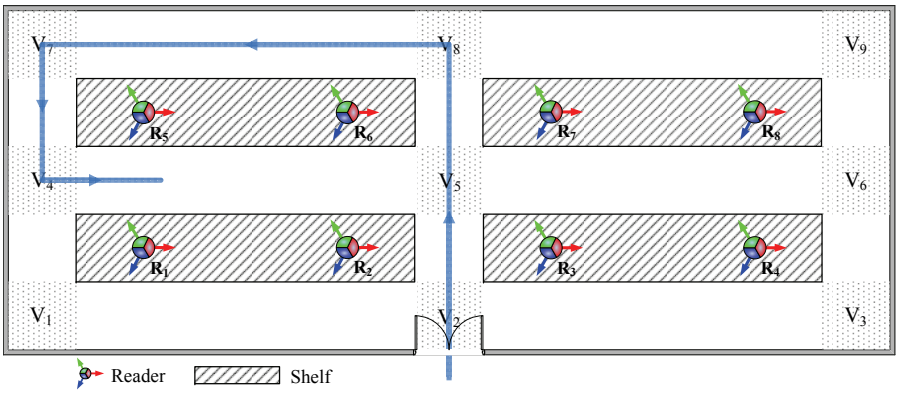

FIGURE 5.1: The RFID system in the considered warehouse layout.

A tagged object moves along the path between two shelves, or the path between a shelf and a wall. The object can go straight or make turns at intersections. For example at a T-shaped intersection the object might turn left or right. The tracking algorithm will account for these directions of movement.

5.2.1 The motion model

The state of the system consists of a vector containing information about a particular tag at time instant t and is denoted by $\boldsymbol{x}_t \in \mathbb{R}^{4\times 1}$, where $\boldsymbol{x}_t = [x_{1,t}\ x_{2,t}\ \dot{x}_{1,t}\ \dot{x}_{2,t}]^\top$ and $t \in \mathbb{R}^+$. The first two elements of the vector are the location of the tag in the two-dimensional Cartesian coordinate system, and the other two elements are the components of the velocity. When we focus on tracking

the direction of movement of the tag, we reformulate the problem in one dimension. The tagged object moves from t_1 to t_2 according to the model

$$\boldsymbol{x}_{t_2} \quad = \quad \boldsymbol{A}_i(t_1, t_2)\boldsymbol{x}_{t_1} + \boldsymbol{B}_i(t_1, t_2)\boldsymbol{u}_{t_2,i}, \tag{5.1}$$

where $i = 1, 2$ denotes the ith motion mode depending if the tag moves horizontally or vertically, respectively, $\boldsymbol{x}_{t_2}$ is the state of the system at time instant t_2, $\boldsymbol{u}_{t,i} \in \mathbb{R}^{2\times 1}$ is a noise vector with a known distribution, and $\boldsymbol{A}_i \in \mathbb{R}^{4\times 4}$ and $\boldsymbol{B}_i \in \mathbb{R}^{4\times 2}$ are known matrices, respectively, given by

$$\boldsymbol{A}_1 = \begin{pmatrix} 1 & 0 & (t_2 - t_1) & 0 \\ 0 & 1 & 0 & 0 \\ 0 & 0 & 1 & 0 \\ 0 & 0 & 0 & 0 \end{pmatrix}, \ \boldsymbol{B}_1 = \begin{pmatrix} \frac{(t_2-t_1)^2}{2} & 0 \\ 0 & 0 \\ (t_2 - t_1) & 0 \\ 0 & 0 \end{pmatrix},$$

$$\boldsymbol{A}_2 = \begin{pmatrix} 1 & 0 & 0 & 0 \\ 0 & 1 & 0 & (t_2 - t_1) \\ 0 & 0 & 0 & 0 \\ 0 & 0 & 0 & 1 \end{pmatrix}, \ \boldsymbol{B}_2 = \begin{pmatrix} 0 & 0 \\ 0 & \frac{(t_2-t_1)^2}{2} \\ 0 & 0 \\ 0 & (t_2 - t_1) \end{pmatrix}.$$

5.2.2 The asynchronous readings

In real RFID systems, all readers start their queries at different time instants. Once a reader receives the response from a tag, it reports the detection to the data processing center. A new query is then started immediately. In the existing literature, the asynchronism of the readers is ignored and the general assumption is that all the observations are obtained synchronously at prefixed sampling instants [62, 61, 48].

Figure 5.2 describes the asynchronous nature of the readings of a tag of interest. Each reading represents the detection of the tag from one reader.

We denote the kth detection by $y_k = \{i_k, j_k, \tau_k\}$, where $i_k \in \{1, 2, \cdots, L\}$ is the

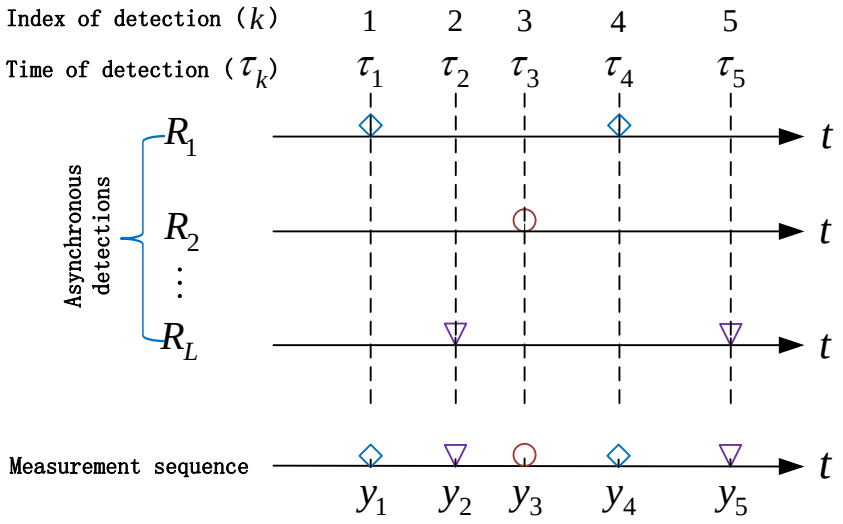

FIGURE 5.2: Asynchronous readings (detections) in a real RFID system of a particular tag.

index of the reader that detected the tag, $j_k \in \{1, 2, 3\}$ is the index of the antenna used in the detection, and $\tau_k \in \mathbb{R}^+$ is the time of the detection. We note that $\tau_1 \leqslant \tau_2 \leqslant \tau_3 \leqslant \cdots$. All the readings up to time instant τ_k are collected in the observation set $\mathcal{Y}_k = \{y_1, y_2, \cdots, y_k\}$. The objective is to track $\boldsymbol{x}_t$ in time given the observations and the assumed model.

5.2.3 The observation model

The observation model constitutes a challenge when tracking with RFID systems especially in indoor environments, since the query and response processes depend on numerous factors including the distance from the antenna, the orientation of the antenna, and the multipath interference [48].

The probability of detecting a tag by a reader, $p(d, \theta)$, is modeled as a random variable following a Beta distribution [62, 73], which is described by a function of both the distance d and the angle θ between the tag and the reader antenna,

$Beta(\alpha(d,\theta),\beta(d,\theta))$, with parameters $\alpha(d,\theta) > 0$ and $\beta(d,\theta) > 0$. The model also accounts for the possibility of a tag being in a dead-zone where the tag will not be detected even within the detecting range. We denote that probability as λ with $\lambda \sim Beta(\alpha_\lambda, \beta_\lambda)$. The observation model is given by [73]

$$\begin{aligned} P(n=1|d,\theta) &= \frac{\beta_\lambda}{\alpha_\lambda+\beta_\lambda}\frac{\alpha(d,\theta)}{\alpha(d,\theta)+\beta(d,\theta)} \\ P(n=0|d,\theta) &= \frac{\beta_\lambda}{\alpha_\lambda+\beta_\lambda}\frac{\beta(d,\theta)}{\alpha(d,\theta)+\beta(d,\theta)} + \frac{\alpha_\lambda}{\alpha_\lambda+\beta_\lambda}. \end{aligned} \tag{5.2}$$

where $n = 1$ and $n = 0$ indicates whether a reader detected the tag or not, respectively.

The mean of the probability of tag detection is given by $\mathbb{E}(p(d,\theta)) = \alpha(d,\theta)/(\alpha(d,\theta)+\beta(d,\theta))$ [70]. Furthermore, we assume that this mean is of the form [73]

$$\mathbb{E}(p(d,\theta)) = \frac{1}{1+e^{(a_1+a_2d+a_3|\theta|)}}, \tag{5.3}$$

where a_1, a_2 and a_3 are model parameters that are estimated from experimental data. Therefore, we express the probability of detection as a function of distance and angle as

$$P(n=1|d,\theta) = \frac{\beta_\lambda}{\alpha_\lambda+\beta_\lambda}\frac{1}{1+e^{(a_1+a_2d+a_3|\theta|)}}. \tag{5.4}$$

5.3 Proposed method

5.3.1 The particle filtering

The nonlinear nature of the observation model motivates the use of the PF methodology for approximation of the posterior distribution of the system state

given the observations [77]. PF approximates the posterior density by using random measures composed of particles and weights associated to the particles [77]. In the considered real-time tracking problem, PF propagates and updates the particles and weights every time we receive a reading.

Suppose that at time instant τ_{k-1}, a random measure of size M, $\chi_{\tau_{k-1}} = \{\boldsymbol{x}_{\tau_{k-1}}^{(m)},\ w_{\tau_{k-1}}^{(m)}\}_{m=1}^{M}$, is available, where $\boldsymbol{x}_{\tau_{k-1}}^{(m)}$ are the particles of the measure, and $w_{\tau_{k-1}}^{(m)}$ denote the corresponding weights. Upon reception of the next observation at τ_k, the particles are propagated according to

$$\boldsymbol{x}_{\tau_k}^{(m)} \sim \pi(\boldsymbol{x}_{\tau_k}|\boldsymbol{x}_{\tau_{k-1}}^{(m)},\ \mathcal{Y}_k), \tag{5.5}$$

where $\pi(\boldsymbol{x}_{\tau_k}|\boldsymbol{x}_{\tau_{k-1}}^{(m)},\ \mathcal{Y}_k)$ is the proposal distribution used for generation of new particles, $\boldsymbol{x}_{\tau_k}^{(m)}$, and $\mathcal{Y}_k$ is the set of all readings up to τ_k. The general expression for computing the weights of the particles is given by

$$w_{\tau_k}^{(m)} \quad \propto \quad w_{\tau_{k-1}}^{(m)} \frac{p(y_k|\boldsymbol{x}_{\tau_k}^{(m)})p(\boldsymbol{x}_{\tau_k}^{(m)}|\boldsymbol{x}_{\tau_{k-1}}^{(m)})}{\pi(\boldsymbol{x}_{\tau_k}^{(m)}|\boldsymbol{x}_{\tau_{k-1}}^{(m)},\ \mathcal{Y}_k)}, \tag{5.6}$$

where $p(y_k|\boldsymbol{x}_{\tau_k}^{(m)})$ is the likelihood of $\boldsymbol{x}_{\tau_k}^{(m)}$, and $p(\boldsymbol{x}_{\tau_k}|\boldsymbol{x}_{\tau_{k-1}}^{(m)})$ is the transition distribution of the state computed at $\boldsymbol{x}_{\tau_k}^{(m)}$.

The transition distribution of the state is readily obtained from (6.1), the layout information, the distribution of the noise vector, and the assumption that $\boldsymbol{u}_{\tau_{k-1}}$ and $\boldsymbol{u}_{\tau_k}$ are independent. For $\pi(\boldsymbol{x}_{\tau_k}|\boldsymbol{x}_{\tau_{k-1}}^{(m)},\ \mathcal{Y}_k)$ we use $p(\boldsymbol{x}_{\tau_k}|\boldsymbol{x}_{\tau_{k-1}}^{(m)})$, and (5.6) simplifies to

$$w_{\tau_k}^{(m)} \quad \propto \quad w_{\tau_{k-1}}^{(m)}\, p(y_k|\boldsymbol{x}_{\tau_k}^{(m)}), \tag{5.7}$$

and it can be computed as

$$w_{\tau_k}^{(m)} \quad \propto \quad w_{\tau_{k-1}}^{(m)}\, f(\boldsymbol{x}_{\tau_k}^{(m)}, y_k), \tag{5.8}$$

where

$$f(\boldsymbol{x}_{\tau_k}^{(m)}, y_k) = \frac{\beta_\lambda}{\alpha_\lambda + \beta_\lambda} \frac{1}{1 + e^{(a_1 + a_2 d_{\tau_k}^{(m)} + a_3 |\theta_{\tau_k}^{(m)}|)}}, \tag{5.9}$$

where $d_{\tau_k}^{(m)}$ and $\theta_{\tau_k}^{(m)}$ can be obtained from $\boldsymbol{x}_{\tau_k}^{(m)}$ and the location of the antenna j_k of the reader i_k that detected the tag, whereas α_λ and β_λ are estimated from experimental data.

We apply a multi-hypothesis propagation by integrating the layout information into the PF framework. Figure 5.3 (a) shows an example of the propagation when the system relies only on RFID readers. The particle cloud is split into three clouds with different moving directions [78]. We keep all the clouds with different hypotheses of the motion model, and update the weight for each cloud after obtaining the new observation. The resulting particle clouds have their own propagation models but the weight normalization and the resampling steps are performed over all the particles. Once more observations are obtained, the number of particles in the cloud with the true hypothesis is expected to increase, and vice versa.

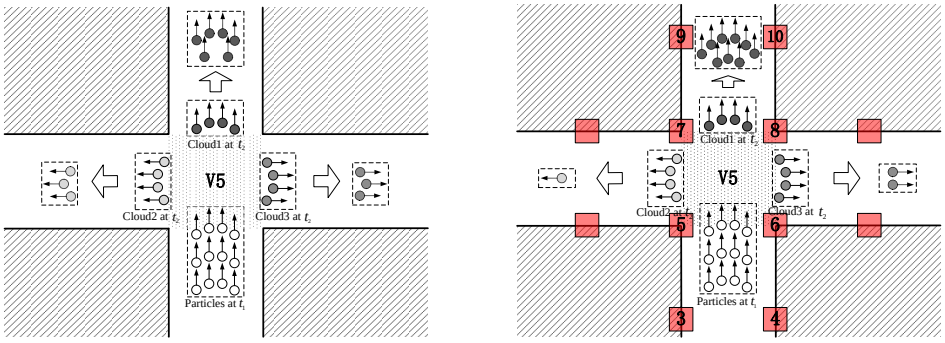

(a) Reader-only system. (b) New system with STs.

FIGURE 5.3: The multi-hypothesis particle propagation.

5.3.2 *The sense-a-tag*

In this section, we discuss a new semi-passive RFID system with ST devices [74, 75] that will improve the accuracy of tracking and will readily resolve the estimation of the direction of movement at intersections.

As pointed out, the ST is a tag-like RFID component with dual functionality. It can not only communicate with the reader like standard tags, but can also sense the communication between the reader and standard tags in its proximity. Based on the information backscattered by the STs to the reader, localization and tracking algorithms based on binary sensor principles can be developed [50, 75, 61].

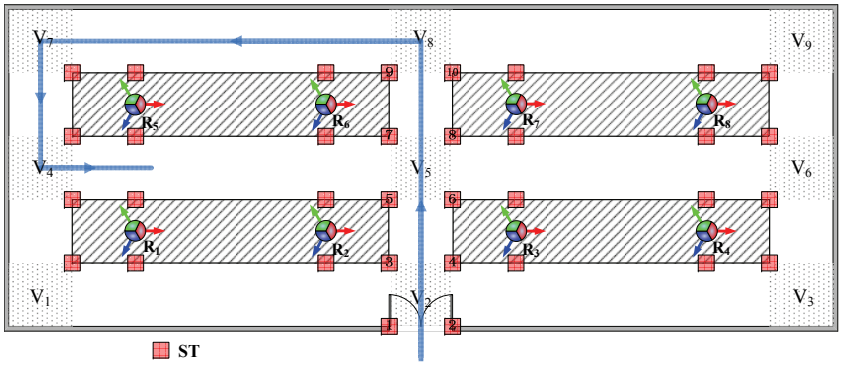

FIGURE 5.4: The RFID system with STs.

Figure 5.4 shows the deployment of a novel RFID system with STs being placed in the corner of the shelves. In the new RFID system with STs, we can also obtain the readings from the STs at time instant τ_k (note that here we ignore the latency due to the reporting from the ST to a reader) and now we denote the kth detection by $y_k = \{i_k, j_k, \tau_k, \boldsymbol{n}_k\}$, where the new argument $\boldsymbol{n}_k$ is a vector of size $\tilde{L} \times 1$, with $\tilde{L}$ being the number of STs in the system. The elements of the vector $\boldsymbol{n}_k$ take values one or zero, depending on if the corresponding ST

detected communication between the reader and the tag. We apply the model of the probability of detection of the STs from [61], which is a function of distance only and is given by $\tilde{p}(\tilde{d}) = 1/(1 + e^{\tilde{\alpha}(\tilde{d}-\tilde{d}_0)})$, where $\tilde{d}$ is the distance between the ST and the tag, whereas $\tilde{\alpha}$ and $\tilde{d}_0$ are model parameters that are estimated from experimental data. The likelihood function in (5.8) is then multiplied by the factor

$$\prod_{i=1}^{\tilde{L}} \left\{ \tilde{p}(\tilde{d}_i^{(m)}) n_{k,i} + (1 - \tilde{p}(\tilde{d}_i^{(m)})(1 - n_{k,i}) \right\}, \tag{5.10}$$

where $n_{k,i} \in \{0, 1\}$ is the ith element of $\boldsymbol{n}_k$, $\tilde{d}_i^{(m)}$ is obtained from the particle state $x_{\tau_k}^{(m)}$ and the known locations of the STs.

An example of the propagation of the particles is shown in Fig. 5.3 (b). The particle cloud quickly merges into one with the proximity information provided by the STs.

5.4 Numerical results

The parameters of the model in (5.3) were obtained by using an Impinj Speedway Reader connected to a single 6 dBIC gain patch antenna and by using Alien Squiggle RFID tags. Both the reader and the tags are compliant with the ISO 180006-C (EPC Gen 2) protocol. The tag was placed in an orientation facing the reader at various distances from the reader's antenna whose power level was set to 23.5 dBm. The reader was programmed to send out queries for a period of 30 s. We measured the probability of detection as a ratio of the number of times the tag was read over the total number of queries sent during the 30 s period.

We simulated two setups. In the first setup, we deployed 8 readers in a warehouse of size 26 m $\times$ 10 m with shelves whose separation was 6 m horizontally

and 4 m vertically as shown in Fig. 5.1. The widths of a path and a shelf were set to 2 m. The noise of the state had a covariance matrix $diag(0.01, 0.01)$ and the initial speed was 1 m/s in the moving direction. The objective was to detect and track the tagged object for a period of 15 s. In the second setup, we included four STs on the shelves' corners with a separation distance of 2 m as shown in Fig. 5.4.

Figure 5.5 shows a tracking run with the two RFID systems. The tracking near the intersections considers the multiple choices. The long detecting range, the short physical distance in the indoor setup and the asynchronism of the detections makes the estimation of direction of movement near intersections challenging. In Fig. 5.5 (a), the target is lost due to the wrong estimation of the direction of movement. However in the system with STs, the direction of movement is estimated correctly with the proximity information given by the STs as shown in Fig. 5.5 (b).

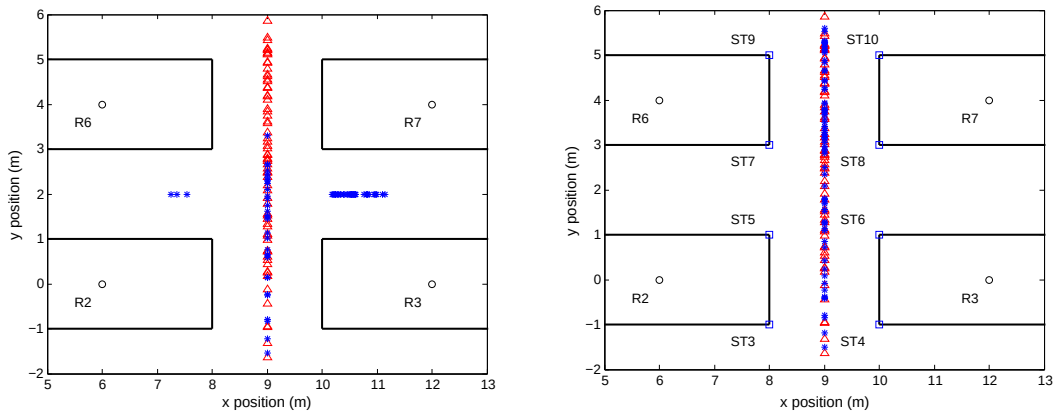

(a) The reader-only system. (b) The system with STs.

FIGURE 5.5: A tracking run in the two systems. The red triangles are the real states and the blue crosses are the tracking results.

Next, we generated 100 independent realizations to measure the tracking performance using the average root mean square error (RMSE) of the position

of the target as a function of time over 100 independent realizations. The RMSE for one realization was calculated as $\sqrt{(\hat{x}_{1,t} - x_{1,t})^2 + (\hat{x}_{2,t} - x_{2,t})^2}$.

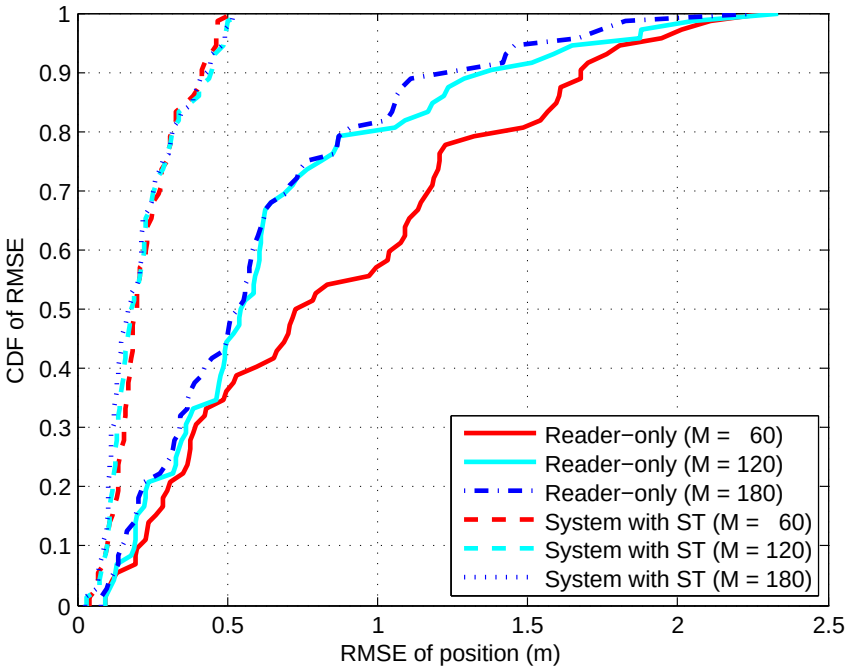

FIGURE 5.6: CDFs of RMSEs for systems with STs and without STs (reader-only).

We compared the performance of the reader-only and the ST-based systems. The cumulative density functions (CDFs) of the RMSEs of the position with the two systems are displayed in Fig. 5.6. The results show that the system with STs has improved tracking performance. The STs reduce the ambiguity of the direction of movement near intersections due to their capability of detecting the tags in their close proximity. We also studied the impact of the particle size M. We can see from Fig. 5.6 that larger M values result in better tracking performance with the reader-only system. For the system with STs, there is no big discrepancy in the tracking performance for different M values. Thus, one can use small particle sizes to

reduce the computation complexity and still achieve satisfactory performance. The advantage brought by the STs is obvious. One can use STs to improve the indoor localization or tracking performance, especially near portals and intersections.

5.5 Summary

In this chapter we addressed the problem of tracking tagged objects in indoor RFID environments using asynchronous binary readings and layout information. The tracking was implemented in an RFID system that contained sense-a-tags with known locations and that provided proximity information to the system about the queried tags. We proposed a multi-hypothesis particle filtering method for tracking so that we account for estimating the direction of movement and/or manoeuvering of the object. We demonstrated the improved accuracy of the proposed method by computer simulations.

6

Real-time Self-tracking with Tag-to-tag Communication

We investigate the problem of real-time self-tracking of tagged objects in a new system with low-cost "smart" tags. These tiny and battery-less devices will play a pivotal role in the infrastructure of the IoT. With capabilities of low-power computation and tag-to-tag backscattered communication, no readers will be needed for running RFID system. In order to allow for low-cost tags, self-tracking has to be performed with simple algorithms while still exhibiting high accuracy. In this chapter we propose a linear observation model for which Kalman filtering is the optimal method. We also consider a nonlinear model for which we apply particle filtering of reduced complexity as the tracking method. The complexity of particle filtering is reduced by a procedure called Rao-Blackwellisation by analytically marginalising some of the linear and Gaussian variables from the joint posterior. The performance and computational complexity of the different methods are compared by computer simulations. The formulation of the self-

tracking problem is presented in Section 6.2. The tracking methods are investigated in Section 6.3. In Section 6.4, performance of the four methods are compared with numerical results. The chapter concludes with some final remarks in Section 6.5.

6.1 Introduction

The Internet of Things is expected to connect physical objects and enable intelligent interactions between them. These objects will have tiny devices that will endow them with the ability to sense signals, process information, and communicate with each other [79]. It is expected that the backbone of the IoT will be the RFID technology and the devices with central role will be RFID tags. A significant progress has been made in developing tags that allow for computing and making decisions based on information collected by onboard sensors. Furthermore, the tags are run by low-power micro-controllers and they harvest ambient energy (e.g., light, RF) [80, 81]. The tags are expected to be cooperative in that they share information whenever necessary. The location and tracking of tags will be of critical importance in the IoT.

Present day RFID systems are composed of two types of components, RFID readers and RFID tags. The latter are of very low cost and the former are rather expensive. Clearly, the cost of the readers raises scalability issues if one envisions large infrastructure of RFID readers in the IoT [79]. On the other hand, one can readily attach tags to trillions of objects with the objective that the tags interact with each other with the ultimate goal of improving daily life [4]. In order to allow for interaction, the RFID tags of today have to be improved.

In this chapter, we investigate the problem of real-time self-tracking of RFID tags that operate in a system *without* RFID readers [82]. The tags harvest energy

from a continuous wave generated by an external exciter or an ambient RF signal [83]. The tags can broadcast information to neighboring tags by backscattering. Thereby, one can argue, these tags can accomplish tag-to-tag communication [84]. Some of the tags in the system know their locations, and they backscatter this information about them periodically. Nearby moving tags read these signals and use it for self-tracking.

Tags with the ability to read other tag signals have already been introduced in [75, 74]. The use of these tags for indoor tracking in systems with RFID readers has been studied, and improved accuracy with them has been reported [85, 61]. We also note that indoor tag tracking with conventional RFID systems has extensively been studied in the wide literature, for instance in [56, 73, 62, 86].

Unlike the work in the previous chapters, here we seek solutions for the self-tracking problem in a system of low-cost RFID tags where the system does not contain readers. The solution is simple enough to perform well on a tag with limited computational ability. The complexity of the self-tracking problem addressed here strongly depends on the considered observation model. We first propose a linear model that can optimally be tackled by Kalman filtering (KF). We also formulate a more precise nonlinear distance-based model for which we propose to use a particle filtering (PF) algorithm of reduced complexity [50]. We compare by computer simulations the tracking performance of four different methods - tracking by association, KF, PF and RBPF. We also analyze the computational complexity of the four methods. The main contributions of this chapter are a) the formulation of the self-tracking problem in a system with RFID tags only where the tags can decode backscattered signals and b) the proposal of self-tracking algorithms with relatively low computational complexity while still exhibiting high accuracy.

6.2 Problem formulation

We consider the problem of self-tracking in a new RFID system with tags only. The tags backscatter information that can be read by tags that are in their proximity. The system has two types of tags: stationary tags that know their locations (also called reference tags) and mobile tags that are tasked to do self-tracking. Figure 6.1 shows an example with three reference tags T_1, T_2, T_3 with known locations and a self-tracking tag T_4. The tags are powered by nearby exciters that emit CWs. The goal of the mobile tag is to perform self-tracking in real time with only backscattered information that comes from the reference tags. This information comes aperiodically at random instants of time.

The main challenges are: 1) only one observation with proximity information can be used at a time due to the requirement of real-time tracking; 2) no complicated tracking algorithms can be applied due to the limited computational ability of the mobile tag; and 3) only simple protocols can be carried out due to the low-power backscattered communication.

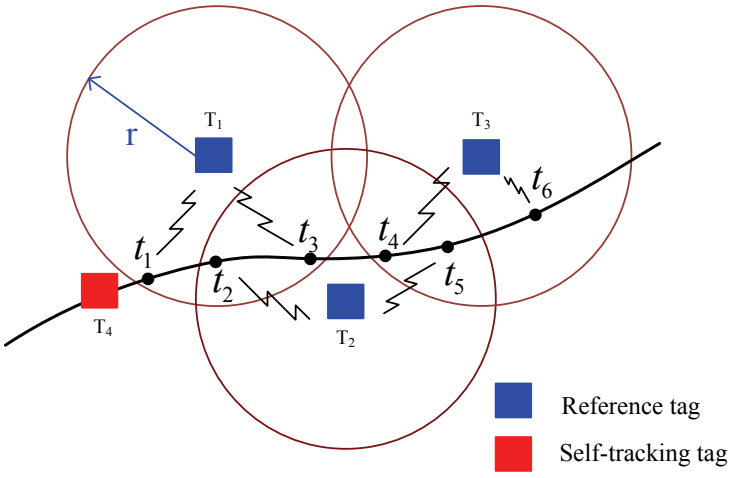

FIGURE 6.1: A self-tracking scenario.

6.2.1 System description

Here we provide a more precise description of the system. As pointed out, the reference tags backscatter information about their locations. If a self-tracking tag moves close to a reference tag that backscatters so that it is in its sensing range r, it will pick up the backscattered signal, decode it, and perform an update of its location. A protocol that the reference tags may use is the all-tag-talk strategy where all the tags have equal rights to "talk" by modulating the external CW. This is done with a certain rate in a randomized Aloha-based strategy to reduce the probability of collision of the backscatterings.

6.2.2 The motion model

The state of the system consists of a vector containing information about the self-tracking tag at time instant t and is denoted by $\boldsymbol{x}_t \in \mathbb{R}^{2J\times 1}$, where $J \in \{1,2,3\}$ is the number of dimensions of interest, $\boldsymbol{x}_t = [x_{1,t}\ \dot{x}_{1,t}\ \cdots\ x_{J,t}\ \dot{x}_{J,t}]^\top$ where $x_{j,t}$ and $\dot{x}_{j,t}$ represent the coordinate and the velocity of the mobile tag in the jth dimension, respectively. That tag moves from t_1 to t_2 according to the model

$$\boldsymbol{x}_{t_2} \;=\; \boldsymbol{A}(t_1,t_2)\boldsymbol{x}_{t_1} + \boldsymbol{B}(t_1,t_2)\boldsymbol{u}_{t_2}, \tag{6.1}$$

where $\boldsymbol{x}_{t_2}$ is the state of the system at time instant t_2, $\boldsymbol{u}_{t_2} \in \mathbb{R}^{J\times 1}$ is a noise vector with a known distribution, and $\boldsymbol{A} \in \mathbb{R}^{2J\times 2J}$ and $\boldsymbol{B} \in \mathbb{R}^{2J\times J}$ are known matrices, respectively, given by

$$\boldsymbol{A} = \boldsymbol{I} \otimes \begin{bmatrix} 1 & \Delta t \\ 0 & 1 \end{bmatrix} \quad \text{and} \quad \boldsymbol{B} = \boldsymbol{I} \otimes \begin{bmatrix} \frac{\Delta t^2}{2} \\ \Delta t \end{bmatrix},$$

where $\otimes$ denotes the Kronecker product, $\Delta t = (t_2 - t_1)$ and $\boldsymbol{I}$ is the identity matrix with size $J \times J$.

6.2.3 *The observation model*

In the system, the reference tags start backscattering rounds asynchronously at different time instants. Without loss of generality, we assume the same rate for all the tags with a period of T_s. Figure 6.2 shows the backscattering time line and the asynchronous measurements for the example from Fig. 6.1. The ith reference tag T_i backscatters signals with information about its location. The backscattering starts at a random slot during each T_s. Here $\Delta\tau$ is the random interval after which T_1 backscatters during the first T_s. As shown in the figure, a collision occurs because T_1 and T_2 chose to backscatter at the same time slot at τ_2. At τ_1, τ_3, τ_4 and τ_5, the backscattered signals cannot reach the mobile tag because it is far away from them.

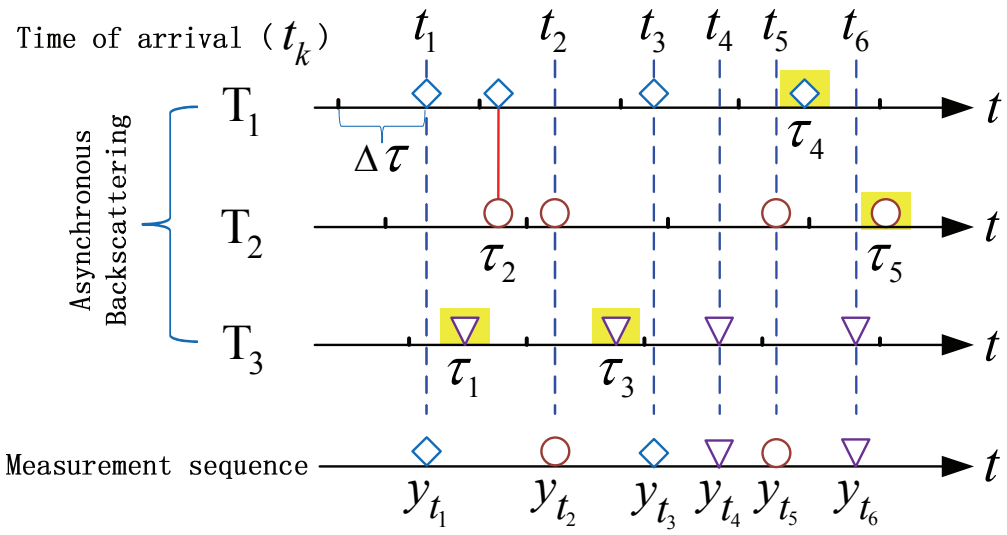

FIGURE 6.2: Backscattering time line with asynchronous measurements. The red solid line represents collision, and the yellow shaded boxes indicate that the backscattered signal cannot reach the target.

We denote the kth signal decoded by the mobile tag by $\boldsymbol{y}_{t_k} = \boldsymbol{l}_i$, where

$i \in \{1, 2, \cdots, L\}$ is the index of the reference tag whose backscattering is picked up at time t_k and $\boldsymbol{l}_i \in \mathbb{R}^{J\times 1}$ is the location of the ith tag in the J-dimensional Cartesian coordinate system. We note that $t_1 < t_2 < t_3 < \cdots$. The objective of the mobile tag is to perform self-tracking given the sequence of asynchronous observations.

6.3 Tracking methods

We assume that there are L reference tags with known positions $\boldsymbol{l}_i$ where $i = 1, 2, \cdots, L$ and one moving tag with unknown positions and velocities, $\boldsymbol{x}_t$. The mobile tag estimates $\boldsymbol{x}_t$ as soon as it receives a backscattered signal from a reference node. Our main goal is to develop an algorithm that can perform well on the mobile tag under the constraints of limited computational ability and real-time processing. Therefore, the processing rate of the mobile tag must be greater than the arriving rate of the measurements. We studied three methods for self-tracking. They are based on i) association or nearest neighbor (NN) [50] ii) KF [29], and iii) PF [66] iv) RBPF [87].

6.3.1 Association

The association method is the simplest, the fastest and the most adaptive to dynamic changes of the environment of all the methods. With this method we simply estimate the target's location by equating it with that of the sensed reference tag [50]. The main drawback of association is that its performance completely relies on the spatial distribution of the reference tags and the sensing range of the mobile tag. When the mobile tag is in an area where it can sense more than one reference tag in a short period of time, and since it only processes one measurement at a

time, the tracking will result in zigzagging.

6.3.2 Kalman Filter

If the mobile tag employs Bayesian inference, it estimates the posterior distribution $p(\boldsymbol{x}_{t_2}|\mathcal{Y}_{t_2})$ at time t_2 given $p(\boldsymbol{x}_{t_1}|\mathcal{Y}_{t_1})$ and the propagation distribution $p(\boldsymbol{x}_{t_2}|\boldsymbol{x}_{t_1})$, where $\mathcal{Y}_{t_k}$ denotes all the measurements collected up to time t_k. The propagation distribution is defined by the motion model in (6.1) and the likelihood function is defined by the observation model. According to Bayes' rule, the states of the target can be obtained by

$$\begin{aligned} f(\boldsymbol{x}_{t_2}|\mathcal{Y}_{t_2}) \quad &\propto \quad f(\boldsymbol{y}_{t_2}|\boldsymbol{x}_{t_2}) \\ &\times \int f(\boldsymbol{x}_{t_2}|\boldsymbol{x}_{t_1}) f(\boldsymbol{x}_{t_1}|\mathcal{Y}_{t_1}) d\boldsymbol{x}_{t_1}. \end{aligned} \tag{6.2}$$

The update from $f(\boldsymbol{x}_{t_1}|\mathcal{Y}_{t_1})$ to $f(\boldsymbol{x}_{t_2}|\mathcal{Y}_{t_2})$ can be accomplished by various types of filters. The KF method has a closed-form solution when the state and observation models are linear and the noises $\boldsymbol{u}_{t_2}$ and $\boldsymbol{v}_{t_2}$ are Gaussian. Because of its simplicity, we first propose a linear observation model. Suppose that at time t_2, the self-tracking tag receives a measurement $\boldsymbol{y}_{t_2}$, which is the location of a reference tag whose backscattering is picked up as described in Section 2.3. We model $\mathcal{Y}_{t_2}$ according to

$$\boldsymbol{y}_{t_2} = \boldsymbol{H}\boldsymbol{x}_{t_2} + \boldsymbol{v}_{t_2}, \tag{6.3}$$

where $\boldsymbol{y}_{t_2} \in \mathbb{R}^{J\times 1}$ and $\boldsymbol{v}_{t_2} = [v_{1,t_2}, \cdots, v_{J,t_2}]^T$ is a random vector that accounts for the location uncertainty. The matrix $\boldsymbol{H}$ is defined by

$$\boldsymbol{H} = \boldsymbol{I} \otimes [1 \quad 0] \tag{6.4}$$

where $\boldsymbol{I}$ is the identity matrix of size $J \times J$.

The distribution of the location uncertainty $\boldsymbol{v}_{t_2}$ can be estimated from experimental measurements and by exploring the spatial relationships among the tags off-line and prior to tracking as discussed in [61]. In order to reduce the complexity and to apply the KF method, here we assume $\boldsymbol{v}_{t_2}$ to be Gaussian-distributed, i.e., $\mathcal{N}(\mathbf{0}, \boldsymbol{G})$, where $\boldsymbol{G}$ is the covariance matrix of the noise. We chose $\boldsymbol{G} = diag(r^2/2, r^2/2)$, where r is the sensing range of the mobile tag.

6.3.3 Particle Filter

A nonlinear distance-based observation model can be also considered as in Chapter 4 [85, 61, 56, 73, 62]. There, the probability of detecting a tag is modeled as a function of the distance. Since this model is nonlinear, an appropriate method for working with it is PF. With PF, one approximates the posterior density of the unknown state by using random measures composed of particles and weights associated to the particles. More specifically, the observation model is a Bernoulli distribution with the probability of detection modeled by

$$p(d) = \frac{1}{1 + e^{a_1 + a_2 d}}, \tag{6.5}$$

where a_1 and a_2 are the model parameters, which can be obtained from real experimental data, and d is the distance between the mobile tag and the backscattering reference tag. The details of the PF algorithm that uses this model can be found Chapter 4 and 5 [62, 85, 61]. Here, however, we attempt to use the method with very low number of particles so that we reduce the computational burden of the mobile tag.

6.3.4 Rao-Blackwellised Particle Filter

There is a linear sub-structure in (6.1), which can be used to obtain better estimates of the linear states using Rao-Blackwellization by analytically marginalising some of the linear and Gaussian variables from the joint posterior. We call it Rao-Blackwellised Particle Filter (RBPF). The idea of RBPF is to use the Kalman filter to solve the linear part of the state space model and the Particle filter to solve the nonlinear part [87, 88, 89].

The mobility model can be rewritten as follows:

$$\begin{bmatrix} \boldsymbol{x}_{t_2}^n \\ \boldsymbol{x}_{t_2}^l \end{bmatrix} = \begin{bmatrix} \boldsymbol{I} & \boldsymbol{A}^n \\ \boldsymbol{0} & \boldsymbol{A}^l \end{bmatrix} \begin{bmatrix} \boldsymbol{x}_{t_1}^n \\ \boldsymbol{x}_{t_1}^l \end{bmatrix} + \begin{bmatrix} \boldsymbol{B}^n \\ \boldsymbol{B}^l \end{bmatrix} \cdot \boldsymbol{u}_{t_2} \tag{6.6}$$

$$\boldsymbol{y}_{t_2} = h(\boldsymbol{x}_{t_2}^n) + \boldsymbol{v}_{t_2} \tag{6.7}$$

where, $\boldsymbol{x}_{t_2}^n = [x_{1,t_2}, ..., x_{J,t_2}]^T$ and $\boldsymbol{x}_{t_2}^l = [\dot{x_{1,t_2}}, ..., \dot{x_{J,t_2}}]^T$ are a partition of the state vector at time instant t_2. The noise $\boldsymbol{u}_{t_2}$ is assumed to be white and Gaussian distributed according to $\boldsymbol{u}_{t_2} = \begin{bmatrix} \boldsymbol{u}_{t_2}^l \\ \boldsymbol{u}_{t_2}^n \end{bmatrix} \sim N(\boldsymbol{0}, \boldsymbol{Q}_{t_2})$

Using Bayes rule, we have

$$P(\boldsymbol{x}_{t_2}^l, \boldsymbol{x}_{t_2}^n | \mathcal{Y}_{t_2}) = \underbrace{P(\boldsymbol{x}_{t_2}^l | \boldsymbol{x}_{t_2}^n, \mathcal{Y}_{t_2})}_{KF} \cdot \underbrace{P(\boldsymbol{x}_{t_2}^n | \mathcal{Y}_{t_2})}_{PF}, \tag{6.8}$$

where $\mathcal{Y}_{t_2}$ is a collection of the measurement up to time t_2.

Since the measurement $\mathcal{Y}_{t_2}$ are conditionally independent on $\boldsymbol{x}_{t_2}^l$, the probability $P(\boldsymbol{x}_{t_2}^l | \boldsymbol{x}_{t_2}^n, \mathcal{Y}_{t_2})$ can be written as $P(\boldsymbol{x}_{t_2}^l | \boldsymbol{x}_{t_2}^n, \mathcal{Y}_{t_2}) = P(\boldsymbol{x}_{t_2}^l | \boldsymbol{x}_{t_2}^n)$

Consider now the linear part of the system and assume a fictitious observation

$\boldsymbol{z}_{t_2}$:

$$KF: \begin{cases} \boldsymbol{x}_{t_2}^l = \boldsymbol{A}^l \boldsymbol{x}_{t_1}^l + \boldsymbol{B}^l \boldsymbol{u}_{t_2}^l \\ \boldsymbol{z}_{t_2} = \boldsymbol{A}^n \boldsymbol{x}_{t_1}^l + \boldsymbol{B}^n \boldsymbol{u}_{t_2}^n \end{cases} \tag{6.9}$$

where $\boldsymbol{z}_{t_2} = \boldsymbol{x}_{t_2}^n - \boldsymbol{x}_{t_1}^n$, since the system (4) is linear and Gaussian, the optimal solution is provided by KF, therefore we can obtain

$$P(\boldsymbol{x}_{t_2}^l | \boldsymbol{x}_{t_2}^n) \sim N(\hat{\boldsymbol{x}}_{t_2|t_1}^l, \boldsymbol{P}_{t_2|t_1}^l) \tag{6.10}$$

where the estimate vector $\hat{\boldsymbol{x}}_{t_2|t_1}^l$ and the corresponding covariance matrix $\boldsymbol{P}_{t_2|t_1}^l$ are calculated by KF.

For the nonlinear part of the system, we apply a KF to solve

$$P(\boldsymbol{x}_{t_2}^n | \mathcal{Y}_{t_2}) = \frac{P(\boldsymbol{y}_{t_2} | \boldsymbol{x}_{t_2}^n) P(\boldsymbol{x}_{t_2}^n | \mathcal{X}_{t_1}^n)}{P(\boldsymbol{y}_{t_2} | \mathcal{Y}_{t_1})} \cdot P(\mathcal{X}_{t_1}^n | \mathcal{Y}_{t_1}), \tag{6.11}$$

where $\mathcal{X}_{t_1}^n = \boldsymbol{x}_{0:t_1}$ and $\mathcal{Y}_{t_1} = \boldsymbol{y}_{0:t_1}$.

The prediction step in PF is done using

$$\boldsymbol{x}_{t_2}^{n,(m)} \sim N\left(\boldsymbol{x}_{t_1}^{n,(m)} + \boldsymbol{A}^n \boldsymbol{x}_{t_1|t_0}^{l,(m)}, \boldsymbol{A}^n \boldsymbol{P}_{t_1|t_0}^l (\boldsymbol{A}^n)^T + \boldsymbol{B}^n \boldsymbol{Q}_{t_1} (\boldsymbol{B}^n)^T\right) \tag{6.12}$$

The prediction of the non-linear variables $\boldsymbol{x}_{t_2}^n$ improves the extimates of $\boldsymbol{x}_{t_2}^l$. Moreover, for each particle, one KF estimate $\boldsymbol{x}_{t_2|t_1}^{l,(m)}, m = 1, ..., M$.

$$\boldsymbol{K}_{t_1} = \boldsymbol{P}_{t_1|t_0}^l (\boldsymbol{A}^n)^T \cdot \boldsymbol{S}_{t_1}^{-1} \tag{6.13}$$

where

$$\boldsymbol{S}_{t_1} = \boldsymbol{A}^n \boldsymbol{P}_{t_1|t_0}^l (\boldsymbol{A}^n)^T + \boldsymbol{B}^n \boldsymbol{Q}_{t_1} (\boldsymbol{B}^n)^T \tag{6.14}$$

$$\boldsymbol{x}_{t_1|t_1}^{l,(m)} = \boldsymbol{x}_{t_1|t_0}^{l,(m)} + \boldsymbol{K}_{t_1} (\boldsymbol{z}_{t_1}^{(m)} - \boldsymbol{A}^n \cdot \boldsymbol{x}_{t_1|t_0}^{l,(m)}) \tag{6.15}$$

$$\boldsymbol{P}^{l}_{t_1|t_1} = \boldsymbol{P}^{l}_{t_1|t_0} - \boldsymbol{K}_{t_1}\boldsymbol{A}^{n} \cdot \boldsymbol{P}^{l}_{t_1|t_0} \tag{6.16}$$

where

$$\boldsymbol{z}^{(m)}_{t_1} = \boldsymbol{x}^{n,(m)}_{t_2} - \boldsymbol{x}^{n,(m)}_{t_1} \tag{6.17}$$

is the fictitious measurement representing difference between the estimated and predicted locations of the particles.

$$\boldsymbol{x}^{l,(m)}_{t_2|t_1} = \bar{\boldsymbol{A}}^{l} \cdot \boldsymbol{x}^{l,(m)}_{t_1|t_1} + \boldsymbol{B}^{l}(\boldsymbol{B}^{n})^{-1} \cdot \boldsymbol{z}^{(m)}_{t_1} \tag{6.18}$$

$$\boldsymbol{P}^{l}_{t_2|t_1} = \bar{\boldsymbol{A}}^{l} \cdot \boldsymbol{P}^{l}_{t_1|t_1} \cdot (\bar{\boldsymbol{A}}^{l})^{T} \tag{6.19}$$

where

$$\bar{\boldsymbol{A}}^{l} = \boldsymbol{A}^{l} - \boldsymbol{B}^{l}(\boldsymbol{B}^{n})^{-1}\boldsymbol{A}^{n} \tag{6.20}$$

Table 6.1 shows the RBPF algorithm for our tracking problem.

6.4 Numerical results

We simulated a setup with 10 reference tags placed on a portal and shelves in a warehouse along where the width between the shelves was 2 m. The setting is displayed in Fig. 6.3. The noise of the state had a covariance matrix $diag(0.01, 0.01)$ and the initial speed was $[0.1, 1]$ m/s. We set $T_s = 0.5$ s. If all the reference tags were in the range of the mobile tag, the maximum arriving rate was 20 measurements per second. Therefore, the processing time for one measurement could not exceed a threshold $\gamma = 1/20 = 0.05$ s. The threshold γ is even smaller with a higher density of the nodes. As a result, only simple algorithms with low

Table 6.1: RBPF algorithm for tracking

INITIALIZATION:
$\boldsymbol{x}_{t_1\|t_0}^{l,(m)} \sim \boldsymbol{P}_{\boldsymbol{x}_0^n}(\boldsymbol{x}_0^n)$ $\left\{\boldsymbol{x}_{t_1\|t_0}^{l,(m)}, \boldsymbol{P}_{t_1\|t_0}^{l}\right\} = \left\{\boldsymbol{x}_0^l, P_0\right\}$ and $w_{t_1}^{(m)} = 1/M, \quad \forall\ m.$ where $[\boldsymbol{x}_0^n; \boldsymbol{x}_0^l]$ is the prior knowledge of the states.
RECURSION:
1) PF Prediction: Predict the particles $\boldsymbol{x}_{t_2}^{n,(m)}, \quad \forall\ m$ according to (6.12). 2) KF Prediction: Predict the particles $\boldsymbol{x}_{t_2\|t_1}^{l,(m)}$ according to (6.13) - (6.20). 3) Weight Update: $\widetilde{w}_{t_2}^{(m)} = w_{t_1}^{(m)} \mathcal{L}(y_{t_2}\|\boldsymbol{x}_{t_2}^{n,(m)})$ where the likelihood $\mathcal{L}(y_{t_2}\|\boldsymbol{x}_{t_2}^{n,(m)})$ is calculated from (6.5) with $d_{t_2}^{(m)} = \sqrt{(x_{1,t_2}^{(m)} - l_{i,x})^2 + (x_{2,t_2}^{(m)} - l_{i,x})^2}$. Normalize the weights $w_{t_2}^{(m)} = \widetilde{w}_{t_2}^{(m)} / \sum_{m=1}^{M} w_{t_2}^{(m)}$. 4) Estimation: $\hat{\boldsymbol{x}}_{t_2}^{n} = \sum_{m=1}^{M} w_{t_2}^{(m)} \boldsymbol{x}_{t_2}^{n,(m)}$ $\hat{\boldsymbol{x}}_{t_2}^{l} = \sum_{m=1}^{M} w_{t_2}^{(m)} \boldsymbol{x}_{t_2\|t_1}^{l,(m)}$ 5) Resampling: Resample $\left\{\boldsymbol{x}_{t_2}^{n,(m)}, \boldsymbol{x}_{t_2}^{l,(m)}\right\}$ in the same way as in the PF. 6) Proceed to t_3: Assign $t_1 = t_2,\ t_2 = t_3$ and repeat 1) - 5).

time-complexity can be accepted for real-time tracking. The mobile tag was self-tracking in a two-dimensional space by using the received observations for a period of 12 s while it moved along the path between the shelves. Figure 6.3 shows a tracking run with the new tag system.

Next, we generated the time sequence of backscattering or "talk" for each tag by simulating the "all-tag-talk" protocol mentioned in Section 2. Then, we generated 100 trajectories for the three methods and for each trajectory 50 independent

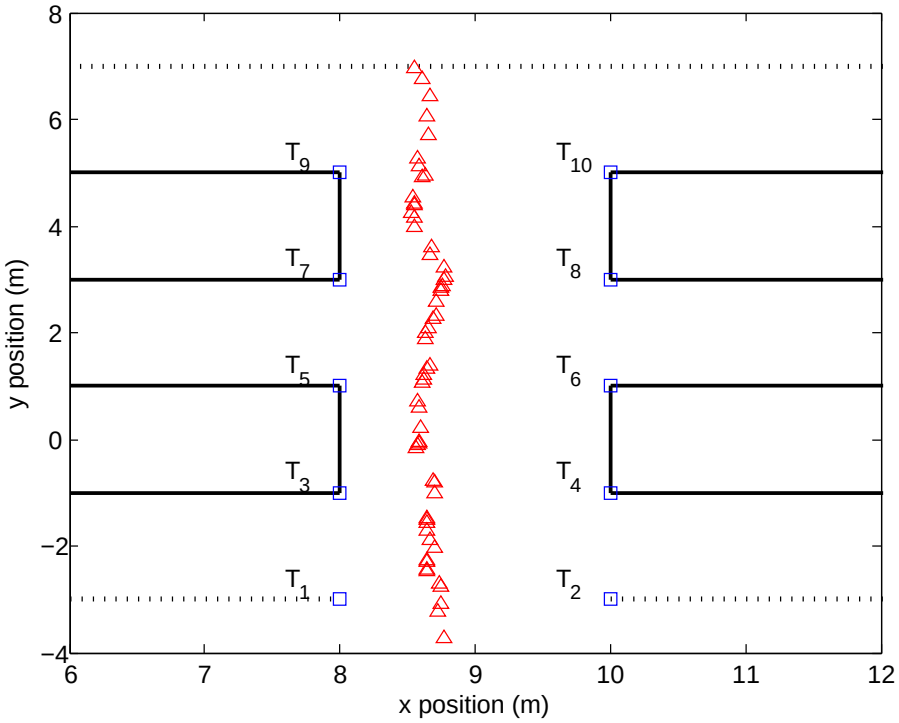

FIGURE 6.3: A tracking realization with the new tag system.

realizations for the PF algorithm. The tracking performance was measured by means of the root mean square error (RMSE) of the position of the mobile tag as a function of time.

In the first experiment, we compared the tracking performance with the four methods. The cumulative density functions (CDFs) of the RMSEs of the position with the four methods are displayed in Fig. 6.4 and note that we used $M = 30$ particles for both PF and RBPF. The results show that the tracking accuracy of RBPF is almost the same as that of the PF method.

In the second experiment, we compared the tracking performance of the NN and KF methods with different sensing ranges. The CDFs of the RMSEs are displayed in Fig. 6.5. The results in Table 6.2 show that the KF method performs better

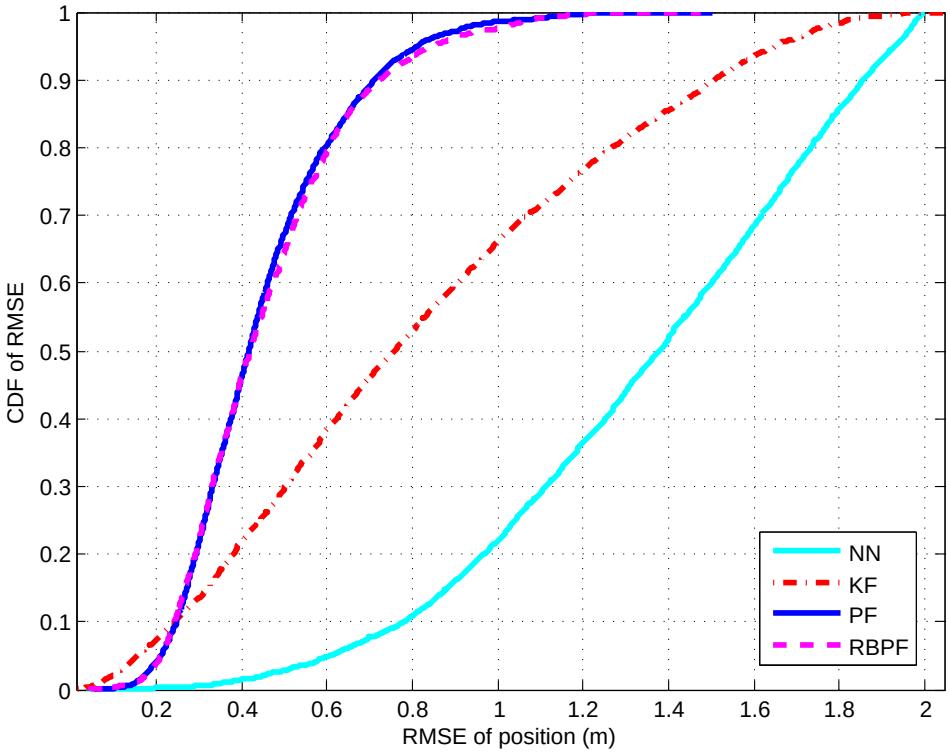

FIGURE 6.4: CDFs of RMSEs for the four methods with $r = 2$ m.

than the NN method with an average improvement of 0.5 m of RMSE. It also shows that the tracking performance with sensing range $r = 1.5$ m performs better than with $r = 2$ m and $r = 2.5$ m. The optimal range depends on the number of reference tags and their deployment topology.

In the third experiment, we also compared the tracking performance of the KF and PF methods with $r = 2$ m and studied the impacts of the particle size M. The results are shown in Fig. 6.6.

Table 6.3 shows the approximate computational complexity scale using the processing time of NN as a baseline. The processing time for the NN method is 0.2855 μs using the Matlab platform with a desktop computer CPU. Clearly, the processing time is platform- and device-dependent and therefore we only compare

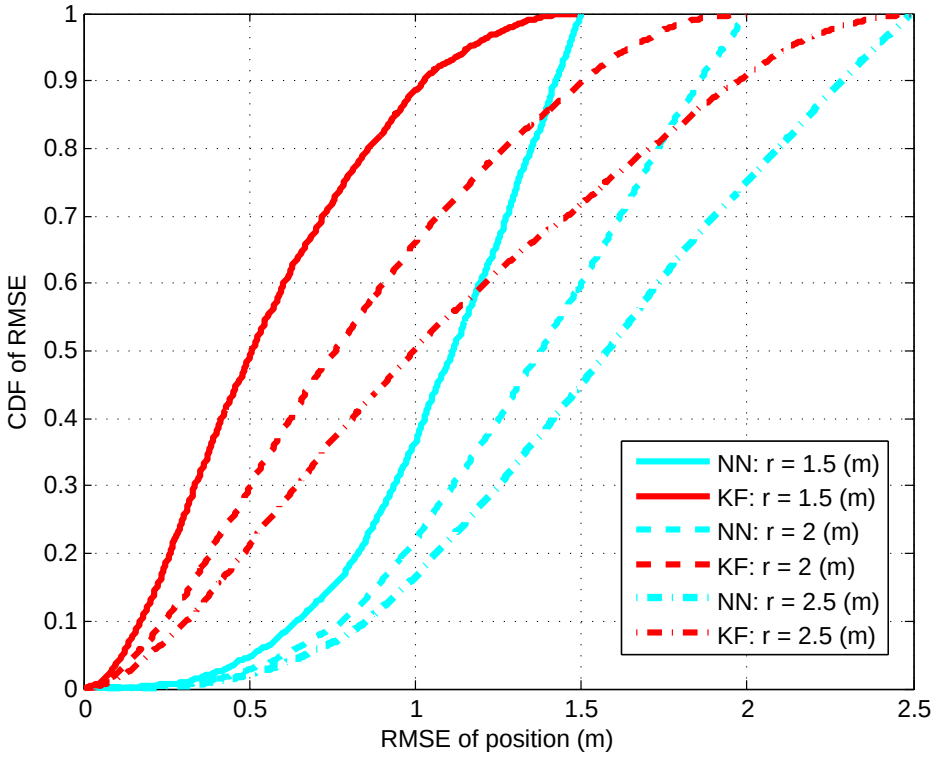

FIGURE 6.5: CDFs of RMSEs for the KF and NN methods with different sensing ranges r.

the ratio of the run-times of the other methods and the NN method. The results show that the KF is about 10 times slower than the NN, while the PF with $M = 10$ particles is 10 times slower than the KF. The processing time for the PF increases linearly with the size of M. Table 6.4 shows the ratio of the runtime between the RBPF and PF methods. It can be seen that the RBPF can achieve a reduction of 15% of the runtime when $M = 30$. One can use RBPF to improve the PF when a linear subspace exists in the state-space equations.

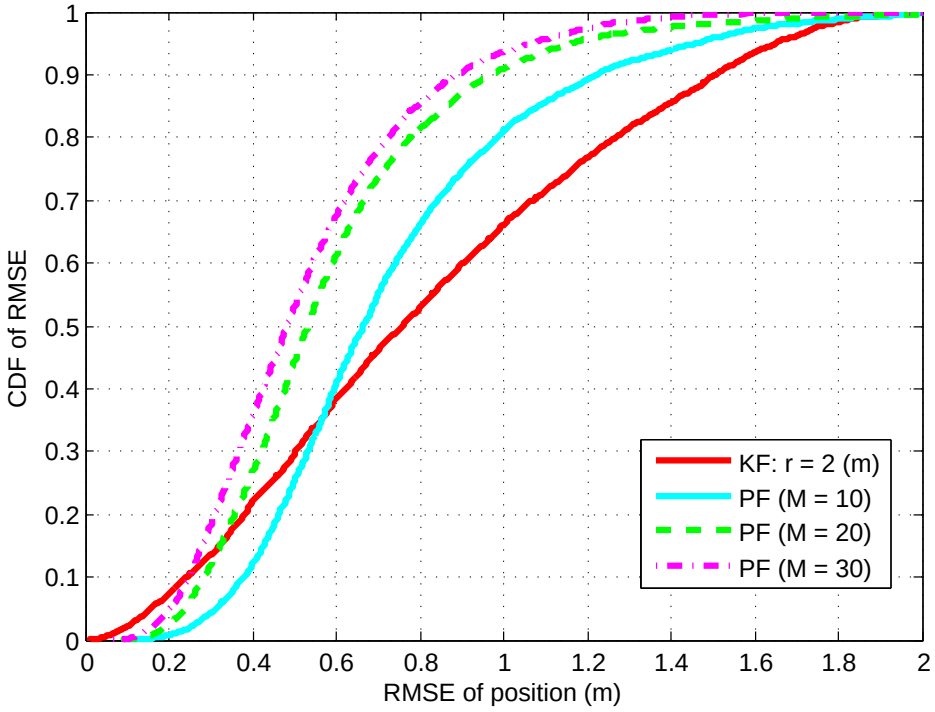

FIGURE 6.6: CDFs of RMSEs of the KF and PF methods (with different number of particles M) for $r = 2$ m.

Table 6.2: The average RMSEs of different methods

r (m)	averageRMSE (m)				
	NN	KF	PF		
			M = 10	M = 20	M = 30
r = 1.5	1.0720	0.5611	0.6466	0.5484	0.5183
r = 2	1.3391	0.8203	0.7351	0.5886	0.5340
r = 2.5	1.5643	1.0782	0.8046	0.6513	0.5812

Table 6.3: Run time of the methods

NN	KF	PF		
		M = 10	M = 20	M = 30
1 (2.8554e-007s)	10	100	200	300

Table 6.4: Run time ratio of the RBPF and PF methods

M = 10	M = 20	M = 30
0.9422	0.8806	0.8435

6.5 Summary

In this chapter, we introduced the problem of self-tracking in a system of low-cost RFID tags where the system does not contain readers. We explored tracking algorithms of low complexity but yet with accurate performance. We introduced a simple linear observation model to allow for the use of Kalman filtering. We also investigated a more ambitious model that is nonlinear and applied particle filtering with a small number of particles. An improvement of the particle filtering was obtained with Rao-Blackwellisation by analytically marginalising the linear part of the state model. We compared the tracking performances and the computational complexities of these methods as well as of the association-based algorithm.

7

Non-centralized Target Tracking in Networks of Binary Directional Sensors

The localization and tracking algorithms discussed in the previous chapters are implemented in a centralized way, where the measurements obtained by all the nodes (readers) are sent to a central unit for the processing. The centralized methods may require energy-intensive communications over large distances or non-negligible delays due to the multiple hops in order to arrive the cental unit, resulting in poor scalability. Furthermore, the centralized processing is not robust because of a possible failure of the central unit. By contrast, a decentralized technique without a central unit use in-network processing and neighbor-to-neighbor communications can achieve low energy consumption, high robustness to node failure, and scalability. In this chapter we will discuss a non-centralized method, where each node implements the algorithm based on its own measurement or measurements received from other nodes. We first present the problem of non-centralized tracking in a general sensor network. Specifically, the directional sensors

are used as the tracking nodes, which detect targets within a range and a predefined direction. The sensors provide only binary decisions regarding whether a target was detected, that is, they transmit a signal only if one of their sensors detects a target. We formulate the problem in section 7.2 and present the proposed solutions to the tracking problem in Section 7.3. The performance of the proposed methods is shown with extensive computer simulations in Section 7.4. We then discuss the extension of the methods into the novel RFID systems in Section 7.5, where a novel device called sense-a-tag is introduced for the non-centralized setup.

7.1 Introduction

We study the target tracking problem with a special class of sensors: directional sensors. These sensors detect targets within a range and a predefined direction. The nodes of the sensors report only binary information indicating their detection of a target [90, 91, 92].

The network is composed of nodes, where each node has four directional sensors providing a coverage of 360° in [93, 94]. The information sensed by the sensors is processed locally by the nodes by some type of cooperative method so that the tracking is conducted in a non-centralized way. The motivation for this comes from the requirement of avoiding intensive communication over large distances so that battery-operated sensor nodes can last longer. In general, non-centralized processing can be implemented by consensus-based methods where sensors locally process their data and exchange their estimates with their neighbors until convergence is reached [95, 96, 97, 98]. The other possibility is to have the nodes exchange and relay the measurements of all the sensors so that all the processing nodes in the network (all or a few of them) have the necessary data

to produce the required estimates [99]. In this chapter, we deal with the second implementation.

To address the challenges of limited communication and power resources, we apply the method which compresses the complete measurements to binary decisions of whether a target is or is not detected by a sensor. Only the excess or non-excess of the observed signal over a threshold indicating the presence or absence of the target in a sensor's proximity is reported as '1's and '0's [55]. With motion models of the target and observation models of the sensors, adaptive filters can be used for estimating position. The observation model depends on the type of sensors. In our work with acoustic sensors, the sensed information is the intensity (signal power) of the transmitted signals by the source that attenuates as a function of distance from the source. And the transmitted information is the binary decisions. Other sensing modalities can also be used. Due to the high nonlinearity of the observation model, we explore the implementation of tracking by particle filtering [29].

7.2 Problem formulation

The mathematical representation of the problem of non-centralized tracking with a network of directional sensors will be introduced in this section.

7.2.1 Directional sensor network description

The targets move in a field of $4N$ directional sensors deployed at N different locations given by $\boldsymbol{r}_n = [r_{1,n}\ r_{2n}]^\top$, $n = 1, 2, \cdots, N$ as shown in Fig. 7.1(a), where at each node there are four collocated directional sensors providing a coverage of 360°. More specifically, each of the sensors at a node "views a 90° of the space"

as shown in Fig. 7.1(b). The first of the four sensors covers the northeast (NE), the second the northwest (NW), the third the southwest (SW), and the fourth, the southeast (SE) direction of the node, respectively.

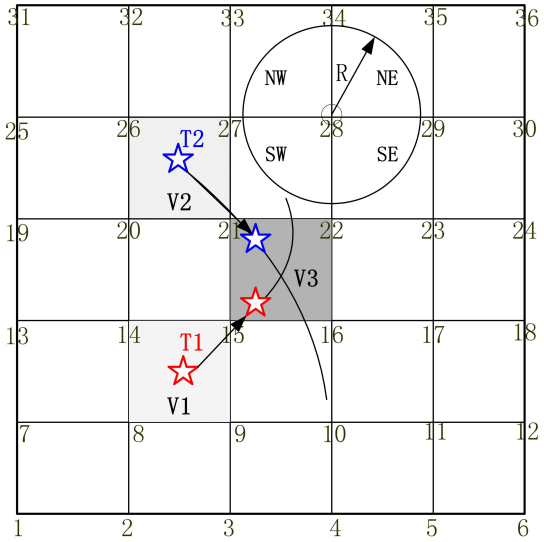

(a) The network deployment.

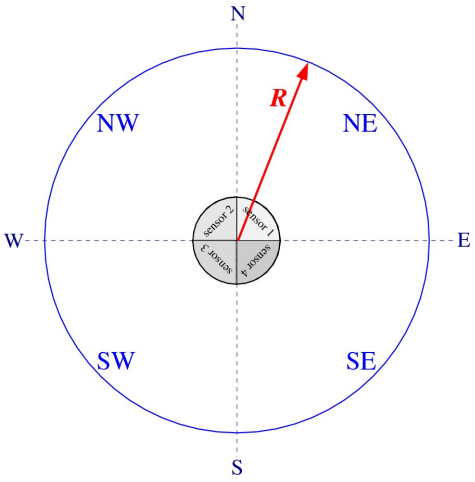

(b) Four co-located sensors at a node.

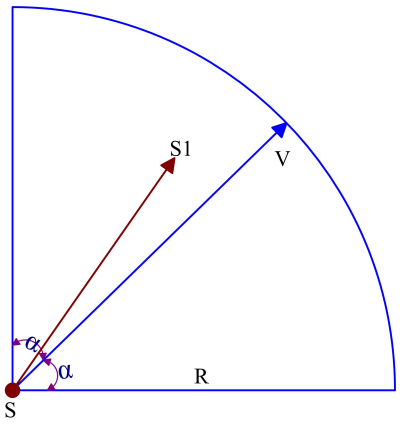

(c) An NE directional sensor.

FIGURE 7.1: The directional sensor network model.

Figure 7.1(c) shows the geometrical model of a directional sensor. Ideally

without noise, a target S_1 is said to be detected by the NE sensor S if and only if $d(S, S_1) \leqslant R$, and the angle of $\overrightarrow{SS_1}$ is within $[\measuredangle\overrightarrow{V} - \alpha, \measuredangle\overrightarrow{V} + \alpha]$, where R is the sensor range and α is half of the field of view. That is, $||\overrightarrow{SS_1}|| \leqslant R$ and $\overrightarrow{SS_1} \cdot \overrightarrow{V} \geqslant ||\overrightarrow{SS_1}|| \cos\alpha$. In our setup, α is fixed at 45° and $\overrightarrow{V}$ is defined as the direction of each sensor with values $\overrightarrow{V_k} = [\frac{\sqrt{2}}{2}, -\frac{\sqrt{2}}{2}]$, $[-\frac{\sqrt{2}}{2}, \frac{\sqrt{2}}{2}]$, $[-\frac{\sqrt{2}}{2}, -\frac{\sqrt{2}}{2}]$ and $[\frac{\sqrt{2}}{2}, -\frac{\sqrt{2}}{2}]$ for $k = 1, 2, 3, 4$ corresponding to the NE, NW, SW and SE sensors of the node, respectively.

The sensors provide only binary decisions regarding whether a target was detected. The nodes of the sensors broadcast the identification number of these sensors to their neighbors and also relay such information from their neighbors. We assume that the communication between nodes is error free.

7.2.2 Target motion model

We describe a general formulation of the tracking problem as follows.

There are J indistinguishable targets that move in a two-dimensional plane according to

$$\boldsymbol{x}_t = \boldsymbol{A}\boldsymbol{x}_{t-1} + \boldsymbol{B}\boldsymbol{u}_t, \tag{7.1}$$

where $t \in \mathbb{N}_0$, $\boldsymbol{x}_t = [\boldsymbol{x}_{1,t}^\top \ \boldsymbol{x}_{2,t}^\top \ \cdots \ \boldsymbol{x}_{J,t}^\top]^\top \in \mathbb{R}^{4J\times 1}$ is the unknown state vector at time instant t, and $\boldsymbol{x}_{j,t} \in \mathbb{R}^{4\times 1}$ is defined by

$$\boldsymbol{x}_{j,t} = [x_{j,1,t} \ x_{j,2,t} \ \dot{x}_{j,1,t} \ \dot{x}_{j,2,t}]^\top,$$

where $x_{j,1,t}$ and $x_{j,2,t}$ represent the coordinates of the jth target in the two-dimensional Cartesian coordinate system, and $\dot{x}_{j,1,t}$ and $\dot{x}_{j,2,t}$ are the respective components of the velocity of that target. The symbol $\boldsymbol{u}_t \in \mathbb{R}^{2J\times 1}$ is the target

propagation noise whose distribution is known. The transition matrices $\boldsymbol{A} \in \mathbb{R}^{4J\times 4J}$ and $\boldsymbol{B} \in \mathbb{R}^{4J\times 2J}$ are known and given by

$$\boldsymbol{A} = \boldsymbol{I} \otimes \begin{pmatrix} 1 & 0 & T_s & 0 \\ 0 & 1 & 0 & T_s \\ 0 & 0 & 1 & 0 \\ 0 & 0 & 0 & 1 \end{pmatrix} \quad \text{and} \quad \boldsymbol{B} = \boldsymbol{I} \otimes \begin{pmatrix} \frac{T_s^2}{2} & 0 \\ 0 & \frac{T_s^2}{2} \\ T_s & 0 \\ 0 & T_s \end{pmatrix},$$

where $\otimes$ denotes the Kronecker product, and $\boldsymbol{I}$ is the identity matrix with size $J \times J$.

7.2.3 Measurement model

The sensors make scalar measurements about the targets in the field, and they are given by

$$y_{k,n,t} \quad = \quad g_{k,n}(\boldsymbol{x}_t) + v_{k,n,t},$$

where $k = 1, 2, 3, 4$ is an index of the sensor at the nth node, and $y_{k,n,t}$ is the measurement of the sensor (identified by k and n), and $v_{k,n,t}$ is noise with distribution that is assumed Gaussian with mean μ_v and variance σ_v^2.

The measurement model depends on the type of sensors. In our work with acoustic sensors, the sensed information is the strength intensity (signal power) of the transmitted signals by the source that attenuates as a function of distance from the source. Thus, we define the functions $g_{k,n}(\cdot)$ by

$$g_{k,n}(\boldsymbol{x}_t) \quad = \quad \sum_{j=1}^{J} \frac{\Psi d_0^{\alpha}}{||\boldsymbol{r}_n - \boldsymbol{l}_{j,t}|\,|^{\alpha}} I(k, n, \boldsymbol{l}_{j,t}), \tag{7.2}$$

where $\Psi(\cdot)$ denotes the emitted power of the target measured at some predefined distance d_0, $\boldsymbol{l}_{j,t} = [x_{j,1,t}\, x_{j,2,t}]^{\top}$ is the location of the jth target at time instant t,

and α is a path-loss parameter. The symbol $I(k, n, \boldsymbol{l}_{j,t})$ is an indicator function given by

$$I(k, n, \boldsymbol{l}_{j,t}) = \begin{cases} 1, & \boldsymbol{l}_{j,t} \in \mathcal{R}_{k,n} \\ 0, & otherwise \end{cases},$$

where $\mathcal{R}_{k,n}$ is the area of sensitivity of the sensor.

The nodes transmit signals to their neighbors that are constructed according to

$$s_{k,n,t} \quad = \quad i, \;\; \gamma_i \leqslant y_{k,n,t} < \gamma_{i+1}, \quad i = 0, 1, 2, \cdots, L-2,$$

where $L \geqslant 3$, and γ_i are thresholds used for constructing $s_{k,n,t}$, with $\gamma_0 = -\infty$, $\gamma_{L-1} = \infty$, and $-\infty < \gamma_i < \infty$, $i = 1, 2, \cdots, L-2$. In the simplest case, when $L = 3$, the signal $s_{k,n,t}$ takes only one of two values, that is, then the sensors provide only binary information. While broadcasting $s_{k,n,t}$, the nodes also broadcast the ID number of the sensors that detected a target. The nodes also have the capability to relay such information from their neighbors. The communication between nodes is assumed to be error free.

The objective is that the nodes, given the available highly compressed information, track the targets in the field with particle filters that run at all the nodes or only at some predefined nodes.

7.3 Proposed methods

In a completely centralized method for tracking, each node takes sensor measurement and transmits them to a fusion center. The fusion center calculates the estimates by processing these measurements. In our non-centralized tracking method, nodes cooperates with each other by way of broadcasting the latest

detections to the neighbors of the nodes. Two schemes are studied, one where all the nodes perform tracking, and another where only one node in the proximity of the target perform it. We refer to these two schemes as all-node method and one-node method.

7.3.1 Tracking by all sensors

Let a target enter the field with directional sensors as shown in Fig. 7.1 (a). Each node has four sensors indexed by $k = 1, 2, 3, 4$, corresponding to the northeast, northwest, southwest and southeast sensor, respectively. It is assumed that upon detection of the target, the nodes that detect it broadcast information about the detected target to their neighbors. The broadcasting continues in stages. In the first stage, the nodes report the detection by their own sensors. In the following stages, they broadcast the new information they have about the detected target. If there is no new information, they stop broadcasting.

In the all-node method case, the broadcasting continues in stages until all the nodes have complete information about the detected target. We describe the first scenario in more detail by way of an example. In Fig.7.1 (a), we depict a target $T1$ that at time instant t was detected by sensors from node 8, 9, 14 and 15. In particular, of node 8, the detecting sensor was $k = 1$ (northeast), of node 9, it was sensor $k = 2$ (northwest), of node 14, it was $k = 4$ (southeast), and of node 15, it was $k = 3$ (southwest). After detecting the target, node 8 sends its information to its neighbors (nodes 2, 7, 9 and 14), node 9 sends it to its own neighbors and so on. In the next stage, node 8 broadcasts to its neighbors the information that specific sensors from node 9 and 14 also detected the target. Similarly, node 9 broadcasts that sensors from nodes 8 and 15 detected the target, and so on. Thus, after two

stages, node 8 knows that, besides its own northwest sensor, specific sensors from node 9, 14 and 15 also detected the target. With the broadcasting being carried on, all the nodes in the network will have the complete information about the detecting sensors.

Once a node has all the information about the detecting sensors, it processes the data using PF. Recall that with PF we represent the posterior density of the unknown state of the target by a random measure χ_t composed of particles of the states, $\boldsymbol{x}_t^{(m)}$ and associated weights to the particles, $w_t^{(m)}$, i.e., $\chi_t = \{\boldsymbol{x}_t^{(m)}, w_t^{(m)}\}_{m=1}^{M}$. The node can apply any of the PF schemes that are popular in the wide literature.

Here, we briefly describe the method we applied in our simulations (the standard PF scheme) [77]. Suppose that at time instant $t-1$, the node has the random measure χ_{t-1}. While waiting for new information, the node propagates the state according to

$$\boldsymbol{x}_t^{(m)} \quad \sim \quad p(\boldsymbol{x}_t|\boldsymbol{x}_{t-1}^{(m)}).$$

When the new information becomes available for processing, the particles $\boldsymbol{x}_t^{(m)}$ are assigned weights. For the weight update, we have

$$w_t^{(m)} \quad \propto \quad w_{t-1}^{(m)} \prod_{k,n} p(s_{k,n,t}|\boldsymbol{l}_{1:J,t}^{(m)})$$

where $\boldsymbol{l}_{1:J,t}^{(m)} \equiv \{\boldsymbol{l}_{1,t}^{(m)}, \boldsymbol{l}_{2,t}^{(m)}, \cdots, \boldsymbol{l}_{J,t}^{(m)}\}$ and $s_{k,n,t} \in \{0,1\}$ is the decision made by the sensor for the binary case. For $p(y_{k,n,t}|\boldsymbol{x}_t^{(m)})$, we use the models from [55]. In other words, we can write for $\boldsymbol{l}_t^{(m)} \in \mathcal{R}_{k,n}$,

$$p\left(s_{k,n,t} = 1|\boldsymbol{l}_{1:J,t}^{(m)}\right) \quad = \quad Q\left(\frac{\gamma - g_{k,n}(\boldsymbol{l}_{1:J,t}^{(m)}) - \mu_v}{\sigma_v}\right)$$

and

$$p\left(s_{k,n,t}=0|\boldsymbol{l}_{1:J,t}^{(m)}\right) \;=\; 1-Q\left(\frac{\gamma-g_{k,n}(\boldsymbol{l}_{1:J,t}^{(m)})-\mu_v}{\sigma_v}\right)$$

where $Q(\cdot)$ is the complementary distribution function of the standard Gaussian distribution, γ is a threshold used for detection and $g(\cdot)$ is given by (7.2). If $\boldsymbol{l}_t^{(m)} \notin \mathcal{R}_{k,n}$, we have

$$p\left(s_{k,n,t}=0|y_{k,n,t},\boldsymbol{x}_t^{(m)}\right)=1.$$

Note that each node can also use their own full RSS measurement. In this case, the weight at node n_0 is computed by

$$w_t^{(m)} \propto w_{t-1}^{(m)}\; p(y_{j,n_0,t}|\boldsymbol{l}_t^{(m)}) \prod_{k,n\in\mathcal{D}_t^*} p(s_{k,n,t}|\boldsymbol{l}_t^{(m)}) \tag{7.3}$$

where $\mathcal{D}_t^*$ is the set of all sensors at time instant t except for sensor j at node n_0, and where

$$p(y_{j,n_0,t}|\boldsymbol{l}_t^{(m)}) \propto \exp\left(-\frac{\left(y_{j,n_0,t}-\mu_v-g_{k,n}(\boldsymbol{l}_t^{(m)})\right)^2}{2\sigma_v^2}\right). \tag{7.4}$$

Once the weights are computed, one can decide if a resampling is needed.

We can extend the analysis to sensors that use multiple thresholds [94]. The difference lies in the computing of the likelihood function

$$p\left(s_{k,n,t}=i|\boldsymbol{l}_{1:J,t}^{(m)}\right)=Q\left(\boldsymbol{\theta}_{k,n,i}^{(m)}\right)-Q\left(\boldsymbol{\theta}_{k,n,i+1}^{(m)}\right),$$

where $\boldsymbol{\theta}_{k,n,i}^{(m)}=[\boldsymbol{l}_{1:J,t}^{(m)}\;\mu_v\;\sigma_v\;\gamma_i\;k\;n]^\top$, and where

$$Q(\boldsymbol{\theta}_{k,n,i}^{(m)}) \;=\; Q\left(\frac{\gamma_i-g_{k,n}\left(\boldsymbol{l}_{1:J,t}^{(m)}\right)-\mu_v}{\sigma_v}\right)$$

7.3.2 Tracking by nearby sensors

In the one-node method, the broadcasting is allowed in only a few stages. The purpose of this is to save on the communication power. the processing node predicts the next location of the target at each time step. If this location is still in the proximity of the processing node (within its detection area), the node will remain as a processing node. Otherwise, it will relinquish the processing. In that case, the processing node transmits the predicted location of the target. We explain the strategy by the same trajectory example shown in Fig. 7.1 (a). Suppose that at time instant $t-1$, it is node 8 that performs the tracking algorithm. This node waits to receive information from other nodes that detected the target, which are nodes 9, 14 and 15 in this example. These information all arrives at node 8 in at most two stages of broadcasting. Node 8 processes the data and then predicts that the target at the next time instant t will be in the sensing region of node 15, 16, 21 and 22. Thus, node 8 relinquishes processing and transmits the estimates of the state of the target through some stages of broadcasting so that at least one of the candidate nodes will get the estimations. One of the candidates (such as with the lowest ID) who receive the information will take over the processing. One recursion of this method was implemented in four steps as follows:

Step 1: The detecting nodes broadcast their own IDs to their neighbors. The nodes that receive this information, rebroadcast it to their neighbors too. Note that with these two broadcasts, the processing node has the IDs of all the detecting nodes.

Step 2: The processing node runs the PF algorithm and obtains an estimate of the state of the target.

Step 3: The processing node propagates the particles and based on the weights from the previous step and the propagated particles, predicts the target location at the next sampling instant. If the next location is still in the vicinity of the processing node, no change of processing nodes take place. Otherwise, the processing node broadcasts the estimate of the projected location of the target to its neighbors and the neighbors to their neighbors. Then the node with the smallest ID in the proximity of the projected location and that detects the target takes over the processing.

Step 4: The processing node, uses the estimated state values to generate particles and proceeds with operation in the same way as the previous processing node.

The processing node applies the PF algorithm for tracking and obtain the estimated states. This node predicts the next location of the target and decides whether to continue to do the processing or to broadcast its estimates to the neighbors. In the later case, when the neighboring nodes receive the estimates, they know based on their IDs, which one of them will be the next processing node. The new processing node generates particles from the prior $p(\boldsymbol{x}_t|\widehat{\boldsymbol{x}}_{t-1})$, where $\widehat{\boldsymbol{x}}_{t-1}$ is the state estimate at the previous time instant. To prevent a possible loss of target, the node may use a larger variance in the generation of $\boldsymbol{x}_t$ given $\widehat{\boldsymbol{x}}_{t-1}$ and may draw larger number particles, or under a severe circumstance it may restart the PF algorithm with the following initialization process: when one or more sensors detect the target, particles are uniformly generated over the region of where the target may be. This region is easily obtained based on the locations of the detecting sensors and their directionality.

When there is more than one target in the sensor field, the number of nodes tasked with tracking will be a function of time, and theoretically, it can vary between one and J. When all the targets are in close proximity to each other in time and space, only one node may be employed for tracking, and by contrast, when they are all separated, J different nodes will be tracking the targets. After estimating the predicted locations of their targets at time instant $t-1$, all of these nodes broadcast the obtained estimates and ID numbers of the targets. The neighboring nodes of the transmitting nodes receive this information, and based on their own ID numbers and the predicted locations of the targets in their proximity decide without ambiguity which nodes will do processing at time instant t.

7.4 Simulation results

We considered a network with $N = 36$ sensors deployed on a square grid, where the neighboring nodes were separated by $d = 40$ m. We set some of the parameters as follows: $\alpha = 2.5$, $\Psi = 5,000$, and $d_0 = 1$ m. The threshold was chosen so that the sensor range was $\rho = 32$ m (that is, $\rho = 0.8d$). The state noise process had a covariance matrix $\boldsymbol{C}_u = \mathrm{d}iag\{0.05, 0.01\}$, whereas the measurement noises had a mean $\mu_v = 1$ and a variance $\sigma_v^2 = 0.01$. The sampling interval was $T_s = 1$ s.

We also applied the same algorithm to a network with $N = 25$ and $N = 100$ nodes in order to verify the advantages of the one-node method regarding the communication cost.

We performed the tracking algorithms for each case for $K = 50$ different runs and used $M = 500$ particles for one target tracking and $M = 1000$ particles for the case of two targets.

To evaluate the performance of the tracking algorithms, we computed the

RMSE of the position of the target as a function of time. In addition, we proposed a new measure of accuracy besides RMSE: effective radius ε_t. It is defined for each time step t as

$$p(||\boldsymbol{l}^{(m)} - \boldsymbol{l}|| < \varepsilon_t) = P_t, \tag{7.5}$$

and represents that the probability of the estimated location deviating from the true location with a value less than ε_t is P_t. In the PF case with a set of weights, we can write equation 7.5 as

$$\sum_{m=1}^{M} w^{(m)} \cdot I(||\boldsymbol{l}^{(m)} - \boldsymbol{l}|| < \varepsilon_t) = P_t, \tag{7.6}$$

where I is an indicator function given by

$$I = \begin{cases} 1, & \text{if } ||\boldsymbol{l}^{(m)} - \boldsymbol{l}|| < \varepsilon_t \\ 0, & \text{otherwise} \end{cases} \tag{7.7}$$

For each t, we get a different radius ε_t when fixing P_t and we call it effective radius. In our simulation we set P_t to a constant value 95%. The simulation results show that the effective radius evaluates the performance well.

Figure 7.2 compares the performance (RMSEs and effective radius) of tracking with omni-directional and directional sensors. The result shows that the performance is improved due to the directional sensors.

Figure 7.3 compares the performance of the all-node and one-node methods. We also compared the communication costs of all-node and one-node methods when they are implemented on the two networks with 25 nodes and 100 nodes with the same density. Note that the tracking performances in these networks were basically the same because the performance doesn't depend on the size of the network when we assume error free communication and no latency. The comparison is given

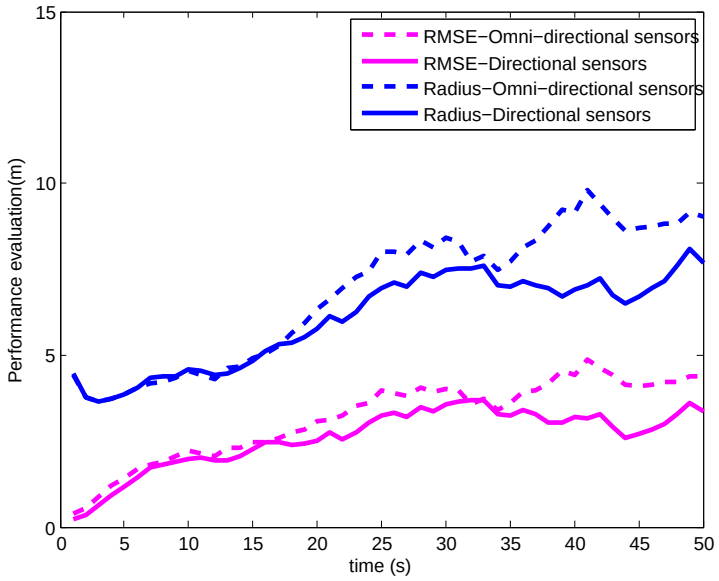

FIGURE 7.2: RMSE and effective radius of position of the all-node method (ANM) as a function of time for omnidirectional and directional sensors.

	Average of total number of transferred bits			
Method	BSN1	BSN2	DBSN1	DBSN2
ANM	27586	120589	38621	168834
ONM	15351	21302	18995	25975

Table 7.1: Average of total number of transferred bits for the (all-node method) ANM and (one-node method) ONM with binary sensor network (BSN) and Directional binary sensor network (DBSN). Here BSN1/DBSN1 indicates a network with 25 nodes, and BSN2/DBSN2 a network with 100 nodes.

in Table 7.1, where we listed the average of total number of transferred bits for the two methods. It can be seen that the all-node method does not scale well. Its average of total number of transferred bits increased by about 4.3 times when the number of nodes is 100 instead of 25. The one-node method had a factor of increase of about only 1.3 when we moved from a network of 25 to a network of 100 nodes. The increase of communication cost of the all-node method when $N = 100$

is due to the larger network size and the need for longer ID numbers of the nodes, whereas one-node method increases its communication cost because of the longer ID numbers.

The sensor range ρ affects the network coverage and the tracking performance. In the previous section, we defined the optimal range of the sensors and found its value numerically. In Fig. 7.4 we show the performance of the all-node method for the following sensor ranges: $\rho = 0.5d$, , $\rho = 0.75d$, $\rho = 0.8d$ and $\rho = d$. The results verify the analysis of the sensor range in the previous section in which $\rho = 0.8d$ obtains the best performance. Note that when $\rho = 0.5d$, the sensors cannot cover the whole region, and in the BSN case they fail to track the target. However with the directional sensors, the performance is not bad because the directional sectors reduce the uncertainty greatly.

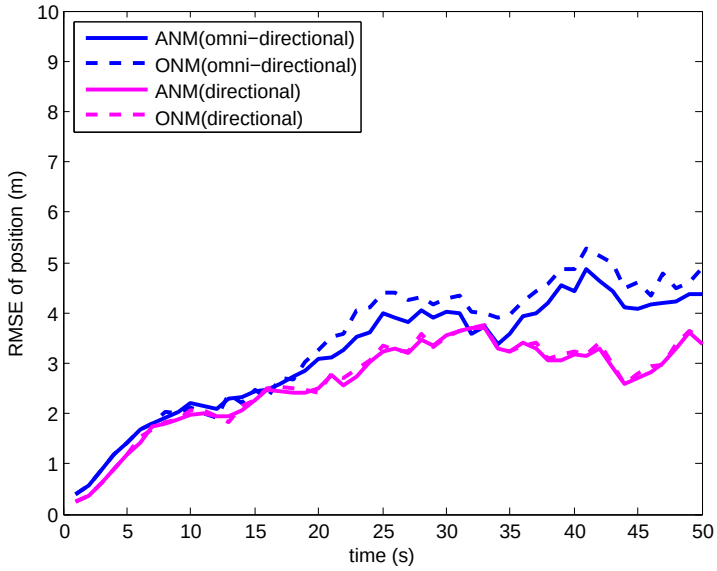

FIGURE 7.3: RMSE performance of the (all-node method) ANM and (one-node method) ONM with omnidirectional and directional sensors.

We analyzed the effect of the sectors for the directional sensors. The result is shown in Fig. 7.5. The overlapped sectors performs better than the non-overlapped sectors.

We also did experiments with two targets. The parameters of the model were selected in a way to allow for having the targets in time-space be in proximity

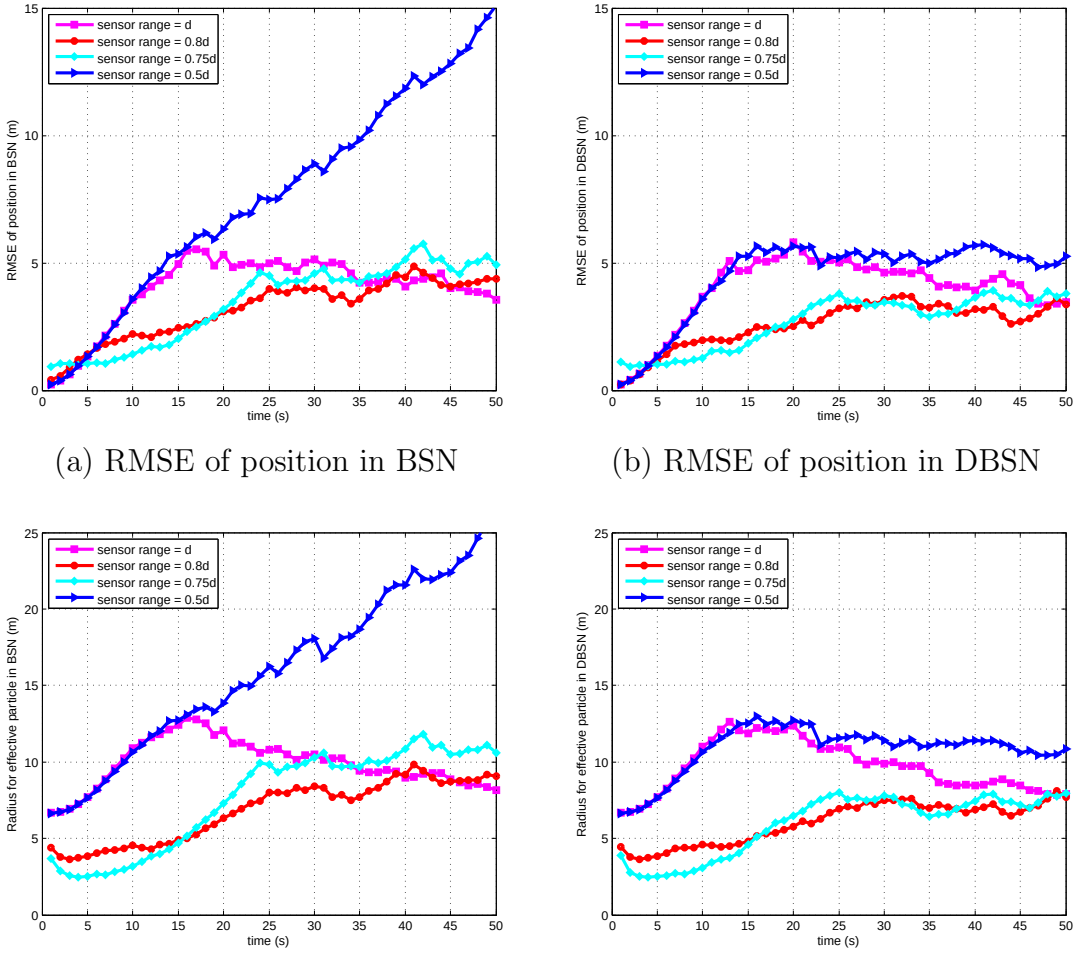

(a) RMSE of position in BSN (b) RMSE of position in DBSN

(c) Effective radius of position in BSN (d) Effective radius of position in DBSN

FIGURE 7.4: Performance evaluation of one target tracking with different sensor ranges as a function of time.

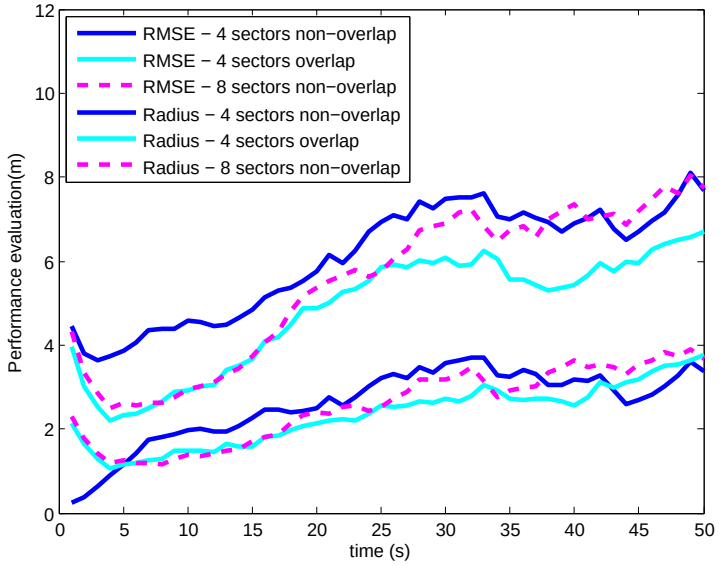

FIGURE 7.5: RMSE and effective error radius of position for directional sensors with different kinds of sectors.

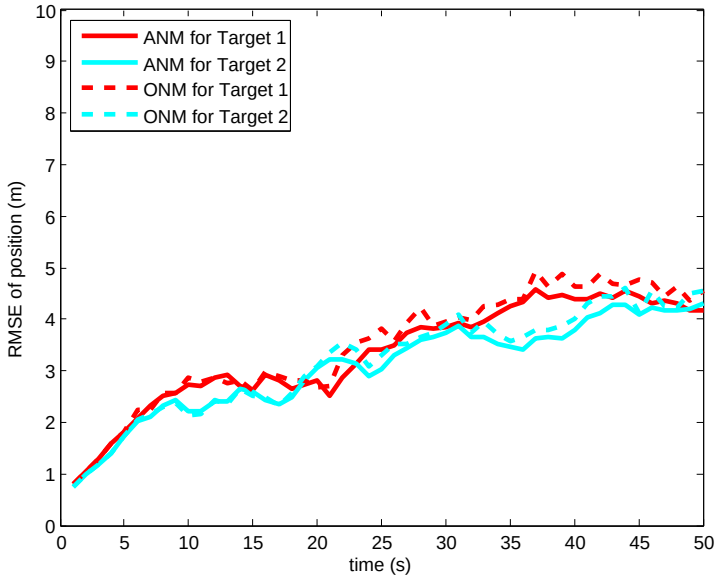

FIGURE 7.6: RMSE of positions for two target tracking with low initial velocities in DBSN

to each other. Figure 7.6 shows the performance for tracking two targets with different methods. We can see that the performance with one-node method is almost as good as that with all-node method.

7.5 Discussion

In the above presentation of the methods, we made strong assumptions about the propagation of the information in the networks before the data were processed. We assumed that the data would arrive on time for processing. In principle, this requirement does not have to be satisfied. If the propagated information in the network contains, besides the IDs of the sensors that detected the target, the time stamp when the target was detected, the nodes can carry on with the processing in the usual way (albeit with some delay).

We proposed these methods to allow for reducing the power for communication that is needed when the sensor network has a fusion center that processes the data. Here the rare communications of the sensors to the distant central unit are substituted with frequent but much less power-demanding communications with neighbors. Therefore, the method is can be readily applied to the novel system introduced in Chapter 6 which is composed of only tags with capability of tag-to-tag communication. However, due to the limited source on the tags, only simple algorithms can be applied such as the ones investigated in Chapter 6.

7.6 Summary

In this chapter we addressed non-centralized target tracking in networks of directional sensors. We proposed two methods, one where all the nodes do tracking at all times and another, where only one node performs tracking at a time. The

cooperation among the nodes is based on broadcasting information about the nodes that have detected the targets. The nodes perform tracking by using particle filtering. Extensive computer experiments were conducted where comparisons were made not only between the two methods but also with the performance in networks with omnidirectional sensors. The effects of the sensor ranges on the performance of the algorithms are also investigated. The results show that the performance of the method based on one processing node, while saving in communication of about 50%, is approximately the same as that of the method where all the nodes process the data.

8

Conclusions and Future Work

8.1 Conclusions

In this dissertation, we have addressed the problem of indoor localization and tracking using only binary information. We have introduced the basics of the indoor localization and tracking techniques and challenges, as well as its application prospects in the construction of IoT. We have also presented an overview of indoor positioning techniques using binary information, which indicates whether a device is present or absent within a predefined area.

We have presented indoor tracking problems using aggregated binary readings with UHF RFID systems within a Bayesian framework. A general probabilistic model of the aggregated binary readings is proposed, in which an accumulation of binary detections is used for tracking. The probability of detection of a tag is modeled as a random variable with a Beta distribution and it is a function of both the distance and the angle between the reader and the tag. The Beta distribution is a conjugate prior of the Binomial distribution and hence the mathematical

tractability is allowed for. The model also accounts for the possibility of a tag being in a dead-zone. We propose the use of a particle filtering algorithm for tracking that operates on asynchronous data.

We have further studied the problem of tracking using asynchronous binary readings, where the modeling of the observation is a special case of the aggregated binary readings where the number of accumulation is one. We have also considered tracking with the layout information and with a novel device called sense-a-tag (ST). The sense-a-tags can passively detect and decode backscatter signals from tags in its proximity and hence improve the positioning accuracy with these extra binary information, especially in areas with intersections and at portals. We have proposed a multi-hypothesis particle filtering method to deal with the tracking problem with intersections.

We have also proposed a novel system containing no RFID readers. This system is composed of low-cost "smart" tags with capability of tag-to-tag communication. These tags can broadcast information to neighboring tags by backscattering and they harvest energy from a continuous wave generated by an external exciter. These tiny and low-cost devices will play a pivotal role in the infrastructure of the IoT. A real-time self-locating problem is formulated in this reader-free system. And we have investigated the performance and computational complexity of several algorithms with low computational complexity, including the simplest association, the kalman filtering (for which a linear observation model is proposed), the particle filtering with the nonlinear observation model for the probability of detection of a tag, and the Rao-Blackwellised particle filtering algorithm which reduced the computational complexity by analytically marginalising the linear part of the state-space function. These algorithms preserve high accuracy in their performance.

Furthermore, we have presented a non-centralized tracking problem in a network of directional binary sensors, where each sensor node implements the algorithm based on its own measurement or measurements received from other nodes. We have proposed two methods where a target is being tracked by all the nodes or by only one of them at a time. The results of the tracking performance and the communication overhead have been presented. The decentralized techniques use in-network processing and neighbor-to-neighbor communications. And they can achieve low energy consumption, high robustness to node failure, and scalability. We have also discussed the extension of the methods with the non-centralized processing into the novel reader-free RFID system. In fact, the wide literature on distributed localization and tracking with sensor networks can also be extended to any system composed of "smart" devices with capability of computation and device-to-device communication.

8.2 Future work

It is expected that an explosion of advances of indoor positioning using binary information will be seen in the near future and the research will be promoted by the development of new technologies as well as the introduction of new applications. We now highlight some of the directions in future work.

- *Distributed localization and tracking*: The vision of IoT aims at connecting anything at anywhere from anytime. The scale of the IoT network will be huge and the connectivity will be rather dynamic. It is non-robust and unpractical to rely on a particular central unit for the localization and tracking purpose. Instead, algorithms that can be implemented in a

distributed way will be required. The literature on distributed localization and tracking can be applied to the systems with the "smart" tags which are capable of device-to-device communication. Methods in the signal processing society such as the consensus, the gossiping and algorithms for diffusion of knowledge can be implemented and investigated in the real-world platform. However, since the devices in IoT are becoming more and more simple, the energy/power requirement for the devices, the available memory and computational capability are becoming less and less, only limited information such as a binary detection can be available. The distributed methods using only binary information while still exhibit high accuracy is still challenging.

- *Anchor uncertainty*: Most of the existing techniques are based on using location information provided by a set of reference nodes which are aware of their exact locations, which is often not the truth in the real world. Therefore, localization and tracking methods must be able to deal with the location uncertainty of the reference nodes.

- *Data filtering and data fusing* : Due to the utilization of multiple mediums and different technologies, data fusing will be one major challenge. On the other hand, data filtering will be necessary due to the large number of objects involved and great volume of data to assist in the indoor localization and tracking. It is absolutely crucial to filter the raw data and extract valuable information in a timely fashion.

- *Interaction analysis*: The IoT vision includes the interaction between any two "things" and hence the interaction analysis between things and people will be of critical importance. In interaction analysis we focus on the detection

of proximity among objects instead of the actual locations of them.

- *Deployment analysis*: The localization and tracking accuracy is greatly affected by the deployment of the devices. The deployment issues include the density of the network, the sensing range of each device (if it is controllable), the deployment patterns and the coverage of the field of interest.

Bibliography

[1] H. Liu, H. Darabi, P. Banerjee, and J. Liu, "Survey of wireless indoor positioning techniques and systems," *IEEE Transactions on Systems, Man, and Cybernetics, Part C: Applications and Reviews*, vol. 37, no. 6, pp. 1067–1080, 2007.

[2] F. Seco, A. Jimenez, C. Prieto, J. Roa, and K. Koutsou, "A survey of mathematical methods for indoor localization," *Intelligent Signal Processing*, pp. 9–14, 2009.

[3] K. Finkenzeller, *RFID handbook*. New York: Wiley, 2010.

[4] B. Khoo, "RFID - from tracking to the Internet of Things: A review of developments," in *Proceedings of IEEE/ACM Int'l Conference on Green Computing and Communications & Int'l Conference on Cyber, Physical and Social Computing*. IEEE Computer Society, 2010, pp. 533–538.

[5] X. Li and V. Jilkov, "Survey of maneuvering target tracking. Part I: Dynamic models," *IEEE transactions on Aerospace and Electronic Systems*, vol. 39, no. 4, pp. 1333–1364, 2003.

[6] *http://www.business2community.com/tech-gadgets/four-internet-of-things-trends-0273289*, 2012.

[7] *ITU Internet Reports 2005: The Internet of Things*, 2005.

[8] *http://dondodge.typepad.com/the_next_big_thing/2013/06/indoor-location-startups-innovating-indoor-positioning.html*, 2013.

[9] A. M. Hossain and W.-S. Soh, "A survey of calibration-free indoor positioning systems," *Computer Communications*, 2015.

[10] D. Dardari, P. Closas, and P. M. Djurić, "Indoor tracking: Theory, methods, and technologies," *IEEE Transactions on Vehicular Technology*, vol. 64, no. 4, pp. 1263–1278, 2015.

[11] C.-H. Lim, Y. Wan, B.-P. Ng, and C. See, "A real-time indoor wifi localization system utilizing smart antennas," *IEEE Transactions on Consumer Electronics*, vol. 53, no. 2, pp. 618–622, 2007.

[12] C. Yang and H.-R. Shao, "Wifi-based indoor positioning," *Communications Magazine, IEEE*, vol. 53, no. 3, pp. 150–157, 2015.

[13] P. Bahl and V. N. Padmanabhan, "RADAR: An in-building RF-based user location and tracking system," in *Proceedings of the Nineteenth Annual Joint Conference of the IEEE Computer and Communications Societies. INFOCOM*, vol. 2. IEEE, 2000, pp. 775–784.

[14] M. A. Youssef, A. Agrawala, and A. Udaya Shankar, "WLAN location determination via clustering and probability distributions," in *Proceedings of the First IEEE International Conference on Pervasive Computing and Communications (PerCom)*. IEEE, 2003, pp. 143–150.

[15] M. Paciga and H. Lutfiyya, "Herecast: an open infrastructure for locationbased services using WiFi." in *WiMob (4)*. Citeseer, 2005, pp. 21–28.

[16] A. LaMarca, Y. Chawathe, S. Consolvo, J. Hightower, I. Smith, J. Scott, T. Sohn, J. Howard, J. Hughes, F. Potter *et al.*, "Place lab: Device positioning using radio beacons in the wild," in *Pervasive computing*. Springer, 2005, pp. 116–133.

[17] H. Liu, J. Yang, S. Sidhom, Y. Wang, Y. Chen, and F. Ye, "Accurate wifi based localization for smartphones using peer assistance," *IEEE Transactions on Mobile Computing*, vol. 13, no. 10, pp. 2199–2214, 2014.

[18] Z. Chen, H. Zou, H. Jiang, Q. Zhu, Y. C. Soh, and L. Xie, "Fusion of wifi, smartphone sensors and landmarks using the kalman filter for indoor localization," *Sensors*, vol. 15, no. 1, pp. 715–732, 2015.

[19] Y. Jin, H.-S. Toh, W.-S. Soh, and W.-C. Wong, "A robust dead-reckoning pedestrian tracking system with low cost sensors," in *IEEE International Conference on Pervasive Computing and Communications (PerCom)*. IEEE, 2011, pp. 222–230.

[20] H. Leppäkoski, J. Collin, and J. Takala, "Pedestrian navigation based on inertial sensors, indoor map, and WLAN signals," *Journal of Signal Processing Systems*, vol. 71, no. 3, pp. 287–296, 2013.

[21] H. Zou, L. Xie, Q.-S. Jia, and H. Wang, "Platform and algorithm development for a RFID-based indoor positioning system," *Unmanned Systems*, vol. 2, no. 03, pp. 279–291, 2014.

[22] Y. Tu, W. Zhou, and S. Piramuthu, "Identifying RFID-embedded objects in pervasive healthcare applications," *Decision Support Systems*, vol. 46, no. 2, pp. 586–593, 2009.

[23] C. Saygin, "Adaptive inventory management using RFID data," *The International Journal of Advanced Manufacturing Technology*, vol. 32, no. 9, pp. 1045–1051, 2007.

[24] J. Choi, D. Oh, and I. Song, "R-LIM: An affordable library search system based on RFID," in *International Conference on Hybrid Information Technology (ICHIT)*, vol. 1. IEEE, 2006, pp. 103–108.

[25] V. Chawla and D. Ha, "An overview of passive RFID," *IEEE Communications Magazine*, vol. 45, no. 9, pp. 11–17, 2007.

[26] D. M. Dobkin, *The RF in RFID: Passive UHF RFID in practice.* Newnes, 2008.

[27] M. R. M. Bolić and P. M. Djurić, "Proximity detection with RFID: a step toward the Internet of Things," *Pervasive Computing*, vol. 14, no. 2, pp. 70–76, 2015.

[28] C. M. Bishop *et al.*, *Pattern recognition and machine learning.* Springer New York, 2006, vol. 4, no. 4.

[29] B. Ristić, S. Arulampalam, and N. Gordon, *Beyond the Kalman filter: Particle filters for tracking applications.* Artech House Publishers, 2004.

[30] J. Zhou and J. Shi, "RFID localization algorithms and applications - A review," *Journal of Intelligent Manufacturing*, vol. 20, no. 6, pp. 695–707, 2009.

[31] L. M. Ni, Y. Liu, Y. Lau, and A. P. Patil, "LANDMARC: Indoor location sensing using active RFID," *Wireless networks*, vol. 10, no. 6, pp. 701–710, 2004.

[32] A. Bekkali and M. Matsumoto, "RFID indoor tracking based on inter-tags distance measurement," in *Proceedings of Wireless Telecommunications Symposium (WTS)*, 2007.

[33] A. Bekkali, H. Sanson, and M. Matsumoto, "RFID indoor positioning based on probabilistic RFID map and Kalman filtering," *Proceedings of the Third IEEE International Conference on Wireless and Mobile Computing (WiMOB)*, 2007.

[34] C. Alippi, D. Cogliati, and G. Vanini, "A statistical approach to localize passive RFIDs," in *Proceedings of International Symposium on Circuits and Systems (ISCAS)*, 2006, p. 4.

[35] T. Tran, C. Sutton, R. Cocci, Y. Nie, Y. Diao, and P. Shenoy, "Probabilistic inference over RFID streams in mobile environments," in *Proceedings of IEEE 25th International Conference on Data Engineering (ICDE)*, 2009, pp. 1096–1107.

[36] S. Jia, E. Shang, T. Abe, and K. Takase, "Localization of mobile robot with RFID technology and stereo vision," in *Proceedings of IEEE International Conference on Mechatronics and Automation (ICMA)*, 2006, pp. 508–513.

[37] D. Zhang, J. Ma, Q. Chen, and L. M. Ni, "An RF-based system for tracking transceiver-free objects," in *Proceedings of Fifth Annual IEEE International Conference on Pervasive Computing and Communications (PerCom)*, 2007, pp. 135–144.

[38] S. Särkkä, V. Viikari, M. Huusko, and K. Jaakkola, "Phase-based UHF RFID tracking with non-linear Kalman filtering and smoothing," *IEEE Sensors Journal*, vol. 12, no. 5, pp. 904–910, 2012.

[39] E. DiGiampaolo and F. Martinelli, "Mobile robot localization using the phase of passive uhf rfid signals," *IEEE Transactions on Industrial Electronics*, vol. 61, no. 1, pp. 365–376, 2014.

[40] D. Joho, C. Plagemann, and W. Burgard, "Modeling RFID signal strength and tag detection for localization and mapping," in *Proceedings of the IEEE International Conference on Robotics and Automation (ICRA)*, 2009, pp. 3160–3165.

[41] D. Hahnel, W. Burgard, D. Fox, K. Fishkin, and M. Philipose, "Mapping and localization with RFID technology," in *Proceedings of IEEE International Conference on Robotics and Automation (ICRA)*, vol. 1, 2004, pp. 1015–1020.

[42] P. Vorst and A. Zell, "Semi-autonomous learning of an RFID sensor model for mobile robot self-localization," in *European Robotics Symposium*. Springer, 2008, pp. 273–282.

[43] A. Milella, G. Cicirelli, and A. Distante, "RFID-assisted mobile robot system for mapping and surveillance of indoor environments," *Industrial Robot: An International Journal*, vol. 35, no. 2, pp. 143–152, 2008.

[44] F. Thiesse, E. Fleisch, and M. Dierkes, "Lottrack: RFID-based process control in the semiconductor industry," *IEEE Pervasive Computing*, vol. 5, no. 1, pp. 47–53, 2006.

[45] J. Song, C. T. Haas, and C. H. Caldas, "A proximity-based method for locating RFID tagged objects," *Advanced Engineering Informatics*, vol. 21, no. 4, pp. 367–376, 2007.

[46] S. Han, H. S. Lim, and J. M. Lee, "An efficient localization scheme for a differential-driving mobile robot based on RFID system," *IEEE Transactions on Industrial Electronics*, vol. 54, no. 6, pp. 3362–3369, 2007.

[47] B. Ferris, D. Hähnel, and D. Fox, "Gaussian processes for signal strength-based location estimation," in *Proceedings of Robotics Science and Systems*, 2006.

[48] L. M. Ni, D. Zhang, and M. R. Souryal, "RFID-based localization and tracking technologies," *IEEE Wireless Communications Magazine*, vol. 18, no. 2, pp. 45–51, 2011.

[49] D. Niculescu and B. Nath, "Dv based positioning in ad hoc networks," *Telecommunication Systems*, vol. 22, no. 1-4, pp. 267–280, 2003.

[50] A. Athalye, V. Savić, M. Bolić, and P. M. Djurić, "Radio Frequency Identification System for accurate indoor localization," in *Proceedings of the IEEE International Conference on Acoustics, Speech and Signal Processing (ICASSP)*, 2011, pp. 1777–1780.

[51] T. He, C. Huang, B. M. Blum, J. A. Stankovic, and T. F. Abdelzaher, "Range-free localization and its impact on large scale sensor networks," *ACM Transactions on Embedded Computing Systems (TECS)*, vol. 4, no. 4, pp. 877–906, 2005.

[52] N. Shrivastava, R. Mudumbai, U. Madhow, and S. Suri, "Target tracking with binary proximity sensors," *ACM Transactions on Sensor Networks (TOSN)*, vol. 5, no. 4, p. 30, 2009.

[53] Y. Shang, W. Rumi, Y. Zhang, and M. Fromherz, "Localization from connectivity in sensor networks," *IEEE Transactions on Parallel and Distributed Systems*, vol. 15, no. 11, pp. 961–974, 2004.

[54] L. Doherty, L. El Ghaoui *et al.*, "Convex position estimation in wireless sensor networks," in *Proceesings of the Twentieth Annual Joint Conference of the IEEE Computer and Communications Societies (INFOCOM).*, vol. 3. IEEE, 2001, pp. 1655–1663.

[55] P. M. Djurić, M. Vemula, and M. F. Bugallo, "Target tracking by particle filtering in binary sensor networks," *IEEE Transactions on Signal Processing*, vol. 56, no. 6, pp. 2229–2238, 2008.

[56] L. Geng, M. F. Bugallo, A. Athalye, and P. M. Djurić, "Indoor tracking with RFID systems," *IEEE Journal of Selected Topics in Signal Processing*, vol. 8, no. 1, pp. 96–105, 2014.

[57] N. Patwari and A. O. Hero III, "Using proximity and quantized RSS for sensor localization in wireless networks," in *Proceedings of the 2nd ACM international conference on Wireless sensor networks and applications*. ACM, 2003, pp. 20–29.

[58] M. Vemula, M. F. Bugallo, and P. M. Djurić, "Sensor self-localization with beacon position uncertainty," *Signal Processing*, vol. 89, no. 6, pp. 1144–1154, 2009.

[59] P. Vorst and A. Zell, "Particle filter-based trajectory estimation for passive UHF RFID fingerprints in unknown environments," in *Proceedings of the IEEE/RJS International Conference on Intelligent Robots and Systems (ICIRS)*, 2009, pp. 395–401.

[60] A. Doucet, N. de Freitas, and N. Gordon, Eds., *Sequential Monte Carlo Methods in Practice*. New York: Springer, 2001.

[61] V. Savić, A. Athalye, M. Bolić, and P. M. Djurić, "Particle filtering for indoor RFID tag tracking," in *Proceedings of the IEEE Statistical Signal Processing (SSP) Workshop*, 2011, pp. 193–196.

[62] L. Geng, M. F. Bugallo, A. Athalye, and P. M. Djurić, "Real time indoor tracking of tagged objects with a network of RFID readers," in *Proceedings of the 20th European Signal Processing Conference (EUSIPCO)*, 2012, pp. 205–209.

[63] Z. Hongsheng, "Analysis of dead zone by mathematical methods," in *Proceedings of the 7th International Conference on Wireless Communications, Networking and Mobile Computing (WiCOM)*, 2011, pp. 1–4.

[64] EPCglobal Inc., "EPC radio frequency identity protocols Class 1 Generation 2 UHF RFID," 2008, available from: http://www.gs1.org/gsmp/kc/epcglobal/uhfc1g2/uhfc1g2_1_2_0-standard-20080511.pdf.

[65] P. M. Djurić, J. H. Kotecha, J. Zhang, Y. Huang, T. Ghirmai, M. F. Bugallo, and J. Miguez, "Particle filtering," *IEEE Signal Processing Magazine*, vol. 20, no. 5, pp. 19–38, 2003.

[66] P. M. Djurić and M. F. Bugallo, *Particle filtering*. Wiley-IEEE Press, 2010, Adaptive Signal Processing: Next Generation Solutions. By S. Haykin and T. Adali (editors).

[67] A. F. García-Fernández and J. Grajal, "Asynchronous particle filter for tracking using non-synchronous sensor networks," *Signal Processing*, vol. 91, no. 10, pp. 2304–2313, 2011.

[68] J. Beaudeau, M. F. Bugallo, and P. M. Djurić, "Target tracking with asynchronous measurements by a network of distributed mobile agents," in *Proceedings of the IEEE International Conference on Acoustics, Speech and Signal Processing (ICASSP)*, 2012, pp. 3857–3860.

[69] F. Gustafsson, F. Gunnarsson, N. Bergman, U. Forssell, J. Jansson, R. Karlsson, and P. Nordlund, "Particle filters for positioning, navigation, and tracking," *IEEE Transactions on Signal Processing*, vol. 50, no. 2, pp. 425–437, 2002.

[70] N. L. Johnson, S. Kotz, and N. Balakrishnan, Eds., *Chapter 21: Beta Distributions*. Wiley-Interscience, 1995, vol. 2, continuous Univariate Distributions.

[71] J. M. Bernardo and A. F. M. Smith, *Bayesian Theory*. New York: John Wiley & Sons, 1994.

[72] N. Bulusu, J. Heidemann, and D. Estrin, "GPS-less low-cost outdoor localization for very small devices," *IEEE Personal Communications Magzine*, vol. 7, no. 5, pp. 28–34, 2000.

[73] L. Geng, M. F. Bugallo, and P. M. Djurić, "Tracking with RFID asynchronous measurements by particle filtering," in *Proceedings of IEEE International Conference on Acoustics, Speech and Signal Processing (ICASSP)*, 2013, pp. 4051–4055.

[74] P. M. Djurić and A. Athalye, "RFID system and method for localizing and tracking a moving object with an RFID tag," patent, Approved on: 2010-06-24; Application Number: 11799257, 2007.

[75] A. Athalye, V. Savić, M. Bolić, and P. M. Djurić, "Novel semi-passive RFID system for indoor localization," *IEEE Sensors Journal*, vol. 13, no. 2, pp. 528–537, 2013.

[76] Y. Oikawa, "Tag movement direction estimation methods in an rfid gate system," in *Proceedings of the 6th International Symposium on Wireless Communication Systems (ISWCS)*. IEEE, 2009, pp. 41–45.

[77] M. S. Arulampalam, S. Maskell, N. Gordon, and T. Clapp, "A tutorial on particle filters for online nonlinear/non-Gaussian bayesian tracking," *IEEE Transactions on Signal Processing*, vol. 50, no. 2, pp. 174–188, 2002.

[78] M. F. Bugallo, S. Xu, and P. M. Djurić, "Performance comparison of ekf and particle filtering methods for maneuvering targets," *Digital Signal Processing*, vol. 17, pp. 774–786, July 2007.

[79] G. Kortuem, F. Kawsar, D. Fitton, and V. Sundramoorthy, "Smart objects as building blocks for the Internet of Things," *IEEE Internet Computing*, vol. 14, no. 1, pp. 44–51, 2010.

[80] A. P. Sample, D. J. Yeager, P. S. Powledge, A. V. Mamishev, and J. R. Smith, "Design of an RFID-based battery-free programmable sensing platform," *IEEE Transactions on Instrumentation and Measurement*, vol. 57, no. 11, pp. 2608–2615, 2008.

[81] H. Zhang, J. Gummeson, B. Ransford, and K. Fu, "Moo: A batteryless computational RFID and sensing platform," *University of Massachusetts Computer Science Technical Report UM-CS-2011-020*, 2011.

[82] L. Geng, M. F. Bugallo, A. Athalye, and P. M. Djurić, "Real-time self-tracking in the Internet of Things," in *Proceedings of IEEE International Conference on Acoustics, Speech and Signal Processing (ICASSP)*, 2015.

[83] V. Liu, A. Parks, V. Talla, S. Gollakota, D. Wetherall, and J. R. Smith, "Ambient backscatter: wireless communication out of thin air," in *Proceedings of the ACM SIGCOMM*, 2013, pp. 39–50.

[84] P. V. Nikitin, S. Ramamurthy, R. Martinez, and K. Rao, "Passive tag-to-tag communication," in *Proceedings of IEEE International Conference on RFID*, 2012, pp. 177–184.

[85] L. Geng, M. F. Bugallo, and P. M. Djurić, "Tracking with asynchronous binary readings and layout information in RFID systems with sense-a-tags," in *Proceedings of the 21st European Signal Processing Conference (EUSIPCO)*, 2013, pp. 1–5.

[86] L. Eslim, W. Ibrahim, and H. S. Hassanein, "GOSSIPY: A distributed localization system for Internet of Things using RFID technology," *IEEE GLOBECOM*, 2013.

[87] A. Doucet, N. J. Gordon, and V. Krishnamurthy, "Particle filters for state estimation of jump markov linear systems," *IEEE Transactions on Signal Processing*, vol. 49, no. 3, pp. 613–624, 2001.

[88] F. Gustafsson, F. Gunnarsson, N. Bergman, U. Forssell, J. Jansson, R. Karlsson, and P.-J. Nordlund, "Particle filters for positioning, navigation, and tracking," *IEEE Transactions on Signal Processing*, vol. 50, no. 2, pp. 425–437, 2002.

[89] L. Mihaylova, D. Angelova, S. Honary, D. R. Bull, C. N. Canagarajah, and B. Ristic, "Mobility tracking in cellular networks using particle filtering," *IEEE Transactions on Wireless Communications*, vol. 6, no. 10, pp. 3589–3599, 2007.

[90] H. Ma and Y. Liu, "Some problems of directional sensor networks," *International Journal of Sensor Networks*, vol. 2, no. 1, pp. 44–52, 2007.

[91] Z. Wang, E. Bulut, and B. K. Szymanski, "Distributed target tracking with directional binary sensor networks," *International Journal of sensor networks*, 2009.

[92] M. Mazo, Jr., A. Speranzon, K. Johansson, and X. Hu, "Multi-robot tracking of a moving object using directional sensors," *IEEE International Conference on Robotics and Automatin*, vol. 2, pp. 1103–1108, 2004.

[93] P. Djuric and L. Geng, "Non-centralized target tracking in networks of directional sensors," in *IEEE Aerospace Conference*, 2011, pp. 1–6.

[94] L. Geng and P. Djuric, "Non-centralized target tracking in networks of directional sensors: Further advances," in *Proceedings of the 4th IEEE International Workshop on Computational Advances in Multi-Sensor Adaptive Processing (CAMSAP)*, 2011, pp. 85–88.

[95] R. Olfati-Saber, J. Fax, and R. Murray, "Consensus and cooperation in networked multi-agent systems," *Proceedings of the IEEE*, vol. 95, no. 1, pp. 215–233, 2007.

[96] A. Dimakis, S. Kar, J. Moura, M. Rabbat, and A. Scaglione, "Gossip algorithms for distributed signal processing," *Proceedings of the IEEE*, vol. 98, no. 11, pp. 1847–1864, 2010.

[97] Z. Weng and P. M. Djuric, "Distributed estimation in the presence of correlated noises," in *Signal Processing Conference (EUSIPCO), 2013 Proceedings of the 21st European*. IEEE, 2013, pp. 1–5.

[98] ——, "Efficient learning by consensus over regular networks," in *IEEE International Conference on Acoustics, Speech and Signal Processing (ICASSP)*. IEEE, 2014, pp. 7253–7257.

[99] T. Zhao and A. Nehorai, "Distributed sequential Bayesian estimation of a diffusive source in wireless sensor networks," *IEEE Transactions on Signal Processing*, vol. 55, no. 4, pp. 1511–1524, 2007.